CONANTOKINS: DEVELOPING PHARMACOLOGY FOR DIFFERENTIATING N-METHYL-D-ASPARTATE RECEPTOR SUBTYPES

by

Vernon D. Twede

A dissertation submitted to the faculty of
The University of Utah
in partial fulfillment of the requirements for the degree of

Doctor of Philosophy

Neuroscience Program

The University of Utah

May 2014

The University of Utah Graduate School

STATEMENT OF DISSERTATION APPROVAL

The dissertation of **Vernon D. Twede**

has been approved by the following supervisory committee members:

Baldomero M. Olivera	, Chair	**10/24/2013** Date Approved
H. Steve White	, Member	**10/24/2013** Date Approved
Kristen Keefe	, Member	**10/24/2013** Date Approved
J. Michael McIntosh	, Member	**10/24/2013** Date Approved
Doju Yoshikami	, Member	**10/24/2013** Date Approved

and by **Kristen Keefe** , Chair/Dean of

the Department/College/School of **Neuroscience**

and by David B. Kieda, Dean of The Graduate School.

ABSTRACT

N-methyl-D-aspartate (NMDA) receptors are members of the ionotropic glutamate receptor family that have critical functions in neural plasticity as well as a number of nervous system pathologies. NMDA receptors have a great deal of diversity in the subtypes expressed in different regions of the nervous system throughout the course of development. A greater understanding of NMDA receptor functioning in the nervous system is therefore highly desirable to researchers and clinicians, but this understanding is limited by the current set of selective pharmacological tools. The goal of the work in this dissertation is to gain a greater understanding of how highly selective NMDA receptor antagonists can be developed from a distinct group of peptides derived from the venom of marine cone snails known as the Conantokins, natural products that block NMDA receptors in a subtype-selective manner. The work in this dissertation aims to further this objective through three separate approaches. In Chapter 2, a novel conantokin, Conantokin-Br, is functionally characterized, and structure-activity relationship studies are performed to identify sequence determinants of subtype selectivity. In Chapter 3, NMDA receptor NR2 subunit chimeras are generated and used to identify determinants of selectivity towards Conantokin-R and Conantokin*Rl*-B on the glutamate binding subdomains of the NR2 subunits. In Chapter 4 the selective conantokin Conantokin*Rl*-B is used to identify NR2B-containing NMDA receptor subtypes present in dissociated Ventral Respiratory Column cells. In Chapter 5, these results are summarized, and the overall significance of the work is described. It is hoped that the experiments performed in this work will one day lead to highly selective compounds that will further the frontiers of investigating the underlying functions and therapeutic potential of targeting NMDA receptors.

TABLE OF CONTENTS

LIST OF TABLES

Table

LIST OF FIGURES

Figure

CHAPTER 1

INTRODUCTION

NMDA Receptors: physiological roles, expression patterns, and pharmacology

N-Methyl-D-Aspartate (NMDA) receptors are members of the ionotropic glutamate receptor superfamily of ion channels. Similar to other members of the glutamate receptor superfamily, including α-Amino-3-hydroxy-5-methyl-4-isoxazolepropionic acid (AMPA) receptors and kainate receptors, NMDA receptors bind the excitatory amino acid glutamate to mediate cation flow across a membrane voltage potential in neurons. A number of functional features distinguish NMDA receptors from other types of ionotropic glutamate receptors, including: 1) the requirement of the co-agonists glycine or D-serine for activation, 2) calcium-permeability through the ion channel pore, and 3) the presence of a voltage-dependent $Mg^{2=}$ blockade of ion flow in the channel. Among these unique functional distinctions, the presence of a voltage-dependent Mg^{2+} blockade of ion flow appears to be important for the process of coincidence detection, a fundamental mechanism thought to underlie the processes of synaptic plasticity and learning and memory in the nervous system (Seeburg et al., 1995). In support of this hypothesis, pharmacological blockade of NMDA receptors has been shown to impede learning and memory of many functional tasks in rodents (Morris, 2013; Davis et al., 1992).

In addition to being implicated in the fundamental processes of learning and memory, the dysfunction of NMDA receptors also plays a role in a number of pathological processes that affect the nervous system. In the spinal cord, NMDA receptors are thought to be involved in the development of chronic neuropathic pain (Zhou et al., 2011). In the brain, NMDA receptors are thought to play a role in epilepsy, Parkinson's disease, Alzheimer's disease, depression, and psychosis (Ghasemi et al., 2011; Xu et al., 2012; Calabresi et al., 2013; Zarate et al., 2013; Pochwat et al., 2013; Cioffi, 2013). Thus, there has been a tremendous amount of interest in developing therapeutics targeted to NMDA receptors. While early studies utilizing nonselective NMDA receptor antagonists demonstrated that they were generally effective at ameliorating many of these conditions, many human trials were not continued due to a number of side effects,

thought to be due to a lack of specificity towards the particular NMDA receptors implicated in these disorders.

Among the obstacles in developing highly specific therapeutics is the tremendous diversity among the NMDA receptor class of glutamate receptors. NMDA receptors comprise at least three different gene families, including the NR1 (which bind glycine), NR2 (which bind glutamate), and NR3 subunit genes (which also bind glycine) (Cull-Candy et al., 2001). To add to this complexity, there are eight different splice variants for the NR1 subunit, for separate NR2 subunit genes (NR2A-NR2D), and two NR3 genes (NR3A and NR3B) (Cull-Candy et al., 2001). Functional NMDA receptors are heterotetramers, consisting of at least two NR1 subunits, and a potential combination of any NR2 or NR3 subunits (Ulbrich and Isacoff, 2008; Schuler et al., 2008).

The precise subunit combinations expressed in the mammalian nervous system are not known; however immunohistochemistry and RNA expression studies have revealed that NMDA receptor subunit genes are distributed in the nervous system in a region-specific and developmentally-regulated manner (Rigby et al, 1996; Riva et al., 1994; Laurie et al., 1997). In general, the obligatory NR1 subunit (and its many splice variants) is ubiquitously-expressed in the nervous system (Pujic et al., 1993; Laurie and Seeburg, 1994). Among the NR2 subunits, the NR2A subunit is expressed in a majority of regions in the central nervous system, the NR2B subunit is expressed predominantly in the forebrain and hippocampal regions, the NR2C subunit is expressed at highest concentrations in the cerebellum, and the NR2D subunit is largely expressed in the midbrain and brainstem regions (Laurie et al., 1997). During development, changes in NMDA receptor subunit expression occur in early postnatal mammals, with the NR2B and NR2D subunits generally declining in expression, and the NR2A and NR2C subunits increasing in abundance (Laurie et al., 1994).

Pharmacological agents targeting specific subtypes have been developed; however, antagonists targeting particular NMDA receptor subtypes are relatively few in comparison to the

number of potential NMDA receptor subtypes. Among the selective antagonists, the majority are targeted towards particular NR2 subunits, which bind the excitatory amino acid glutamate. Small molecules, including ifenprodil and derivatives, are highly specific to NMDA receptor subtypes containing NR2B subunits (Fischer et al., 1997; Gill et al., 2002). In addition, novel classes of small molecules have been developed that target the NR2C and NR2D subunits with some preference over NR2A and NR2B subtypes (Mosley et al., 2010). Notably, many of these molecules have been reported to have off-target (non-NMDA receptor) activities that should be considered when assessing the effects of these compounds (see Supplementary Information, Gowd et al., 2012). Thus, additional selective antagonists, with minimal activity on non-NMDA receptor targets, would be highly desirable for research and therapeutics.

Conantokins: subtype selective conopeptide NMDA receptor antagonists

Conantokins are peptide antagonists of NMDA receptors derived from the venom of marine cone snails of the genus *Conus*. Conantokins are distinct among the conopeptides in that they generally lack disulfide bonds are enriched in the posttranslationally-modified amino acid gamma carboxyglutamate (gla). The presence of gla residues contribute to the helical structure of conantokins in solution upon binding of divalent cations (Chen et al., 1998; Rigby et al., 1997; Warder et al., 1998). Thus far, 15 different conantokins from 8 different species have been functionally characterized in the literature (Gowd et al., 2008; Gowd et al., 2010; Gowd et al., 2012; Haack et al., 1990; Jiminez et al., 2002; Mena et al., 1990; Platt et al., submitted; Teichert et al., 2007; Twede et al., 2009a; White et al., 2000).

Conantokins are thought to competitively inhibit ion flow through NMDA receptors by acting at the glutamate binding site on the NR2 subunits (Donevan and McCabe, 2000). In accordance with this hypothesis, conantokins generally selectively block NMDA receptor subtypes depending on which NR2 subunits are expressed in the complex (see Twede et al., 2009b). The majority of conantokins preferentially target NMDA receptors containing the NR2B

subunit, and have varying degrees of inhibition on NMDA receptor subtypes containing other NR2 subunits (Reviewed in Twede et al., 2009b). Recently, however, conantokins were identified that show some preference for NR2D-containing NMDA receptor subtypes (Platt et al., submitted).

Along with other conantokins, Conantokin*G* (Con*G*) from *Conus geographus*, has demonstrated therapeutic potential in preclinical trials for the treatment of epilepsy, neuroprotection from focal ischemia, and neuropathic pain (Bialer et al., 2002; Malmberg et al., 2003; Reviewed in Twede et al., 2009b; Williams et al., 2000;). Con*G* has additionally reached Phase I clinical trials for the treatment of epilepsy in humans (Bialer et al., 2002). Unlike many other NMDA receptor antagonists, conantokins have shown relatively low toxicity and few side effects in animal models (Malmberg et al., 2003). This relatively low toxicity has been attributed to specificity towards the particular NMDA receptor subtypes affected in these nervous system disorders, in addition to a lack of off-target activity (Malmberg et al., 2003; see Gowd et al., 2012). Recently, the discovery of Conantokin*Rl*-B (Con*Rl*-B), a conantokin with anticonvulsant activity and unprecedented selectivity among the conantokin family (greater than ~100-fold against all other subtypes) for the NR2B subunit (Gowd et al, 2012) has demonstrated further potential for the development of highly selective antagonists targeted towards each NMDA receptor subtype.

To develop and discover additional highly selective conantokin peptides and analogues more effectively, two problems must first be addressed. First, a greater understanding is needed of how and to what extent the primary amino acid sequences (and subsequent structures) of conantokin peptides can be used to predict (and design) conantokin sequences that are capable of targeting each particular NMDA receptor subtype with a high degree of selectivity. Structure-activity relationship studies have demonstrated, for instance, that certain amino acid positions within these peptides are critical for governing both rudimentary activity and, to some extent, subunit selectivity (Klein et al., 2001; Sheng et al., 2007; Sheng et al., 2010). Second, a greater

understanding is needed of how conantokins interact with the binding site(s) on the each of the NR2 subunits to determine selectivity towards each NMDA receptor subtype. While some work has been performed to address both of these questions, these studies were largely performed, by examining differences between selectivity towards two of the NMDA receptor subtypes (those containing either the NR2A or NR2B subunits) (Klein et al., 2001; Sheng et al., 2007; Sheng et al., 2009; Sheng et al., 2010). Thus, the question of how each conantokin interacts with each of the four NR2 subunits to result in subtype selectivity is an area of potential research interest. In addition, the question of how subtype-selective conantokins can be used to dissect the expression patterns of particular NMDA receptor subtypes in the nervous system is an area of research interest.

Work described in this dissertation

The work described in this dissertation aims to further the efforts of developing and characterizing highly selective NMDA receptor antagonists derived from the Conantokin family of peptides. In Chapter 2, a novel conantokin from *Conus brettinghami*, Conantokin-Br, is functionally characterized; high potency on NR2D-containing NMDA receptors allowed for a structure-activity relationship study to be performed, resulting in the identification of the amino acid at position 5 in the peptide as a determinant of NR2D selectivity. In Chapter 3, structure function studies are used to elucidate the regions of interaction between two conantokins, Conantokin-R and Conantokin*Rl*-B and the two NR2 subunits, NR2B and NR2D; results indicate that the two conantokins interact with similar regions (yet different amino acids) in the glutamate binding domains to determine the subunit selectivities of the peptides. In Chapter 3, the NR2B subtype-selective conantokin Con*Rl*-B is used in a calcium-imaging assay of dissociated ventral respiratory column cells to identify NMDA receptor subtypes expressed in this region; results indicate a distinction between NR2B-containing and other NMDA receptor subtypes among two major cell classes with in this region of the brain. Lastly, in Chapter 5, future directions of

research are discussed in the context of the results described in the experiments herein. It is hoped that this work can be used to ultimately gain an understanding of the individual functional roles and therapeutic potential of each NMDA receptor subtype capable of being targeted in the nervous system.

References

Bialer M., Johannessen S.I., Kupferberg H.J., Levy R.H., Loiseau P., Perucca E., 2002. Progress report on new antiepileptic drugs: a summary of the Sixth Eilat Conference (EILAT VI). Epilepsy Res. 51, 31-71.

Calabresi P., Di Filippo M., Gallina A., Wang Y., Stankowski J.N., Picconi B., Dawson V.L., Dawson T.M., 2013. New synaptic and molecular targets for neuroprotection in Parkinson's disease. Mov. Disord. 28, 51-60.

Chen Z., Blandl T., Prorok M., Warder S.E., Li L., Zhu Y., Pedersen L.G., Ni F., Castellino F.J., 1998. Conformational changes in conantokin-G induced upon binding of calcium and magnesium as revealed by NMR structural analysis. J. Biol. Chem. 273, 16248-58.

Cioffi C.L., 2013. Modulation of NMDA receptor function as a treatment for schizophrenia. Bioorg. Med. Chem. Lett. 23, 5034-44.

Cull-Candy S., Brickley S., Farrant M., 2001. NMDA receptor subunits: diversity, development and disease. Curr. Opin. Neurobiol. 11, 327-35. Review.

Davis S., Butcher S.P., Morris R.G., 1992. The NMDA receptor antagonist D-2-amino-5-phosphonopentanoate (D-AP5) impairs spatial learning and LTP in vivo at intracerebral concentrations comparable to those that block LTP in vitro. J. Neurosci. 12, 21-34.

Donevan S.D., McCabe R.T., 2000. Conantokin G is an NR2B-selective competitive antagonist of N-methyl-D-aspartate receptors. Mol. Pharmacol. 58, 614-23.

Fischer G., Mutel V., Trube G., Malherbe P., Kew J.N., Mohacsi E., Heitz M.P., Kemp, J.A., 1997. Ro 25-6981, a highly potent and selective blocker of N-methyl-D-aspartate receptors containing the NR2B subunit. Characterization in vitro. J. Pharmacol. Exp. Ther. 283, 1285−1292.

Ghasemi M., Schachter S.C., 2011. The NMDA receptor complex as a therapeutic target in epilepsy: a review. Epilepsy Behav. 22, 617-40. Review.

Gill R., Alanine A., Bourson A., Buttelmann B., Fischer G., Heitz M.P., Kew J.N., Levet-Trafit, B., Lorez H.P., Malherbe P., Miss M.T., Mutel V., Pinard E., Roever S., Schmitt M., Trube G., Wybrecht R., Wyler R., and Kemp J.A., 2002. Pharmacological characterization of Ro 63-1908 (1-[2-(4-hydroxy-phenoxy)-ethyl]-4-(4-methyl-benzyl)-piperidin-4-ol), a novel subtype-selective N-methyl--aspartate antagonist. J. Pharmacol. Exp. Ther. 302, 940−948.

Gowd K.H., Han T.S., Twede V., Gajewiak J., Smith M.D., Watkins M., Platt R.J., Toledo G., White H.S., Olivera B.M., Bulaj G., 2012. Conantokins derived from the Asprella clade impart conRl-B, an N-methyl d-aspartate receptor antagonist with a unique selectivity profile for NR2B subunits. Biochemistry. 51, 4685-92.

Gowd K.H., Twede V., Watkins M., Krishnan K.S., Teichert R.W., Bulaj G., Olivera B.M., 2008. Conantokin-P, an unusual conantokin with a long disulfide loop. Toxicon. 52, 203-13.

Gowd K.H., Watkins M., Twede V.D., Bulaj G.W., Olivera B.M., 2010. Characterization of conantokin Rl-A: molecular phylogeny as structure/function study. J. Pept. Sci. 16, 375-82.

Haack J.A., Rivier J., Parks T.N., Mena E.E., Cruz L.J., Olivera B.M., 1990. Conantokin-T. A gamma-carboxyglutamate containing peptide with N-methyl-d-aspartate antagonist activity. J. Biol. Chem. 265, 6025-9.

Jimenez E.C., Donevan S., Walker C., Zhou L.M., Nielsen J., Cruz L.J., Armstrong H., White H.S., Olivera B.M., 2002. Conantokin-L, a new NMDA receptor antagonist: determinants for anticonvulsant potency. Epilepsy Res. 51, 73-80.

Klein R.C., Prorok M., Galdzicki Z., Castellino F.J., 2001. The amino acid residue at sequence position 5 in the conantokin peptides partially governs subunit-selective antagonism of recombinant N-methyl-D-aspartate receptors. J. Biol. Chem. 276, 26860-7.

Laurie D.J., Bartke I., Schoepfer R., Naujoks K., Seeburg P.H., 1997. Regional, developmental and interspecies expression of the four NMDAR2 subunits, examined using monoclonal antibodies. Brain Res. Mol. Brain Res. 51, 23-32.

Laurie D.J., Putzke J., Zieglgänsberger W., Seeburg P.H., Tölle T.R., 1995. The distribution of splice variants of the NMDAR1 subunit mRNA in adult rat brain. Brain Res. Mol. Brain Res. 32, 94-108.

Laurie D.J., Seeburg P.H., 1994. Regional and developmental heterogeneity in splicing of the rat brain NMDAR1 mRNA. J. Neurosci. 14, 3180-94.

Malmberg A.B., Gilbert H., McCabe R.T., Basbaum A.I., 2003. Powerful antinociceptive effects of the cone snail venom-derived subtype-selective NMDA receptor antagonists conantokins G and T. Pain. 101, 109-16.

Mena E.E., Gullak M.F., Pagnozzi M.J., Richter K.E., Rivier J., Cruz L.J., Olivera B.M., 1990. Conantokin-G: a novel peptide antagonist to the N-methyl-D-aspartic acid (NMDA) receptor. Neurosci Lett. 118, 241-4.

Morris R.G., 2013. NMDA receptors and memory encoding. Neuropharmacology. 74, 32-40.

Mosley C.A., Acker T.M., Hansen K.B., Mullasseril P., Andersen K.T., Le P., Vellano K.M., Brauner-Osborne H., Liotta D.C., and Traynelis S.F., 2010. Quinazolin-4-one derivatives: a novel class of noncompetitive NR2C/D subunit-selective N-methyl-D- aspartate receptor antagonists. J. Med. Chem. 53, 5476−5490.

Platt R.J., Curtice K.J., Twede V.D., Watkins M., Gruszczynski P., Bulaj G., Horvath M.P., Olivera B.M., *submitted*. Conantokins from *Conus bocki*: from molecular phylogeny

towards differentiating pharmacology for NMDA receptor subtypes.

Pochwat B., Szewczyk B., Sowa-Kucma M., Siwek A., Doboszewska U., Piekoszewski W., Gruca P., Papp M., Nowak G., 2014. Antidepressant-like activity of magnesium in the chronic mild stress model in rats: alterations in the NMDA receptor subunits. Int. J. Neuropsychopharmacol. 17, 393-405.

Pujic Z., Matsumoto I., Wilce P.A., 1993. Expression of the gene coding for the NR1 subunit of the NMDA receptor during rat brain development. Neurosci. Lett. 162, 67-70.

Rigby A.C., Baleja J.D., Li L, Pedersen L.G., Furie B.C., Furie B., 1997. Role of gamma-carboxyglutamic acid in the calcium-induced structural transition of conantokin G, a conotoxin from the marine snal Conus geographus. Biochemistry. 36, 15677-84.

Rigby M., Le Bourdellès B., Heavens R.P., Kelly S., Smith D., Butler A., Hammans R., Hills R., Xuereb J.H., Hill R.G., Whiting P.J., Sirinathsinghji D.J., 1996. The messenger RNAs for the N-methyl-D-aspartate receptor subunits show region-specific expression of different subunit composition in the human brain. Neuroscience. 73, 429-47.

Riva M.A., Tascedda F., Molteni R., Racagni G., 1994. Regulation of NMDA receptor subunit mRNA expression in the rat brain during postnatal development. Brain Res. Mol. Brain Res. 25, 209-16.

Schüler T., Mesic I., Madry C., Bartholomäus I., Laube B. 2008. Formation of NR1/NR2 and NR1/NR3 heterodimers constitutes the initial step in N-methyl-D-aspartate receptor assembly. J Biol Chem. 283, 37-46.

Seeburg P.H., Burnashev N., Köhr G., Kuner T., Sprengel R., Monyer H., 1995. The NMDA receptor channel: molecular design of a coincidence detector. Recent Prog. Horm. Res.50, 19-34. Review.

Sheng Z., Dai Q., 2007. Prorok M., Castellino F.J., Subtype-selective antagonism of N-methyl-D-aspartate receptor ion channels by synthetic conantokin peptides. Neuropharmacology. 53, 145-56.

Sheng Z., Liang Z., Geiger J.H., Prorok M., Castellino F.J., 2009. The selectivity of conantokin-G for ion channel inhibition of NR2B subunit-containing NMDA receptors is regulated by amino acid residues in the S2 region of NR2B. Neuropharmacology. 57, 127-36.

Sheng Z., Prorok M., Castellino F.J., 2010. Specific determinants of conantokins that dictate their selectivity for the NR2B subunit of N-methyl-D-aspartate receptors. Neuroscience. 170, 703-10.

Teichert R.W., Jimenez E.C., Twede V., Watkins M., Hollmann M., Bulaj G., Olivera B.M., 2007. Novel conantokins from Conus parius venom are specific antagonists of N-methyl-D-aspartate receptors. J. Biol. Chem. 282, 36905-13.

Twede V.D., Teichert R.W., Walker C.S., Gruszczyński P., Kaźmierkiewicz R., Bulaj G., Olivera B.M., 2009. Conantokin-Br from Conus brettinghami and selectivity determinants for the NR2D subunit of the NMDA receptor. Biochemistry. 48, 4063-73.

Twede V.D., Miljanich G., Olivera B.M., Bulaj G., 2009. Neuroprotective and cardioprotective conopeptides: an emerging class of drug leads. Curr. Opin. Drug Discov. Devel. 12, 231-9. Review.

Ulbrich M.H., Isacoff E.Y., 2008. Rules of engagement for NMDA receptor subunits. Proc. Natl. Acad. Sci. USA. 105, 14163-8.

Warder S.E., Prorok M., Chen Z., Li L., Zhu Y., Pedersen L.G., Ni F., Castellino F.J., 1998. The roles of individual gamma-carboxyglutamate residues in the solution structure and cation-dependent properties of conantokin-T. J. Biol. Chem. 273, 7512-22.

White H.S., McCabe R.T., Armstrong H., Donevan S.D., Cruz L.J., Abogadie F.C., Torres J., Rivier J.E., Paarmann I., Hollmann M., Olivera B.M., 2000. In vitro and in vivo characterization of conantokin-R, a selective NMDA receptor antagonist isolated from the venom of the fish-hunting snail Conus radiatus. J. Pharmacol. Exp. Ther. 292, 425-32.

Williams A.J., Dave J.R., Phillips J.B., Lin Y., McCabe R.T., Tortella F.C., 2000. Neuroprotective efficacy and therapeutic window of the high-affinity N-methyl-D-aspartate antagonist conantokin-G: in vitro (primary cerebellar neurons) and in vivo (rat model of transient focal brain ischemia) studies. J. Pharmacol. Exp. Ther. 294, 378-86.

Xu Y., Yan J., Zhou P., Li J., Gao H., Xia Y., Wang Q., 2012. Neurotransmitter receptors and cognitive dysfunction in Alzheimer's disease and Parkinson's disease. Prog. Neurobiol. 97, 1-13. Review.

Zarate C., Duman R.S., Liu G., Sartori S., Quiroz J., Murck H., 2013. New paradigms for treatment-resistant depression. Ann. NY Acad. Sci. 1292, 21-31. Review.

Zhou H.Y., Chen S.R., Pan H.L., 2011. Targeting N-methyl-D-aspartate receptors for treatment of neuropathic pain. Expert. Rev. Clin. Pharmacol. 4, 379-88. Review.

CHAPTER 2

CONANTOKIN-BR FROM CONUS BRETTINGHAMI AND SELECTIVITY DETERMINANTS FOR THE NR2D SUBUNIT OF THE NMDA RECEPTOR

Reprinted with permission from: Twede V.D., Teichert R.W., Walker C.S., Gruszczyński P., Kaźmierkiewicz R., Bulaj G., Olivera B.M., 2009. Conantokin-Br from Conus brettinghami and selectivity determinants for the NR2D subunit of the NMDA receptor. Biochemistry. 48, 4063-73.

BIOCHEMISTRY
including biophysical chemistry & molecular biology
Article

Biochemistry **2009,** *48,* 4063–4073 4063
DOI:10.1021/bi802259a

Conantokin-Br from *Conus brettinghami* and Selectivity Determinants for the NR2D Subunit of the NMDA Receptor†

Vernon D. Twede,*,‡ Russell W. Teichert,‡ Craig S. Walker,‡ Paweł Gruszczyński,§,∥ Rajmund Kaźmierkiewicz,§ Grzegorz Bulaj,⊥ and Baldomero M. Olivera‡

‡*Department of Biology, University of Utah, Salt Lake City, Utah 84112,* §*Intercollegiate Faculty of Biotechnology of University of Gdańsk and Medical University of Gdańsk, 80-822 Gdańsk, Poland,* ∥*Faculty of Chemistry, University of Gdańsk, 80-952 Gdańsk, Poland, and* ⊥*Department of Medicinal Chemistry, University of Utah, Salt Lake City, Utah 84108*

Received December 11, 2008. Revised Manuscript Received March 18, 2009

ABSTRACT: Conantokins are venom peptides from marine cone snails that are NMDA receptor antagonists. Here, we report the characterization of a 24 AA conantokin from *Conus brettinghami* Coomans, H. E., Moolenbeek, R. G., and Wils, E. (1982) *Basteria 46* (1/4), 3−67, conantokin-Br (con-Br), the first conantokin that does not have the conserved glutamate residue at position 2. Molecular modeling studies suggest that con-Br has a helical structure between residues 2−13. In contrast to other characterized conantokins, con-Br has a high potency for NMDA receptors with NR2D subunits. To identify determinants for NR2D potency, we synthesized chimeras of con-Br and conantokin-R (con-R); the latter has a ∼30-fold lower potency for the NR2D subtype. The characterization of two reciprocal chimeras (con-Br/R and con-R/Br), comprising the first 9−10 N-terminal AAs of each conantokin followed by the corresponding C-terminal AAs of the other conantokin demonstrates that determinants for NR2D selectivity are at the N-terminal region. Additional analogues comprising 1−3 amino acid substitutions from each peptide into the homologous region of the other led to the identification of a key determinant; a Tyr residue in position 5 increases potency for NR2D, while Val at this locus causes a decrease. The systematic definition of key determinants in the conantokin peptides for NMDA receptor subtype selectivity is an essential component in the development of conantokin peptides that are highly selective for each specific NMDA receptor subtype.

The glutamate receptor superfamily comprises a large number of different genes, each encoding a subunit that assembles to form the functional receptor complex, believed to be composed of four primary subunits (*2*). Glutamate receptors are traditionally divided into three classes, α-amino-3-hydroxy-5-methyl-4-isoxazole propionic acid (AMPA[1]) receptors, NMDA receptors, and kainate receptors, on the basis initially of pharmacological criteria (*3*−*5*). Each class has separate, but overlapping physiological roles and corresponding links to various pathologies in the nervous system. Dysfunction among all three classes has been implicated in epilepsy (*6*), Parkinson's disease and Alzheimer's disease (*7*) as well as excitotoxic neuronal death (*8*). Additionally, NMDA receptors are thought to be involved in chronic pain (*9*) and mechanisms of drug and alcohol addiction (*10*, *11*).

NMDA receptors have many properties that distinguish them from other members of the glutamate receptor superfamily (i.e., voltage-dependent Mg^{2+} inhibition, permeability to Ca^{2+}, and the requirement of the coagonists glycine or D-serine), and multiple NMDA receptor subunit genes contribute to their functional diversity (*12*). The NR1 subunit, which binds glycine, has eight splice variants, and is ubiquitously expressed in the central nervous system (*5*). Four separate genes (NR2A-NR2D) encode different isoforms of the NR2 subunit, which binds glutamate; expression of different NR2 genes varies according to both regional and temporal expression patterns in the brain (*12*). In addition, two NR3 genes have been identified (NR3A-NR3B), which also vary in their regional and temporal expression patterns (*13*). The assembly of a functional tetrameric complex is thought to require the presence of two obligatory NR1 subunits and a combination of modulatory NR2 or NR3 subunits; studies examining receptor subunit assembly indicate that NR1 subunits form heterodimers with NR2 or NR3 subunits at the initial stage in assembly (*14*).

†This work was supported by GM48677 from the National Institute of General Medical Science (to B.M.O.). V.D.T. was funded by a student fellowship from the Neuroscience Training Grant NIH NIDCD 5T32 DC008553. R.K. acknowledges support from the fund DS/B50A-4-162-8.

*To whom correspondence should be addressed. Tel: 801-581-8370. Fax: 801-585-5010. E-mail: vernon.twede@utah.edu.

[1]Abbreviations: NMDA, *N*-methyl-D-aspartate; AMPA, α-amino-3-hydroxy-5-methyl-4-isoxazole propionic acid; con, conantokin; Gla, γ, γ-carboxyglutamate; ACN, acetonitrile; HPLC, high performance liquid chromatography; MD, molecular dynamics; rms, root-mean-square; rmsd, root-mean-square deviation; DSSP, define secondary structure of protein; PDB, protein data bank.

Published on Web 3/23/2009

Although much remains to be elucidated, pharmacological evidence suggests that different NMDA receptor subunit combinations may play different roles in the physiology and corresponding pathology of the central nervous system. For instance, NMDA receptor antagonists that selectively inhibit receptors containing the NR2B subunit have been implicated in the treatment of epilepsy and chronic pain, whereas more broadly selective NMDA receptor antagonists generally result in toxicity or intolerable side effects in the same assays (*15*). Conversely, more broadly targeted NMDA receptor antagonists were effective at preventing axonal demyelination in models of ischemia, whereas NR2B-specific antagonists had no effect on myelin degradation, suggesting that the antagonism of non-NR2B subtypes mediates this protective effect (*16*).

Interestingly, evidence suggests the effects of NR2B-selective antagonists show correspondence to temporal and regional expression patterns in the brain. For instance, NR2B expression is enriched in hippocampal and temporal regions in adult rats (*17*), corresponding to areas of the brain affected in many types of epilepsy, and suggesting a possible mechanism of action. It remains to be determined whether antagonists targeted to other NR2 subunits, such as NR2D, which is enriched in midbrain regions (*12*), affect the physiology and pathophysiology associated with these brain regions.

In order to understand the function of each individual receptor subtype in the intact nervous system, the standard approach that has been employed is gene knockout technology. As is the case for all ion channel complexes with multiple subunits, glutamate receptor gene knockouts need to be complemented with pharmacological agents that are as highly subtype selective as possible. It is particularly desirable to find ligands that bind at subunit interface sites that permit the ligand to interact with determinants on two different subunits. There is a fundamental difficulty with using knockout technology exclusively to assess ion channel function for those families in which a wide variety of different receptor subunits can be assembled as heteromeric complexes *in vivo*. Ablating the function of a gene that encodes a single type of subunit can result in a very complex phenotype, in which multiple functional complexes with different subunit compositions and physiological roles are affected. The phenotype of NMDA receptor NR1 subunit gene knockout mice, for instance, is not straightforward: concomitant expression of the NR2B subunit is markedly reduced, and neonates do not survive long after birth (*18*).

One often-effective approach to obtaining subtype selective pharmacological agents to complement gene knockout technology is to start with the pharmacologically active components of animal venoms. Unfortunately, there have not been a large number of venom components characterized to date that target glutamate receptors. The polyamine toxins found in spider venoms are one such class (*19*). A promising general source that needs to be explored further are the venoms of cone snails; these have proven to be very rich in families of peptides targeted to ion channels. There are two *Conus* peptide families that target glutamate receptors identified so far, the conantokins, that act as NMDA receptor antagonists (*15*, *20*−*22*), and the recently identified con-ikot-ikots, which are targeted to AMPA receptors (Walker, C. et al., submitted for publication). All members of the conantokin family target NMDA receptors but with differing subtype selectivity; conversely, the con-ikot-ikots appear to exclusively target AMPA receptors, although many properties of this peptide family remain to be investigated (*23*−*25*).

For both of these families, the number of *Conus* species that have been identified with venom components targeted to glutamate receptors has been surprisingly small. Among the conantokins, peptides from only six species have been characterized (*20*, *24*−*28*), and within the con-ikot-ikot family, a peptide from a single *Conus* species has been characterized.

We recently initiated an expanded effort to systematically examine new *Conus* species (*29*) for venom components that selectively target glutamate receptor subtypes. Previous work has used synthetic peptide analogues to identify some of the determinants of NR2A and NR2B subunit selectivity in conantokins (*30*) (reviewed in ref *31*). To expand upon this approach, we have begun to search for sequence variations among native conantokins that govern target specificity.

In this article, we describe a new peptide, conantokin-Br, from *Conus brettinghami* (*1*) that has a number of properties that are novel, including higher relative potency for the NR2D subunit than has been previously reported for conantokin peptides. We also characterized chimeras between conantokin-Br and a conantokin with different subunit selectivity, conantokin-R. This provided an opportunity to assess the relative importance of primary sequence variations with respect to activity on different NMDA receptor subtypes. This study has led to a number of structure/function insights for developing ligands with divergent selectivity for different NMDA receptor subtypes based on the conantokin family of conopeptides.

MATERIALS AND METHODS

Isolation of the Conantokin-Br Clone. An oligo (DHOG 450 5′-GCCCGTGCCTAGGATTA-3′) was designed to the signal sequence of known conantokins, conantokin-R and conantokin-G. This oligo was used to probe a cDNA library constructed from the venom duct of *C. brettinghami* using Southern hybridization as previously described (*32*). The identified clone was sequenced using Sequenase version 2.0.

Peptide Synthesis and Cleavage. Native peptides and analogues were synthesized using Fmoc-protected amino acids in an ABI model 430A automated peptide synthesizer, courtesy of Dr. Bob Schackmann and Scott Endicott of the Peptide/DNA Core Facility at the University of Utah. Each peptide was cleaved from 25 to 50 mg resin using 1 mL of Reagent K (trifluoroacetic acid/H_2O/1,2-ethanedithiol/phenol/thioanisole, 82.5:5:2.5:5:5 by volume). Each peptide was agitated for a minimum of 1.5 h at room temperature, with an additional 0.5 h for each arginine residue in the individual amino acid sequence. The cleavage mixture was filtered and precipitated with cold methyl-*tert*-butyl ether (MTBE). The crude peptides were then collected by centrifugation at 5000*g* for 8 min and washed two times with cold MTBE. The washed peptide pellet was dissolved in 60% acetonitrile in

0.1% trifluoroacetic acid and purified using a Vydac C_{18} semipreparative HPLC column (10 × 250 mm, 5 μm particle size). Each peptide was eluted from the column using a linear gradient of 10% buffer B (90% ACN, 0.1% TFA) to 50% buffer B in 40 min, at 4 mL/min.

Oxidative Peptide Folding. Conantokins containing two C-terminal cysteines (con-R and con-R variants) were oxidized using either Clear-Ox resin (Peptides International, Inc.), as described previously (*33*), or 1:1 oxidized/reduced glutathione. To prepare Clear-Ox resin for the oxidation reaction, 20 mg of the resin was activated in dichloromethane for 30 min and washed two times each with 1 mL of dimethyl formamide, 1 mL of methanol, and 1 mL of acetonitrile H_2O (1:1) solution. For the Clear-Ox reaction, 200 nmol of peptide per reaction was oxidized for 2 h in a solution containing 20 mg of the activated resin and 100 mM Tris HCl. The reaction was then quenched by adding formic acid (8% final concentration), filtered under vacuum, and washed with 0.01% TFA in H_2O to remove the peptide from the resin. For the glutathione reaction, 200 nmol of peptide per reaction was oxidized using a mixture of the following reagents: 0.01% TFA in H_2O, 1 M tris HCl/100 mM EDTA, 10 mM oxidized/10 mM reduced glutathione, and nanopure H_2O (1:1:1:7; final peptide concentration: 20 μM). Glutathione reactions were carried out for 45−60 min and quenched with 8% formic acid. Folded peptides were purified on a Vydac C_{18} semipreparative HPLC column (10 × 250 mm, 5um particle size) and eluted using a gradient of 10% buffer B to 50% buffer B in 40 min, at 4 mL/min.

Heterologous Expression of NMDA Receptors in Xenopus Oocytes. The rat NMDA receptor clones used were NR2A, NR2B, NR2C, NR2D, and NR1−3b; GenBank numbers AF001423, U11419, U08259, U08260, and U08266, respectively. *In vivo*, the NR1−3 and NR1-b splice variants are expressed in the hippocampus and cerebral cortex of adult rats (*34*); the NR2 subunits vary in their regional and developmental expression (see ref *12*). All of the expression clones were driven by a T7 promoter and were used to make capped RNA (cRNA) for injection into the oocytes of *Xenopus laevis* frogs. cRNA was prepared *in vitro* using Ambion RNA transcription kits (Ambion, Inc.) according to the manufacturer's protocols. To express NMDA receptors, 2−5 ng of cRNA for each subunit was injected per oocyte. Oocytes were maintained at 18 °C in ND96 solution (96.0 mM NaCl, 2.0 mM KCl, 1.8 mM $CaCl_2$, 1 mM $MgCl_2$, and 5 mM HEPES at pH 7.2−7.5) containing antibiotics (septra, amikacin, and pen/strep). All voltage-clamp electrophysiology was done using oocytes 1−6 days postinjection.

Two-Electrode Voltage Clamp Electrophysiology. All oocytes were voltage clamped at −70mV at room temperature. Oocytes were gravity perfused with Mg^{2+}-free ND96 buffer (96.0 mM NaCl, 2.0 mM KCl, 1.8 mM $CaCl_2$, and 5 mM HEPES at pH 7.2−7.5). Mg^{2+} was not included in the ND96 buffer because Mg^{2+} blocks NMDA receptors at the voltage potential used to clamp oocytes (−70 mV). To reduce nonspecific absorption of peptide, bovine serum albumin (BSA) was added to ND96 buffer at a final concentration of 0.1 mg/mL. To elicit current from oocytes expressing NMDA receptors, one-second pulses of gravity-perfused agonist solution were administered at intervals of 60 s, 90 s, or 120 s, depending on the rate of receptor recovery from desensitization. Agonist solution comprised glutamate and coagonist glycine suspended in Mg^{2+}-free ND96 buffer at final concentrations of 200 μM and 20 μM, respectively. Buffer was perfused continuously over the oocytes between agonist pulses, except during equilibration periods. During the equilibration period, buffer flow was halted for either 5 or 10 min to create a static bath for application of either peptide (suspended in ND96 buffer at various concentrations) or control solution (ND96 buffer alone). The length of equilibration period for each peptide was equal to or greater than the time necessary to achieve maximal current inhibition at a given concentration. The effect of a peptide on NMDA receptor-mediated current was determined by measuring the amplitude of the first agonist-elicited current pulse immediately following the equilibration period as a percentage of the amplitude of the baseline current (agonist-elicited current immediately preceding the equilibration period). Data acquisition was automated by a virtual instrument made by Doju Yoshikami of the University of Utah. Concentration−response curves were generated using Prism software (GraphPad Software, Inc.), using the following equation, where nH is the Hill coefficient, and IC_{50} is the concentration of peptide causing half-maximal block: % response = $100/\{1 + ([\text{peptide}]/IC_{50})^{nH}\}$.

Molecular Modeling. Conantokin-T (con-T) and con-G sequences were aligned to con-Br and its chimera con-R/Br using the CLUSTALW (*35*) web-based program (Table S1, Supporting Information). Since the alignments with con-T had a higher percentage identity score, the con-T coordinates (PDB code-name: 1ONT) were used for homology modeling. Modeling of con-R and con-Br/R chimera was precluded due to a lack of an appropriate conantokin model containing a disulfide bridge. γ-Carboxyglutamate residues were replaced with glutamic acid residues using the PyMOL (*36*) program. PSIPRED (*37*), a protein secondary structure prediction program, was employed to verify the homology modeling results. To further expand the structural analysis of the modeled conantokins, we submitted the resulting coordinates to molecular dynamics (MD) simulation with the AMBER 8.0 (*38*) program and ff99SB AMBER force field. Conantokins were solvated with the explicit water model TIP3P (*39*), with the box-size extended approximately 12 Å away from the solute atoms. To neutralize the charge of the system, a magnesium cation was added using the LEaP program from the AmberTools package. To monitor conformational changes for all amino acid residues, we used the DSSP method (*40*) from the Ptraj program. The energy minimization procedure involved 5000 steps of the steepest descent (*41*) (SD) method and 15000 steps of the conjugate gradient (*42*) (CG) method. To heat up the system, a 50 ps MD simulation was carried out. The initial temperature was 100 K, and the final was 298 K. Neither restraints nor constrains were applied during the heating step. Next, a 1.25 ns MD simulation with the 2.0 fs time step was performed. The temperature

was kept at 298 K with Berendsen coupling (*43*) and 10 Å cutoff applied. The SHAKE algorithm (*44*) was used on hydrogen atoms with a tolerance of 0.00005 Å.

RESULTS

Analysis of a Clone Encoding a Conantokin from C. brettinghami. A specimen of *Conus brettinghami* collected by trawlers from around Manila Bay, Philippines was used to construct a cDNA library. *Conus brettinghami* is conventionally regarded as a form or subspecies of *Conus sulcatus*: in this view, *Conus sulcatus* is regarded as a variable species distributed broadly in the IndoPacific region from Japan to the Bay of Bengal in South India, and east to Fiji. *Conus sulcatus* is a somewhat confusing taxon. However, the Manila Bay populations are not typical *Conus sulcatus* but rather the form known by most taxonomists as *Conus sulcatus brettinghami*, which has a narrower and smoother shell than the typical form (see Figure 1). Although the standard treatise on cone snail taxonomy (*45*) regards *Conus sulcatus brettinghami* as merely a form of *Conus sulcatus*, more recent data suggests that it is a different species from typical *Conus sulcatus* (Olivera, B., and Bouchet, P., manuscript in preparation). The conantokin peptide described below was characterized from a cDNA clone from *C. brettinghami*; no independent assessment of cDNAs from typical *Conus sulcatus* has been carried out to date. Although there is no molecular phylogenetic data on this species complex available at the present time, we regard *C. brettinghami* as a distinct species from *C. sulcatus*.

A cDNA clone encoding a peptide precursor highly homologous to previously identified sequences in the conantokin gene superfamily was identified, as described under Materials and Methods. The amino acid sequence predicted from the encoded open reading frame of the clone (Figure 2) is compared to the sequences of three previously characterized conantokin precursors. The high degree of homology is consistent with the gene belonging to the conantokin superfamily.

As a member of the conantokin superfamily, most glutamate residues in the mature toxin region are predicted to be post-translationally modified to γ-carboxyglutamate. The glutamate residue at position 12, however, was predicted not to be post-translationally modified based on the pattern of γ-carboxylation of previously characterized conantokins purified from venom (i.e., a Gla every 3−4 residues in the N-terminal-to-middle of the mature peptide). It has been shown for con-G in NMR studies that this pattern results in the alignment of Gla residues on one face of the peptide in a linear fashion to form a calcium binding motif allowing for stabilization of the α helix conformation (*46*). Analysis of the conantokin-T sequence purified from venom suggests that Glu residues in positions that do not adhere to this pattern are not modified to Gla; for instance, the

FIGURE 1: Forms of *Conus sulcatus* and *Conus brettinghami*, the species that produces conantokin-Br. The shells on the extreme left and right are *Conus sulcatus*; the two middle shells are generally called *Conus sulcatus brettinghami*; two varieties are shown. As is discussed in the text, we regard *Conus brettinghami* as a distinct species, not as a subspecies or form of *C. sulcatus*. The shell on the extreme left is a variant of the typical form. Venom ducts of several specimens of *Conus sulcatus brettinghami* from Manila Bay were pooled; this was the source of the cDNA clone that yielded the conantokin sequence. The specimens resembled the shell that is second from left.

Propeptide region

```
Con-Br   MQLYTYLYLLVPLVTFHLILGTGTLDHGGALTERRSTDATALKPEPVL-QKSAARSTDDNGKDRLTQMKRILKKRGKNAR
Con-R    MQLYTYLYLLVSLVTFYLILGTGTLGHGGALTERRSTDATALKPEPVLLQKSSARSTDDNGNDRLTQMKRILKKRGNKAR
Con-P    MQLYTYLYLLVPLVTFHLILSTGTLAHGGTLTERRSTDTTALKPEPVLLQKSDARSTDDNDKDRLTQMKRILKKRGNKAR
Con-G    MHLYTYLYLLVPLVTFHLILGTGTLDDGGALTERRSADATALKAEPVLLQKSAARSTDDNGKDRLTQMKRILKQRGNKAR
```

Mature toxin region

```
Con-Br  GDγγYSKFIγRERγAGRLDLSKFP
Con-R   GEγγVAKMAAγLARγNIAKGCKVNCYP
Con-P   GEγγHSKYQγCLRγIRVNKVQQγC
Con-G   GEγγLQγNQγLIRγKSN
```

FIGURE 2: Con-Br peptide precursor and predicted mature toxin sequences, compared to previously characterized conantokin precursors. In the mature toxin region, Glu residues either known or predicted to be post-translationally modified to Gla are indicated by γ.

Glu at position 16 (1 AA from the nearest Gla) is not post-translationally modified in the native sequence (*20*). The predicted sequence of con-Br was chemically synthesized as described under Materials and Methods.

The mature toxin sequences of the venom-purified conantokins con-G and con-R are shown in Figure 2 and Table 1 for comparison. Unlike any other conantokin characterized thus far, the sequence of the *C. brettinghami* clone predicts an aspartate at sequence position 2 rather than the canonical (nonpost-translationally modified) glutamate; the conserved glutamate at this position was found to be critical for NMDA receptor activity in other conantokins (*47*, *48*).

Functional Characterization of Conantokin-Br. The amino acid sequence of con-Br is clearly homologous with other members of the conantokin family, which are NMDA receptor antagonists. To assess its effects on NMDA receptors, we used two-electrode voltage-clamp electrophysiology to measure current traces from *Xenopus* oocytes heterologously expressing various combinations of NR1−3b and NR2 subunits. Con-Br was applied to oocytes and allowed to equilibrate for 10 min. The effect of the peptide was determined by measuring the agonist-elicited current in the absence (as a control) and presence of the peptide.

Con-Br (1 μM) blocked most of the current in the NR1−3b/NR2B subtype (Figure 3A), confirming its activity as an NMDA receptor antagonist. Strikingly, a similar level of current inhibition was observed at the same concentration for the NR1−3b/NR2D subtype (Figure 3B), suggesting con-Br is the most potent conantokin active on NR2D-containing NMDA receptors of any characterized thus far.

Concentration−response curves for each of the NR2 subunits (A−D) separately coexpressed with the NR1−3b subunit were determined (see Table 2 and Figure 4A); con-Br had the greatest inhibitory effect on the NR2B subunit, and the order of potency for con-Br was NR2B > NR2D > NR2A > NR2C.

Localization of Determinants for Subtype Selectivity. Previous studies have demonstrated that, for NMDA receptors containing NR2A and NR2B subunits, the structural determinants of subtype selectivity in conantokin-G and conantokin-T can be localized to discrete amino acid residues within the peptides (*30*, *49*). To determine whether the unique subtype selectivity profile of con-Br can be attributed to key localized amino acid residues, we synthesized chimeric analogues of con-Br, which weakly discriminates between NR2B and NR2D, and conantokin-R (con-R), which discriminates strongly against NR2D in favor of NR2B (*28*). Two chimeric analogues were synthesized with the N-terminal end of one peptide attached to the C-terminal end of the other peptide with a crossover point at the third Gla residue (Gla 10 in con-Br and Gla 11 in con-R). Thus, con-Br/R had the N-terminal residues of con-Br and the C-terminal residues of con-R and con-R/Br, the N-terminal amino acids of con-R, and the C-terminal amino acids of con-Br. The analogues were tested for subtype selectivity on NR1−3b/NR2B and NR1−3b/NR2D receptors expressed in *Xenopus* oocytes (Figure 4 and Table 2). Parent peptides were used as controls. Because previously published results for the con-R activity on NR2D were obtained using different methods (*28*), a concentration−response curve for con-R was generated to obtain an IC_{50} value for the NR1−3b/NR2D subtype using the present protocol (see Table 2).

The concentration−response curves for the chimeric and parent peptides are shown in Figure 4. As expected, con-R discriminated heavily against the NR2D subunit in favor of NR2B (Figure 4B), whereas con-Br did not (Figure 4A). Con-R/Br showed selectivity that favors NR2B, in a fashion similar to that of con-R (Figure 4D). Con-Br/R discriminated much more weakly between the NR2B and NR2D, more closely resembling the selectivity of con-Br (Figure 4C). Interestingly, both analogues were far less potent on both receptor subtypes than the parent peptides (Table 2). The IC_{50} ratios for NR2D/NR2B of con-Br and con-Br/R are approximately equal (∼2−3), while the corresponding ratios of con-R and con-R/Br are also similar (> 30). These results suggest that one or more N-terminal residues in con-Br are responsible for the lack of discrimination between NR2B and NR2D.

Localization of Key Amino Acid Residues Important for Subtype Selectivity. To further localize key N-terminal amino acid determinants for subtype selectivity, we synthesized six con-R and con-Br variants, in which groups of 1−4 amino acids at differing N-terminal sequence positions of one peptide were replaced with the amino acids from the corresponding regions of the other peptide (see Table 3). The subtype selectivity of these analogues with respect to NR1−3b/NR2B and NR1−3b/NR2D was assessed. Variants in which the middle amino

Table 1: Comparison of Predicted Mature Con-Br Sequence with Other Conantokins[a]

conus species	conantokin	amino-acid sequence	ref
C. brettinghami	con-Br	G**D** $\gamma\gamma$ YS K FI γ RER γ AGRLDLSKFP^	this work
C. purpurascens	con-P	GE $\gamma\gamma$ HS K YQ γ CLR γ IRVNKVQQγC (^)	*24*
C. parius	con-Pr1	GE Dγ YA γ GIR γ YQL I HGKI^	*25*
C. parius	con-Pr2	DE Oγ YA γ AIR γ YQL K YGKI^	*25*
C. parius	con-Pr3	GE Oγ VA K WA γ GLR γ KASSN*	*25*
C. radiatus	con-R	GE $\gamma\gamma$ VA K MAA γ LAR γ NIAKGCKVNCYP^	*28*
C. lynceus	con-L	GE $\gamma\gamma$ VA K MAA γ LAR γ DAVN*	*26*
C. tulipa	con-T	GE $\gamma\gamma$ YQ K ML γ NLR γ AEVKKNA*	*20*
C. geographus	con-G	GE $\gamma\gamma$ LQ γ NQ γ LIR γ KSN*	*27*

[a] ^ = COOH; * = $CONH_2$.

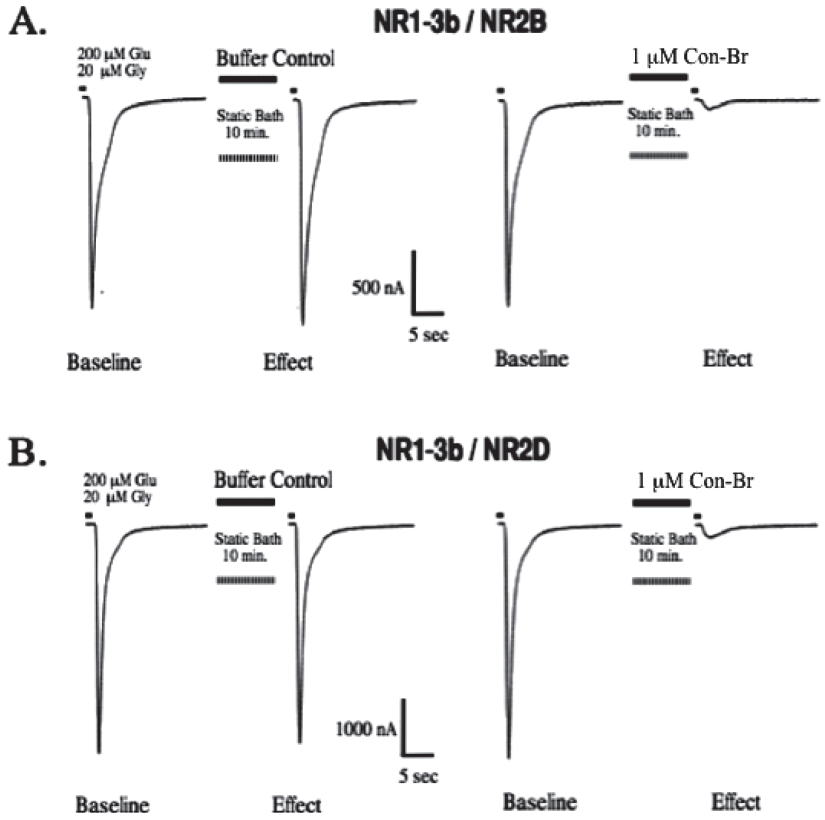

FIGURE 3: NMDA receptor current traces in the presence and absence of con-Br. (A) Left: NR2B current elicited by agonist pulse before and after buffer control. Right: baseline NR2B response followed by current elicited following a 10 min application of 1 μM con-Br. (B) Effects of buffer control (left) and 1 μM con-Br (right) on NR2D.

Table 2: Approximate IC_{50} Values of Con-Br, Con-R, and Analogues

peptide	NR2A IC_{50} (μM)	NR2B IC_{50} (μM)	NR2C IC_{50} (μM)	NR2D IC_{50} (μM)	NR2D/ NR2B IC_{50} ratio
con-Br	0.68	0.14	4.9	0.31	2.2
con-R	0.53	0.35	~10	> 10	> 30
Br/R		2		5.5	2.75
R/Br		3.7		> 100[a]	> 30[a]
Br [R 5−6]		5.2		> 100	> 20
R [Br 5−6]		0.40		3.1	7.8
Br [Y5V]		3.3		> 100	> 30
R [V5Y]		0.35		3.4	9.7

[a] Predicted values are based on curve fit (see Materials and Methods).

acids were replaced (R [Br 7−9] and Br [R 7−10]) were rendered inactive or greatly diminished in potency (Figure 5A−B). Substituting the amino acids from positions 5−6 of con-Br into the corresponding regions of con-R resulted in a peptide with activity similar to that of con-R with respect to NR2B but a 3-fold increase in potency for NR2D (Figure 5C and Table 2). In the context of con-Br, replacing residues at positions 5−6 with those in con-R led to a decrease in activity on both receptor subtypes but with a 10-fold relative increase in selectivity toward NR2B (Figure 5D and Table 2). These data suggest that one or both residues at positions 5−6 of both peptides are important for determining selectivity among these receptor subtypes.

Two recently characterized conantokins from *C. parius* (con-Pr1 and con-Pr2) with relatively high affinities for NR2D have a tyrosine at sequence position 5 (*25*), sharing conserved sequence homology with con-Br (see Table 1). We therefore examined the role of the con-R and con-Br amino acids at position 5 with respect to NR2B-NR2D subtype selectivity. In the context of con-R, replacing the valine at position 5 with tyrosine resulted in a peptide with an NR2B potency equal to that of con-R and a 3-fold increase in potency for NR2D, indicating that the amino

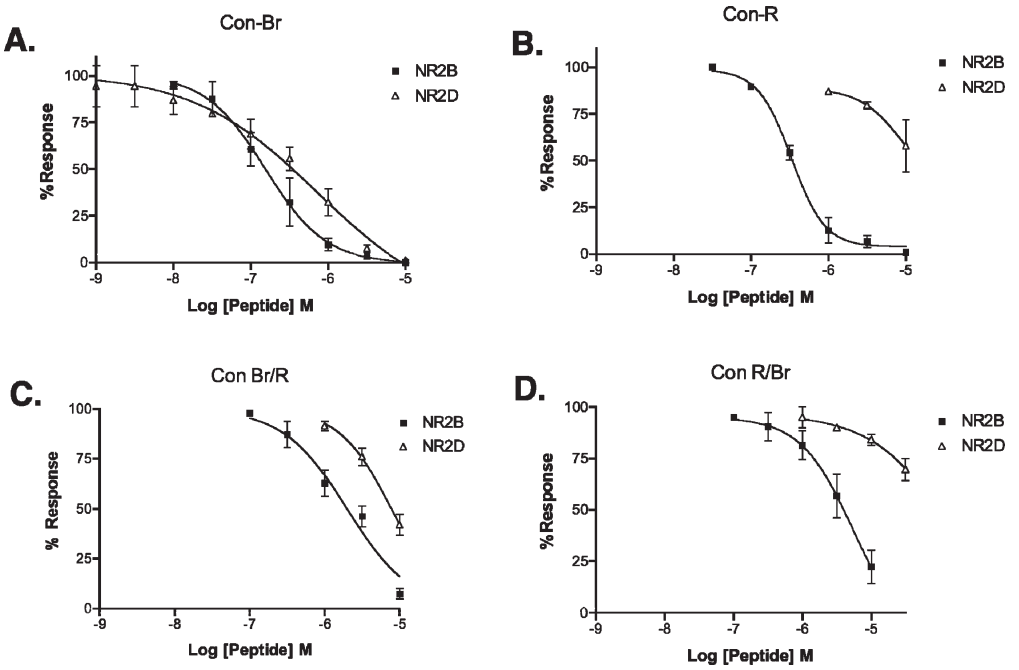

FIGURE 4: NR2B and NR2D discrimination of con-Br, con-R, and chimeras. (A) Concentration−response curves for con-Br on NR1−3b/NR2B and NR1−3b/NR2D, showing weak discrimination between the two subtypes. (B) Con-R concentration−response curves for NR2B and NR2D, showing high selectivity toward NR2B. (C) Br/R concentration−response curves for NR2B and NR2D. (D) R/Br concentration−response curves for NR2B and NR2D. R/Br and Br/R sequences are shown in Table 3.

Table 3: Amino Acid Sequences of Con-Br and Con-R Variants[a]

peptide name	amino-acid sequence
con-Br	GD $\gamma\gamma$ YS K FI γ RER γ AGRLDLSKFP
con-R	GE $\gamma\gamma$ VA K MAA γ LAR γ NIAKGCKVNCYP
Br/R	**GD $\gamma\gamma$ YS K FI** γ LAR γ NIAKGCKVNCYP
R/Br	**GE $\gamma\gamma$ VA K MAA** γ RER γ AGRLDLSKFP
con-Br [R7−10]	GD $\gamma\gamma$ YS K **MAA** γ RER γ AGRLDLSKFP
con-R [Br7−9]	GE $\gamma\gamma$ VA K **FI** γ LAR γ NIAKGCKVNCYP
con-Br [R5−6]	GD $\gamma\gamma$ **VA** K FI γ RER γ AGRLDLSKFP
con-R [Br5−6]	GE $\gamma\gamma$ **YS** K MAA γ LAR γ NIAKGCKVNCYP
con-Br [Y5V]	GD $\gamma\gamma$ **VS** K FI γ RER γ AGRLDLSKFP
con-R [V5Y]	GE $\gamma\gamma$ **YA** K MAA γ LAR γ NIAKGCKVNCYP

[a] Amino acid substitutions are shown in bold.

acid at position 5 is a significant determinant of the subtype selectivity seen in R [Br5−6] (Figure 6E and Table 2). Replacing the tyrosine in con-Br with a valine resulted in a 20-fold decrease in potency for NR2B (Figure 6F and Table 2). Despite this marked decrease in potency, however, this single amino acid substitution dramatically shifted the selectivity of con-Br toward NR2B, resulting in a NR2D/NR2B IC_{50} ratio similar to that seen in con-R (see Table 2). The shifts in selectivity profiles of the two position 5 variants suggest that the amino acid at this position is a key determinant of NR2B-NR2D selectivity.

Molecular Modeling. A characteristic feature of conantokins is their helical conformation stabilized by interactions of Gla residues with divalent cations (*31*, *46*, *50*). Modeling of two linear conantokins, con-Br and the con-R/Br chimera, was performed using the NMR model of con-T, as described in the Materials and Methods section. Con-Br and the chimera exhibited a substantial amount of helical conformation (Figure S1, Supporting Information) that was further confirmed using the secondary structure prediction program, PSIPRED (*37*, *51*) (Figure S2, Supporting Information). To better characterize conformational properties of con-Br and con-R/Br, the initial model structures containing Mg^{2+} cations (used as counterions to neutralize the charge and solvated by the explicit water model) were submitted to molecular dynamics analysis. The MD results are summarized in Figure 6 and Tables S2 and S3 (Supporting Information).

Figure 6 shows the superimposition of five averaged structures of con-Br and con-R/Br generated from 1.25 ns MD run with 250 ps frequency. The results of the MD simulations confirmed that the helical structure between residues 2−13 is dominant for both conantokins. The helical structure is particularly pronounced in con-Br between residues 2 and 12 and for the con-R/Br chimera between residues 2−13 with three additional residues (17−19) forming a short helical fragment. From the superimposition, we are able to observe that the conformation of the con-R/Br chimera is somewhat less stable in an aqueous environment than con-Br. However, the structure of con-Br is very stable during the MD simulation. In both cases, the helical motif is present between residues 2−13. To measure the stability of the conformations, we calculated the rms value during MD simulations for both conantokins as well as for the selected helical region between residues 2−13 (Figure 6C). It is notable

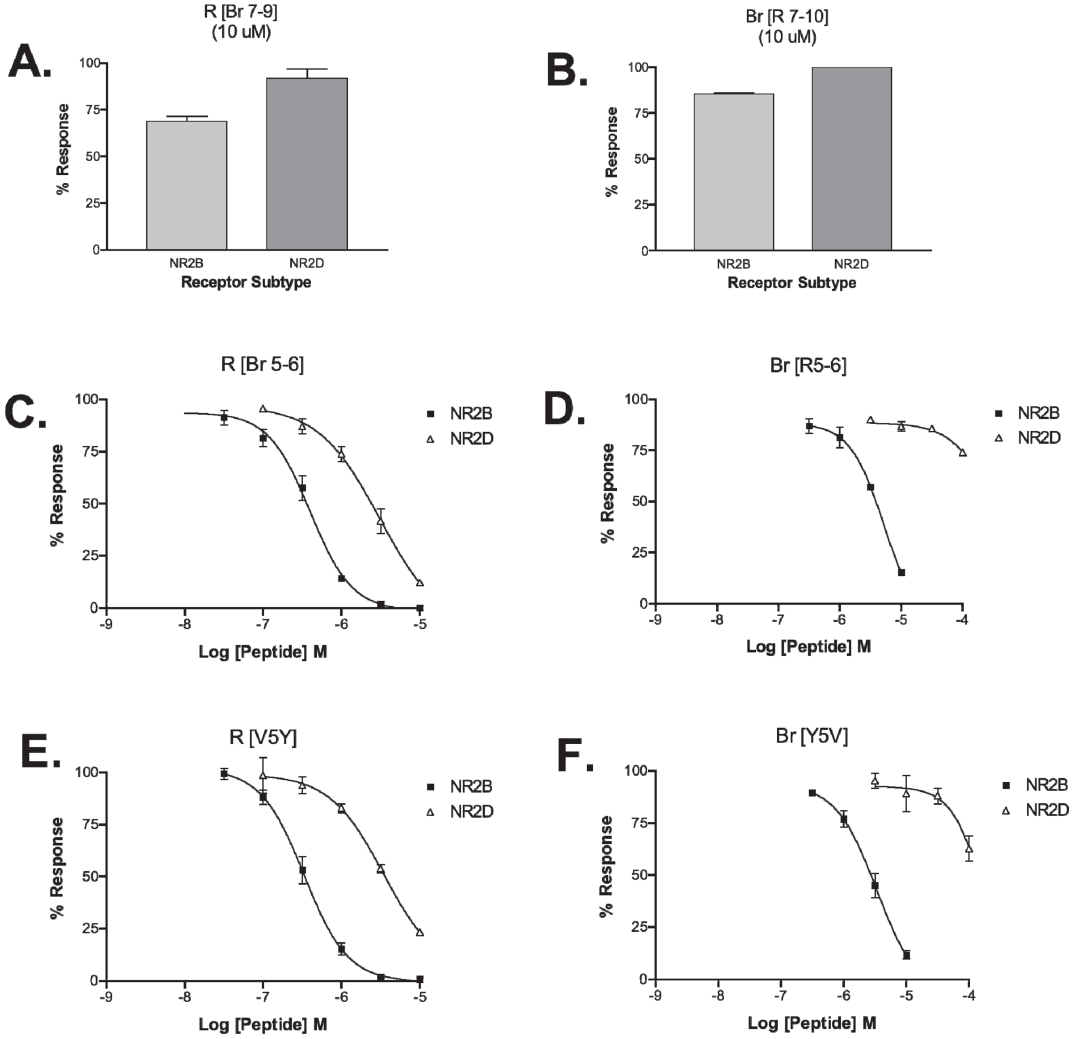

FIGURE 5: Relative inhibitory potencies of con-Br and con-R variants on NR1−3b/NR2B and NR1−3b/NR2D. Con-R [Br 7−9] and con-Br [R 7−10] have greatly reduced potency on NR2B and NR2D (A,B). Con-R [Br 5−6] and con-R [V5Y] retain their potency on NR2B and discriminate less strongly against NR2D (C,E). Con-Br [R 5−6] and con-Br [Y5V] have reduced potency on both subtypes and discriminate strongly against NR2D (D,F). Sequences of con-Br and con-R variants are shown in Table 3.

that the calculated values of the rmsd are lower for the calculation of the helical region, suggesting that the helices stabilize the structure of the peptides.

DISCUSSION

In this work, we characterized con-Br, a conantokin peptide from a species not previously analyzed, *Conus brettinghami*. A comparison of the sequence of con-Br to known conantokins is shown in Table 1. One functional difference between conantokin-Br and previously characterized conantokins is the relatively high potency for NMDA receptors that have an NR2D subunit. All conantokins characterized so far have a preference for NR2B; presumably the relevant target in the fish prey of these piscivorous species is an NMDA receptor complex with a subunit similar to that of the mammalian NR2B subtypes. However, the relative affinities for other NMDA receptor subtypes vary, and conantokin-Br is noteworthy in the relatively high potency for NR2D containing NMDA receptor complexes. In contrast, con-R has low potency (> 10um) for the NR2D subtype.

We used the differential affinities of conantokin-Br and conantokin-R for the NR2D subunit to evaluate chimeras and analogues of conantokin-Br and conantokin-R for activity on NMDA receptors containing the NR2B and NR2D subunits. When chimeras were made of conantokin-Br and conantokin-R, both of the resulting chimeras had a significantly lowered potency for both NMDA receptor subtypes, compared to the native parent peptides. However, even at the lower affinities, the ratio between

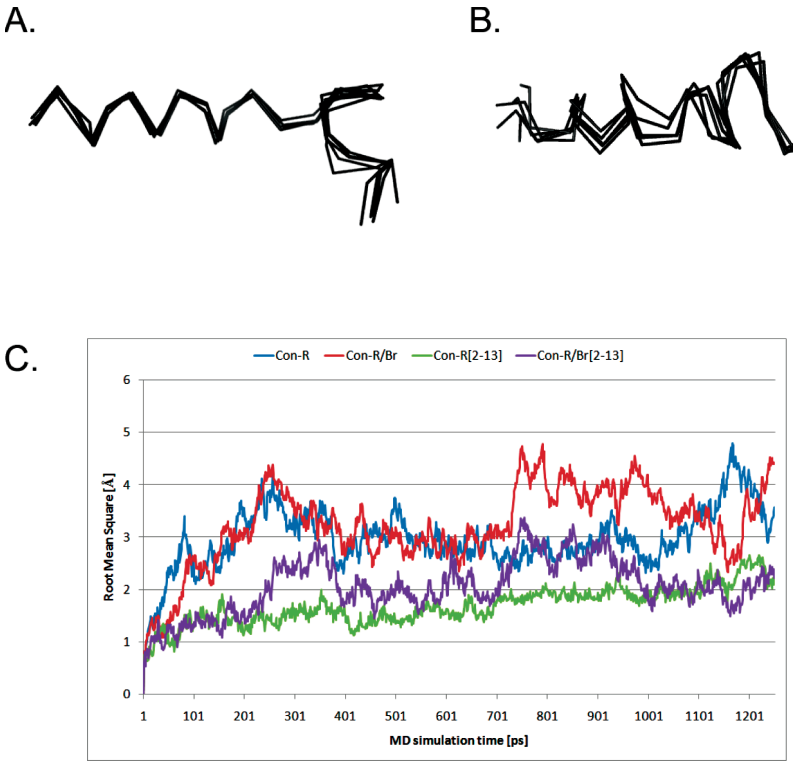

FIGURE 6: Molecular modeling of con-Br and con-R/Br. Ribbon representation of con-Br (A) and con-R/Br chimera (B). Superimposion of five averaged structures generated with a frequency of 250 ps from a 1.25 ns MD simulation run. (C) rms deviation for conantokins con-Br and the con-R/Br chimera calculated during the MD simulation for each residue (all atoms were included). rms deviation was also calculated for the chosen helical region, which included residues 2−13 for both peptides.

NR2B and NR2D differed between the chimeras; only the chimera with the N-terminal half of con-Br showed a comparable potency for NR2D and NR2B, while the chimera with the N-terminal half of con-R showed a ~30-fold lower potency for NR2D compared to that of NR2B. These results suggest that despite the fall in potency for both receptor subtypes, there were determinants for differential binding to NR2D in the N-terminal region. A residue switch at position 5 between con-Br and con-R was particularly revealing. In (V5Y) con-R, the potency of the peptide for the NR2B subtype was not significantly perturbed, but a higher potency for NR2D subtype was observed. This result suggests that the presence of tyrosine in con-Br contributes to its higher potency for the NR2D subtype, although there may be other determinants that further improve the potency for this subtype that remain to be identified. To this end, we also synthesized a chimeric peptide to test the role of Asp at position 2 in con-Br, the other likely determinant of selectivity; however, the data suggest that this is not a significant determinant of NR2D selectivity (not shown). The reciprocal analogue, (Y5V) con-Br had very poor relative potency for NR2D, thus confirming that position 5 is an important determinant of NR2D selectivity; however, this single residue substitution also lowered the potency for NR2B approximately 20-fold, suggesting that it had lower binding energy for shared sites in both the NR2B and NR2D subtypes. Interestingly, the amino acid at position 5 has been shown to be essential for activity in conantokin-T (*48*) and is a key determinant of NR2A-NR2B selectivity in conantokin-G (*49*). Furthermore, all native conantokins that have a tyrosine at position 5 have a relatively higher potency for NR2D (see ref *25*). Thus, the residue at this position may be partially predictive of the subunit selectivity of a given conantokin.

From the data included in this work, it cannot be directly ruled out that the C-terminal disulfide loop in con-R analogues may confer properties that govern peptide activity and subunit selectivity. Several lines of evidence suggest this possibility is highly unlikely, however. First, earlier structure function studies of con-R using circular dichroism analysis and [^{3}H]MK-801 binding displacement assays suggest that structure and NMDA receptor activity are virtually unchanged in C-terminal truncation variants comprising the first 17 amino acids of con-R, which exclude the C-terminal disulfide bond (*47*, *52*). Second, unpublished data from our recent characterization of con-P, which contains an unusually long disulfide loop, (*24*) shows similar activity and subunit selectivity in both reduced alkylated and oxidized forms, indicating that the disulfide bond plays little or no role in the NMDA antagonist activity of the peptide. Finally, extensive structure−activity studies of con-G and con-T, in addition to con-R (reviewed in ref *31*), and the data in this work,

suggest that structural properties important for peptide activity are conferred by the N-terminal amino acids of the peptide.

From the discovery of the first conantokins and the presence of γ-carboxyglutamate residues in these peptides, combined with the similarity in the spacing of the Gla residues to the Gla domains of mammalian blood-clotting factors, it was immediately hypothesized that these peptides assumed a helical structure stabilized by Gla residues chelated to Ca^{2+} or other divalent cations. This has been strongly supported by a variety of NMR studies (*31*, *46*, *50*, *53*). Molecular modeling and MD studies on con-Br and con-R/Br confirmed substantial amount of the α-helical conformation in the N-terminal parts of the peptides. The data obtained here also suggest that the conantokin framework of Gla residues should not be regarded as a rigid helical scaffold from which side chains are displayed that can interact with partner residues on their specific NMDA receptor targets. Such a model works reasonably well for the (V5Y) con-R analogue: the substitution of Tyr for Val clearly increases the potency of conantokin-R for the NR2D subunit, without a large effect on the potency for the NR2B subunit. However, in most other chimeras or substitutions, the significant decrease in potency observed for the different NMDA subunits tested indicate that the potency of conantokins for particular NMDA receptors is a more subtle function of the entire structure; the nonreciprocal nature of the complementary substitutions at position 5 of con-R and con-Br in terms of NR2B potency emphasize this general perception.

Although differences in selectivity uncovered so far are modest, the lack of subtype selective NMDA receptor ligands makes the development and further exploration of the conantokin family highly desirable. The conantokins are widespread across *Conus*, and clearly, the concerted discovery strategy used for other families of *Conus* peptides (*29*, *54*) gives grounds for optimism that a broader survey of the conantokin gene family across the entire phylogenetic range of cone snails may yield novel conantokin peptides and their derivatives that will prove useful for identifying additional determinants of subtype selectivity. The first step in being able to efficiently scan a library of natural sequences for potentially novel-targeting specificity is to have information regarding which residues may be selectivity determinants; the work that we have described in this article is a significant step in this important direction.

It is highly desirable to continue developing NR2D specific ligands. The NR2D subunit confers a number of physiologically distinct properties to NMDA receptor complexes, including low sensitivity to Mg^{2+} block, resistance to H^+ block, and prolonged deactivation kinetics (reviewed in ref *12*), which may make neurons expressing this subunit particularly vulnerable to excitotoxicity. In addition, expression of the NR2D subunit is more regionally restricted within the brain than NR2A or NR2B subunits, with expression primarily localized to the diencephalons and midbrain (*34*), and an enrichment of expression in the substantia nigra and striatum (*55*, *56*). Thus, the development of an NR2D-specific ligand may help to evaluate the role of this NMDA receptor subtype in a number of pathological conditions affecting these regions, such as Parkinson's disease.

ACKNOWLEDGMENT

We thank Tiffany Han and Aleksandra Walewska for their assistance with some of the bioassays and oxidation reactions.

SUPPORTING INFORMATION AVAILABLE

Summary of homology modeling experiments and homology models and secondary structure prediction results. This material is available free of charge via the Internet at http://pubs.acs.org.

REFERENCES

1. Coomans, H. E., Moolenbeek, R. G., and Wils, E. (1982) Alphabetical revision of the (sub)species in recent Conidae 5. *baccatus to byssinus*, including *Conus brettinghami nomen novum*. *Basteria 46* (1/4), 3–67.
2. Simeone, T. A., Sanchez, R. M., and Rho, J. M. (2004) Molecular biology and ontogeny of glutamate receptors in the mammalian central nervous system, *J. Child Neurol. 19*, 343−360; discussion 361.
3. Dingledine, R., Borges, K., Bowie, D., and Traynelis, S. F. (1999) The glutamate receptor ion channels. *Pharmacol. Rev. 51*, 7–61.
4. Hille, B. (2001) *Ion Channels of Excitable Membranes*, 3rd ed., Sinauer Associates, Inc., Sunderland, MA.
5. Hollmann, M., and Heinemann, S. (1994) Cloned glutamate receptors. *Annu. Rev. Neurosci. 17*, 31–108.
6. Meldrum, B. S. (1994) The role of glutamate in epilepsy and other CNS disorders. *Neurology 44*, S14–23.
7. Ulas, J., Weihmuller, F. B., Brunner, L. C., Joyce, J. N., Marshall, J. F., and Cotman, C. W. (1994) Selective increase of NMDA-sensitive glutamate binding in the striatum of Parkinson's disease, Alzheimer's disease, and mixed Parkinson's disease/Alzheimer's disease patients: an autoradiographic study. *J. Neurosci. 14*, 6317–6324.
8. Ozawa, S., Kamiya, H., and Tsuzuki, K. (1998) Glutamate receptors in the mammalian central nervous system. *Prog. Neurobiol. 54*, 581–618.
9. Childers, W. E.Jr., and Baudy, R. B. (2007) N-methyl-D-aspartate antagonists and neuropathic pain: the search for relief. *J. Med. Chem. 50*, 2557–2562.
10. Bisaga, A., Popik, P., Bespalov, A. Y., and Danysz, W. (2000) Therapeutic potential of NMDA receptor antagonists in the treatment of alcohol and substance use disorders. *Expert Opin. Invest. Drugs 9*, 2233–2248.
11. Bisaga, A., and Popik, P. (2000) In search of a new pharmacological treatment for drug and alcohol addiction: N-methyl-D-aspartate (NMDA) antagonists. *Drug Alcohol Depend. 59*, 1–15.
12. Cull-Candy, S., Brickley, S., and Farrant, M. (2001) NMDA receptor subunits: diversity, development and disease. *Curr. Opin. Neurobiol. 11*, 327–335.
13. Cavara, N. A., and Hollmann, M. (2008) Shuffling the deck anew: how NR3 tweaks NMDA receptor function. *Mol. Neurobiol 38* 16–26.
14. Schuler, T., Mesic, I., Madry, C., Bartholomaus, I., and Laube, B. (2008) Formation of NR1/NR2 and NR1/NR3 heterodimers constitutes the initial step in N-methyl-D-aspartate receptor assembly. *J. Biol. Chem. 283*, 37–46.
15. Layer, R. T., Wagstaff, J. D., and White, H. S. (2004) Conantokins: peptide antagonists of NMDA receptors. *Curr. Med. Chem. 11*, 3073–3084.
16. Micu, I., Jiang, Q., Coderre, E., Ridsdale, A., Zhang, L., Woulfe, J., Yin, X., Trapp, B. D., McRory, J. E., Rehak, R., Zamponi, G. W., Wang, W., and Stys, P. K. (2006) NMDA receptors mediate calcium accumulation in myelin during chemical ischaemia. *Nature (London) 439*, 988–992.
17. Monyer, H., Burnashev, N., Laurie, D. J., Sakmann, B., and Seeburg, P. H. (1994) Developmental and regional expression in the rat brain and functional properties of four NMDA receptors. *Neuron 12*, 529–540.
18. Forrest, D., Yuzaki, M., Soares, H. D., Ng, L., Luk, D. C., Sheng, M., Stewart, C. L., Morgan, J. I., Connor, J. A., and Curran, T. (1994) Targeted disruption of NMDA receptor 1 gene abolishes NMDA response and results in neonatal death. *Neuron 13*, 325–338.
19. Estrada, G., Villegas, E., and Corzo, G. (2007) Spider venoms: a rich source of acylpolyamines and peptides as new leads for CNS drugs. *Nat. Prod. Rep. 24*, 145–161.

20. Haack, J. A., Rivier, J., Parks, T. N., Mena, E. E., Cruz, L. J., and Olivera, B. M. (1990) Conantokin T: a γ-carboxyglutamate-containing peptide with N-methyl-D-aspartate antagonist activity. *J. Biol. Chem. 265*, 6025–6029.
21. Hammerland, L. G., Olivera, B. M., and Yoshikami, D. (1992) Conantokin-G selectively inhibits NMDA-induced currents in *Xenopus* oocytes injected with mouse brain mRNA. *Eur. J. Pharmacol. 226*, 239–244.
22. Mena, E. E., Gullak, M. F., Pagnozzi, M. J., Richter, K. E., Rivier, J., Cruz, L. J., and Oivera, B. M. (1990) Conantokin-G: a novel peptide antagonist to the N-methyl-D-aspartate acid (NMDA) receptor. *Neurosci. Lett. 118*, 241–244.
23. Donevan, S. D., and McCabe, R. T. (2000) Conantokin-G is an NR2B-selective competitive antagonist of N-methyl-D-aspartate receptors. *Mol. Pharmacol. 58*, 614–623.
24. Gowd, K. H., Twede, V., Watkins, M., Krishnan, K. S., Teichert, R. W., Bulaj, G., and Olivera, B. M. (2008) Conantokin-P, an unusual conantokin with a long disulfide loop. *Toxicon 52*, 203–213.
25. Teichert, R. W., Jimenez, E. C., Twede, V., Watkins, M., Hollmann, M., Bulaj, G., and Olivera, B. M. (2007) Novel conantokins from Conus parius venom are specific antagonists of N-methyl-D-aspartate receptors. *J. Biol. Chem. 282*, 36905–36913.
26. Jimenez, E. C., Donevan, S. D., Walker, C., Zhou, L.-M., Nielsen, J., Cruz, L. J., Armstrong, H., White, H. S., and Olivera, B. M. (2002) Conantokin-L, a new NMDA receptor antagonist: determinants for anticonvulsant potency. *Epilepsy Res. 51*, 73–80.
27. McIntosh, J. M., Olivera, B. M., Cruz, L. J., and Gray, W. R. (1984) γ-Carboxyglutamate in a neuroactive toxin. *J. Biol. Chem. 259*, 14343–14346.
28. White, H. S., McCabe, R. T., Armstrong, H., Donevan, S., Cruz, L. J., Abogadie, F. C., Torres, J., Rivier, J. E., Paarman, I., Hollmann, M., and Olivera, B. M. (2000) *In vitro* and *in vivo* characterization of conantokin-R, a selective NMDA antagonist isolated from the venom of the fish-hunting snail *Conus radiatus*. *J. Pharmacol. Exp. Ther. 292*, 425–432.
29. Olivera, B. M., and Teichert, R. W. (2007) Diversity of the neurotoxic Conus peptides: a model for concerted pharmacological discovery. *Mol. Interventions 7*, 251–260.
30. Sheng, Z., Dai, Q., Prorok, M., and Castellino, F. J. (2007) Subtype-selective antagonism of N-methyl-D-aspartate receptor ion channels by synthetic conantokin peptides. *Neuropharmacology 53*, 145–156.
31. Prorok, M., Warder, S. E., Blandl, T., and Castellino, F. J. (1996) Calcium binding properties of synthetic gamma-carboxyglutamic acid-containing marine cone snail "sleeper" peptides, conantokin-G and conantokin-T. *Biochemistry 35*, 16528–16534.
32. Woodward, S. R., Cruz, L. J., Olivera, B. M., and Hillyard, D. R. (1990) Constant and hypervariable regions in conotoxin propeptides. *EMBO J. 1*, 1015–1020.
33. Green, B. R., and Bulaj, G. (2006) Oxidative folding of conotoxins in immobilized systems. *Protein Pept. Lett. 13*, 67–70.
34. Laurie, D. J., Bartke, I., Schoepfer, R., Naujoks, K., and Seeburg, P. H. (1997) Regional, developmental and interspecies expression of the four NMDAR2 subunits, examined using monoclonal antibodies. *Brain Res. Mol. Brain Res. 51*, 23–32.
35. Thompson, J. D., Higgins, D. G., and Gibson, T. J. (1994) CLUSTAL W: improving the sensitivity of progressive multiple sequence alignment through sequence weighting, position-specific gap penalties and weight matrix choice. *Nucleic Acids Res. 22*, 4673–4680.
36. DeLano, W. L. (2002) *The PyMOL Molecular Graphics System*, DeLano Scientific, Palo Alto, CA.
37. Jones, D. T. (1999) Protein secondary structure prediction based on position-specific scoring matrices. *J. Mol. Biol. 292*, 195–202.
38. Case, D. A., Cheatham, T. E.3rd, Darden, T., Gohlke, H., Luo, R., Merz, K. M.Jr., Onufriev, A., Simmerling, C., Wang, B., and Woods, R. J. (2005) The Amber biomolecular simulation programs. *J. Comput. Chem. 26*, 1668–1688.
39. Jorgensen, W. L., Chandrasekhar, J., Madura, J., Impey, R. W., and Klein, M. L. (1983) Comparison of simple potential functions for simulating liquid water. *J. Chem. Phys. 79*, 10.
40. Kabsch, W., and Sander, C. (1983) Dictionary of protein secondary structure: pattern recognition of hydrogen-bonded and geometrical features. *Biopolymers 22*, 61.
41. Arfken, G. (1985) The Method of Steepest Descents, in *Mathematical Methods for Physicists*, 3rd ed., pp 428−443, Academic Press, Orlando, FL.
42. Fletcher, R., and M., R. C. (1964) Function minimization by conjugate gradients. *Comput. J. 7*, 6.
43. Berendsen, H. J. C., Postma, J. P. M., Vangunsteren, W. F., Dinola, A., and J.R., , H. (1984) Molecular-dynamics with coupling to an external bath. *J. Chem. Phys. 81*, 7.
44. Ryckaert, J.-P., Ciccotti, G., and Berendsen, H. J. C. (1977) Numerical integration of the cartesian equations of motion of a system with constraints: molecular dynamics of n-alkanes. *J. Comput. Phys. 23*, 15.
45. Röckel, D., Korn, W., and Kohn, A. J. (1995) *Manual of the Living Conidae*, Vol. *I*, Indo-Pacific Region, Verlag Christa Hemmen, Wiesbaden, Germany.
46. Rigby, A. C., Baleja, J. D., Li, L., Pedersen, L. G., Furie, B. C., and Furie, B. (1997) Role of gamma-carboxyglutamic acid in the calcium-induced structural transition of conantokin G, a conotoxin from the marine snail Conus geographus. *Biochemistry 36*, 15677–15684.
47. Blandl, T., Zajicek, J., Prorok, M., and Castellino, F. J. (2001) Sequence requirements for the N-methyl-D-aspartate receptor antagonist activity of conantokin-R. *J. Biol. Chem. 276*, 7391–7396.
48. Warder, S. E., Blandl, T., Klein, R. C., Castellino, F. J., and Prorok, M. (2001) Amino acid determinants for NMDA receptor inhibition by conantokin-T. *J. Neurochem. 77*, 812–822.
49. Klein, R. C., Prorok, M., Galdzicki, Z., and Castellino, F. J. (2001) The amino acid residue at sequence position 5 in the conantokin peptides partially governs subunit-selective antagonism of recombinant N-methyl-D-aspartate receptors. *J. Biol. Chem. 276*, 26860–26867.
50. Chen, Z., Blandl, T., Prorok, M., Warder, S. E., Li, L., Zhu, Y., Pedersen, L. G., Ni, F., and Castellino, F. J. (1998) Conformational changes in conantokin-G induced upon binding of calcium and magnesium as revealed by NMR structural analysis. *J. Biol. Chem. 273*, 16248–16258.
51. McGuffin, L. J., Bryson, K., and Jones, D. T. (2000) The PSIPRED protein structure prediction server. *Bioinformatics 16*, 2.
52. Blandl, T., Warder, S. E., Prorok, M., and Castellino, F. J. (2000) Structure-function relationships ofthe NMDA receptor antagonist peptide, conantokin-R. *FEBS Lett. 470*, 139–146.
53. Skjaebaek, N., Nielsen, K. J., Lewis, R. J., Alewood, P., and Craik, D. J. (1997) Determination of the solution structures of conantokin-G and conantokin-T by CD and NMR spectroscopy. *J. Biol. Chem. 272*, 2291–2299.
54. Olivera, B. M., Quik, M., Vincler, M., and McIntosh, J. M. (2008) Subtype-selective conopeptides targeted to nicotinic receptors: Concerted discovery and biomedical applications, *Channels (Austin) 2*.
55. Counihan, T. J., Landwehrmeyer, G. B., Standaert, D. G., Kosinski, C. M., Scherzer, C. R., Daggett, L. P., Velicelebi, G., Young, A. B., and Penney, J. B.Jr. (1998) Expression of N-methyl-D-aspartate receptor subunit mRNA in the human brain: mesencephalic dopaminergic neurons. *J. Comp. Neurol. 390*, 91–101.
56. Kuppenbender, K. D., Standaert, D. G., Feuerstein, T. J., Penney, J. B.Jr., Young, A. B., and Landwehrmeyer, G. B. (2000) Expression of NMDA receptor subunit mRNAs in neurochemically identified projection and interneurons in the human striatum. *J. Comp. Neurol. 419*, 407–421.

CHAPTER 3

CONANTOKIN-R AND CONANTOKIN*RL*-B DISCRIMINATE BETWEEN THE NR2B AND NR2D SUBUNITS THROUGH COMMON REGIONS IN THE S1 AND S2 SUBDOMAINS OF NR2B

Abstract

Conantokins are peptide antagonists of NMDA receptors derived from the venom of marine cone snails. Conantokins exhibit subtype selectivity depending on the NR2 subunit composition present in the NMDA receptor complex. Here, we describe experiments to identify the regions of the NR2D and NR2B subunits important for the differential sensitivity to two NR2B-preferring conantokins: Conantokin-R (Con-R) and Conantokin*Rl*-B (Con*Rl*-B). To this end, we designed chimeras of the NR2B and NR2D subunits, heterologously expressed chimeric receptor complexes in *Xenopus* oocytes, and assessed the sensitivities to Con-R and Con*Rl*-B using two-electrode voltage clamp electrophysiology. Our results show that both the S1 and S2 glutamate-binding subdomains are important for sensitivity to Con-R and Con*Rl*-B, with the C-terminal regions of S1 and S2 from NR2B yielding the greatest increases in sensitivity upon homologous substitution into NR2D. Evaluation of point mutants shows that two amino acids in NR2B, Tyr 507 and Val 510, import the sensitivity of the S1 domain to Con-R when substituted for the corresponding residues (Asp 531 and Ile 534) in NR2D. These amino acid substitutions, however, had no effect on sensitivity to Con*Rl*-B or ifenprodil. The results in this work suggest that each conantokin interacts with a distinct set of amino acids on the NR2 subunits to determine selectivity.

Abbreviations are as follows: HPLC, High-Performance Liquid Chromatography; Con, Conantokin; NMDA, N-methyl-D-aspartate; NMDAR, N-methyl-D-aspartate receptor; NR1, N-methyl-D-aspartate receptor subunit 1; NR2, N-methyl-D-aspartate receptor subunit 2, NR3, N-methyl-D-aspartate receptor subunit 3, NTD, N-terminal domain of NR subunits; S1 and S2, extracellular glutamate-binding subdomains 1 and 2, respectively, of NR subunits; TM, transmembrane domain of NR subunits; CTD, C-terminal domain of NR subunits; P, Pore-lining region of NR subunits; Gla, γ-carboxyglutamate

Introduction

N-methyl-D-aspartate receptors (NMDARs) are members of the glutamate receptor superfamily of ion channels that have critical function in learning and memory (Morris, 2013), as well as an array of neuropathic conditions, such as stroke, epilepsy, and chronic pain (Meldrum, 1994; Childers et al., 2007; Gonda, 2012). A large diversity of genes encoding NMDA receptor subunits have been identified, with one NR1 gene (with eight splice variants), four NR2 genes, and two NR3 genes (Cavara et al., 2008; Hollman and Heinemann, 1994; Matsuda et al., 2002; Simeone et al., 2004). In the nervous system, NMDARs are tetrameric, comprising two NR1 subunits and a combination of NR2 or NR3 subunits (Schuler et al., 2008; Simeone et al, 2004). The given set of NMDA receptor subunit genes can potentially generate a tremendous diversity of receptor subtypes.

As of yet, a set of pharmacological tools capable of targeting individual NMDA receptor subtypes with a high degree of specificity has not been assembled. Ifenprodil and derivatives define one class of noncompetitive NMDA receptor antagonist that exhibits high specificity for NMDA receptors containing the NR2B subunit (Chenard and Menniti, 1999; Fischer et al., 1997; Mosley et al., 2009). Additionally, some small molecules have been developed that are capable of targeting NR2C- and NR2D- containing subtypes with some degree of specificity over those containing NR2A or NR2B (Costa et al., 2009; Feng et al., 2004; Mosley et al., 2010).

Conantokins are a unique group of peptidic NMDA receptor antagonists derived from the venom of marine cone snails (genus *Conus*). Conantokins are generally selective towards NMDA receptors containing the NR2B subunit, but vary in their selectivity towards NMDA receptors containing other NR2 subunits (Donevan and McCabe, 2000; Sheng et al., 2007; Twede et al., 2009a; Twede et al., 2009b). A number of studies have shown a competitive interaction at the glutamate-binding site on the NR2 subunits (Donevan and McCabe, 2000; Hammerland et al., 1992; Wittekindt et al., 2001). Conantokin*G* (Con*G*) was found to exhibit a preference for NR2B- over NR2A- containing NMDA receptors by interacting with amino acid residues in the

S2 subdomain, near the glutamate binding pocket (Sheng et al., 2009). Whether other conantokins interact with NR2 subunits in a similar manner, and whether similar regions are important for the differences in selectivity between subunits (e.g., NR2B vs. NR2D or NR2C) is not known.

Conantokin-R (Con-R), is a previously characterized conantokin that is highly potent on NR2B-containing NMDA receptors and little affinity for NMDA receptors containing the NR2D subunit (Twede et al., 2009; White et al., 2000). More recently, Conantokin*Rl*-B (Con*Rl*-B) was shown to have a high degree of NR2B specificity (Gowd et al., 2012). Here, we describe experiments that identify determinants of sensitivity of NR2B-containing NMDA receptors to Con-R and Con*Rl*-B. Unlike Con*G*, Con-R and Con*Rl*-B interact with both the S1 and S2 subdomains to discriminate between NR2B and NR2D. The results described herein comprise necessary steps towards the rational design of selective antagonists capable of distinguishing among the various NR2 NMDA receptor subtypes.

Materials and methods

Construction of chimeras. Clones of cDNA encoding rat NR1-b NR2B, and NR2D were obtained from Dr. Michael Hollman (Ruhr University, Bochum, Germany). Chimeric NR2B and NR2D subunits were made using standard molecular biology methods. Figure 3.1 shows the approximate regions of substitution for NR2B into NR2D. Chimera 2 comprised a substitution from the N-terminal extracellular domain in NR2D (AAs 1-567) for that of NR2B (AAs 1-543). Chimera 4 comprised a substitution of the "S2" subdomain (the extracellular transmembrane domain 2-3 linker) from NR2D (AAs 684-823) for the "S2" subdomain of NR2B (AAs 660-799). Chimera 5 included both of the substitutions in Chimera 2 and Chimera 4. Chimera 3 involved substitutions at the "S1" subdomain (412-567 NR2D for 390-543 NR2B). All other chimeric constructs involved amino acid substitutions within these regions (see Table 3.1). All point mutants were constructed by site-directed mutagenesis, using a site-directed mutagenesis kit,

according to the manufacturer's protocols (Stratagene, Inc.). All mutant constructs were subcloned into a sp72 vector (Promega, Inc.) for subsequent in vitro transcription, and heterologous expression in *Xenopus* oocytes.

Heterologous expression of NMDA receptors in Xenopus oocytes. Rat NMDA receptor clones NR2B, NR2D, and NR1-2b were used (GenBank entries U11419, U08260, and U08264,), in addition to subunit chimeras using the NR2B and NR2D clones as templates. NR2B, NR2D, and subunit chimeras were co-expressed with the NR1-2b subunit. All expression clones and mutant variants were under control of a T7 promoter. For each clone, Ambion transcription kits (Ambion, Inc.) were used to make capped RNA for injection into Xenopus oocytes. To express NMDA receptors, 2-5 ng of RNA encoding each subunit was injected into each oocyte. Oocytes were incubated in ND96 solution [96 mM NaCl, 2 mM KCl, 1.8 mM $CaCl_2$, 1 mM $MgCl_2$, and 5 mM HEPES (pH 7.2-7.5) with antibiotics (Gentamicin and Pen/Strep). All voltage-clamp electrophysiology was performed prior to 7 days following injection.

Electrophysiology. All oocytes were voltage clamped at -70 mV. Experiments were performed at room temperature, and oocytes were gravity-perfused with Mg^{2+} free ND96 buffer [96.0 mM NaCl, 2.0 mM KCl, 1.8 mM $CaCl_2$, and 5 mM HEPES (pH 7.2-7.5)]. BSA (0.1 mg/mL) was added to reduce nonspecific absorption of peptides. Previous work has shown similar responses of NMDA receptors expressed in oocytes to conantokins in the presence of ND96 containing either calcium or substituted with barium (Gowd et al., 2012).

The sensitivity to glutamate was assessed for all native and chimera NMDA receptor subunit combinations tested. To determine the response to glutamate, oocytes were administered a 20 μL bolus of glutamate combined with saturating (20 μM) glycine perfused in Mg^{2+} -free ND96 buffer. Glutamate was administered in increasing concentrations until saturating concentration, or the concentration at which there was no further increase in current response was determined. All glutamate responses were normalized to the maximum current response

(saturating current) for each oocyte. EC_{50} values were determined using the following equation: response = $100/[1+(EC_{50}/[\text{agonist}])^{nH}]$.

For experiments assessing the block of heterologously expressed NMDA receptors by antagonists, NMDA receptor-mediated current was elicited by 1-second pulses of 200 μM glutamate and 20 μM glycine in Mg^{2+}-free ND96. Agonist concentrations elicited greater than 90% of maximal current in oocytes for all NMDA receptor subtypes tested. To measure the effect of antagonists on oocytes expressing NMDA receptors, the buffer flow was halted, and antagonists were applied for a minimum of 5 minutes, or sufficient time to reach equilibrium. Inhibition of NMDA receptor-mediated current was measured by normalizing the first response to agonist following application of antagonist to the baseline response to agonist. A virtual instrument was used for data acquisition (made by D. Yoshikami, University of Utah). Concentration response curves were calculated using Prism software (Graphpad Software, Inc.). The following equation was used to fit the concentration response curves: % response = $100/[1+([\text{peptide}]/IC_{50})^{nH}]$, where nH is the Hill coefficient, and IC_{50} is the concentration required to achieve half-maximal block.

Peptide synthesis. Con-R and Con*Rl*-B were synthesized using standard *N*-(9-fluorenyl) methoxycabonyl (Fmoc)-protected amino acids, in an ABI model 430A peptide synthesizer. Synthesis was performed by Dr. Scott Endicott of the DNA/Peptide Facility at the University of Utah. The peptide was cleaved from resin by treatment with 1 mL of a mixture of trifluoroacetic acid/H20/1,2-ethanedithiol/phenol/thioanisole (82.5/5/2.5/5/5 by volume). Peptide was agitated in the mixture for 2 hours at room temperature, and the mixture was filtered under vacuum into methyl-*tert*-butyl ether at -10 degrees C. Peptide was precipitated from the mixture and collected by centrifugation at 5000 x *g* for 5 minutes. The supernatant was removed, and the pellet was washed with methyl-*tert*-butyl ether and centrifuged twice more. The pellet was dissolved in 20% ACN in 0.1% trifluoroacetic acid. Purification was carried out by High-Performance Liquid

Chromatography (HPLC) using a Vydac C_{18} semipreparative column (10 x 250 mm, 5 mM particle size), using a flow rate of 5ml/minute and a gradient of solvent B. Con-R was oxidatively folded in a 1:1 mixture of reduced and oxidized glutathione (1mM each) in a solution of 100mM Tris and 0.1mM EDTA. The folded peptide was purified by HPLC using a Vydac C_{18} analytical column (at a flow rate of 1ml/minute) and a gradient of Solvent B.

Use of other agents for electrophysiology. Ifenprodil was obtained from Sigma (St Louis, MO). For use in electrophysiology assays, a stock solution of ifenprodil was made by dissolving in Dimethyl Sulfoxide (DMSO) at a concentration of 10 mM. Subsequent dilutions for electrophysiology assays were made in Mg^{2+}-free ND96 with BSA.

Results

Design of NR2 subunit chimeras. NR2 subunits of the NMDA receptor comprise structural and functional subdomains homologous to those of other genes in the ionotropic glutamate receptor family (Dani and Mayer, 1995). These domains include the extracellular N-terminal regulatory and glutamate binding subdomains (NTD and S1, respectively), three transmembrane (M1-M3) domains, a re-entrant pore loop (P), a second extracellular glutamate binding subdomain (S2) and an intracellular C-terminal domain (CTD) (See Figure 3.1). Studies indicate a competitive interaction of conantokins at the glutamate-binding site (S1 and S2 domains), including shifts in glutamate EC50 values with increasing conantokin concentrations, and point mutations in the glutamate binding pocket affecting glutamate binding (i.e., Donevan and McCabe, 2000; Wittekindt et al., 2001; but see Skolnick et al., 1992).

To determine which regions were most important for the high sensitivity of NR2B and corresponding low sensitivity of NR2D to Con-R and Con*Rl*-B, we examined the contribution of the extracellular domains (NTD, S1 and S2) of these subunits to the conantokin inhibition. To this end, we made substitutions in specific regions in the DNA encoding the extracellular domains of the NR2B and NR2D subunits. The resulting NMDA receptor subunit variants are

termed Chimeras 1-12, along with variants and point mutants. Domain topologies of Chimeras 2-9 are shown in Figure 3.1. We first designed a construct comprising the NTD of NR2D, and the remaining NR2 domains of NR2B. This construct (Chimera 1), however, did not express sufficient current to perform our assays when mRNA encoding the subunit was co-injected with NR1-b into *Xenopus* oocytes (<20 nA, not shown). We next made the converse construct, with the N-terminal domain of NR2B, and the remaining domains of NR2D (Chimera 2). This construct yielded much greater current levels upon expression in oocytes (ranging from 500 to 5000 nA) upon application of saturating concentrations of agonists (200 μM glutamate and 20 μM glycine), sufficient for use in further experiments. To differentiate between the contribution of the NTD and S1 to Con-R sensitivity, we then constructed a chimera containing the NTD of NR2D, S1 of NR2B, and the remaining domains of NR2D (Chimera 3). We also constructed an NR2D variant with a substitution of S2 from NR2B (Chimera 4). Chimeras 6-7 and 8-9 were NR2D variants with NR2B substitutions in subregions of Chimeras 4 and 3, respectively. Chimeras 10-12, along with all variants and point mutants were constructed as substitutions in subregions of Chimera 9, based on the results obtained with functional tests of Chimeras 1-9. Similar to Chimera 2, Chimeras 3-12 and all variants yielded sufficient current levels for subsequent experiments.

Localization of regions important for Con-R sensitivity. Con-R has a high potency on NR2B subtypes, and a low potency on NR2D subtypes (Twede et al., 2009; White et al., 2000). Other conantokins, such as Con*G*, while NR2B selective, typically target NR2D-containing NMDA receptor subtypes with much greater potency (Twede et al., 2009). We therefore used Con-R as a tool to discriminate between the two subunits and identify regions important for conantokin sensitivity. Figure 3.2A shows the contrast in selectivity profiles of Con-R for NR2B and NR2D, co-expressed with NR1-b in *Xenopus* oocytes. Con-R has an approximately 30-fold higher potency on the NR1-b/NR2B subtype than the NR1-b/NR2D subtype (Twede et al., 2009;

also see Table 3.1). As shown in Figure 3.2B and Table 3.1, the sensitivity of NR2D to Con-R was increased to a similar extent (~ 6 fold) by both substitutions in the N-terminal extracellular (Chimera 2) and S2 (Chimera 4) domains. The simplest interpretation of this result is that Con-R interacts with both the S1 and S2 domains of the NR2B subunit. The amino-terminal domain may also contribute to the observed increase in sensitivity, however. Comparison of Chimera 2 with Chimera 3, which differ only in the identity of residues in the NTD, show a relatively minor contribution: there was an approximately 2-fold difference between the IC_{50} values of Chimera 2 and Chimera 3 (0.81 and 1.7 μM, respectively). Thus, a subtle shift in sensitivity was observed upon substitution of the NTD. Lastly, the simultaneous substitution of the extracellular NTD, S1, and S2 subdomains (Chimera 5) resulted in a sensitivity to Con-R that was equal to that of the native NR2B subtype (Table 3.1; Fig. 3.2B), suggesting that these regions completely recapitulate the sensitivity of the native NR2B subtype to Con-R.

Given that the data suggest determinants of sensitivity reside in both S1 and S2, these subdomains were divided into substitutions in four subregions so as to construct Chimeras 6 -9, that contain more highly localized substitutions (See Figure 3.1). Interestingly, replacement of NR2D residues with NR2B residues in all four subregions enhanced the sensitivity to Con-R (Table 3.1, Figure 3.2C). However, replacements within the C-terminal half of S2 in Chimera 7 appeared to make a greater contribution to sensitivity than replacements within the N-terminal half of S2 in Chimera 6 (9-fold and 4-fold increases, respectively) (Table 3.1, Fig. 3.2C). More surprisingly, the sole substitution of the C-terminal half of NR2B S1 (Chimera 9) completely restored the sensitivity to Con-R seen in native NR2B (Table 3.1, Fig. 3.2C). Among the constructs, replacements of entire subdomains from NR2B (either NTD, S1 or S2) appeared to be additive, reconstituting the sensitivity of the native NR2B subunit when combined (as in Chimera 5); mutants with smaller substitutions (i.e., Chimeras 6-9), however, did not retain the additivity of the parent chimeras (see Table 3.1).

Localization of residues important for Con-R sensitivity. Although the data suggest determinants important for sensitivity to Con-R reside in both S1 and S2, the high contribution to sensitivity of the C-terminal half of the S1 subdomain led us to investigate this region further. To localize contributing residues, we further subdivided this region into three segments, and the resulting sensitivities are shown in Table 3.1 and Figure 3.3. Of the three substitutions in the C-terminal half of S1 (Chimeras 10-12), only one (Chimera 11; 7 divergent AAs) had an increase in sensitivity to Con-R, suggesting residues in this region were predicted to account for a degree of the sensitivity observed in Chimera 9 (Figure 3.3B). Interestingly, the Con-R IC_{50} value for Chimera 11 (1.9 μM) was more similar to that of Chimera 3 than to that of Chimera 9 (1.7 μM and 0.15 μM, respectively). Therefore, although Chimera 9 had an unusually high sensitivity to Con-R, these data suggest residues in this subregion reconstitute the partial sensitivity of the NR2B S1 subdomain, rather than the complete sensitivity of the NR2B subunit. To further verify the significance of this subregion in the overall contribution to Con-R sensitivity, we combined the seven divergent NR2B residues in Chimera 11 with the entire NR2B S2 subdomain. The resulting construct (Chimera 11 [S2]) had Con-R sensitivity similar to NR2B (0.18 μM, compared to 0.14 μM, respectively) (Figure 3.3C). Lastly, we examined the effects of further amino acid substitutions within the Chimera 11 region (Table 3.1). Of the substitutions made within these seven amino acids, the simultaneous replacement of two residues (D531Y and I534V) in Chimera 15 appeared to contribute most to Con-R sensitivity (Table 3.1, Figure 3.3C).

Response of NR2 chimeras to glutamate. Previous studies have shown that some substitutions in the S1 and S2 subdomains of NR2 subunits at or near the glutamate-binding locus can potentially affect sensitivity to glutamate-site agonists (Anson et al., 1998; Chen et al., 2004; Kinarsky et al., 2005; Maier et al., 2004). To determine whether replacement of residues in these regions alter the response to glutamate, and to verify the appropriate agonist concentrations for our assays, each NMDA receptor subunit variant was co-expressed with NR1-b in *Xenopus*

oocytes and the resulting assembled channels were assessed for sensitivity to glutamate using two-electrode voltage clamp electrophysiology. Figure 3.4A shows concentration-response curves of glutamate on the native NR2B and NR2D subunit combinations co-expressed with NR1-b. NR2D had a slightly lower glutamate EC_{50} value (3.7 μM) than NR2B (6.3 μM); however, in our assay, this difference was within the margin of error. Examples of glutamate concentration-response curves for chimeras are shown in Figure 3.4B. The EC_{50} for Chimera 2 (13.7 μM) was approximately 2-fold higher than the EC_{50} for NR2B (Table 3.1, Figure 3.4B). In addition, Chimera 15 (with an EC_{50} of 1.9 μM) was approximately 2-fold more responsive to glutamate than NR2D (Figure 3.4B). All other chimeras or point mutants had EC_{50} values within the margin of error of those for one or both of the native subtypes (Table 3.1).

Sensitivity of chimeras to other NR2B-selective antagonists. Data presented here demonstrate that residues imparting sensitivity to Con-R are distributed among several regions of the NR2 subunit, including S1 and S2. To test whether conantokins, as a class of NMDA receptor antagonists, generally interact with one or multiple regions we challenged each of the chimera receptors with Con*Rl*-B. Con*Rl*-B is a conantokin recently characterized from the species *Conus rolani* (Gowd et al., 2012) that has a high potency on NR2B subtypes, and shows little or no potency on NMDA receptor subtypes containing other NR2 subunits (also, see Figure 3.5A). Thus, similar to Con-R, Con*Rl*-B selectively inhibits NR2B over NR2D; however, the conantokin from *C. rolani* diverges considerably from Con-R in selectivity towards other NR2 subtypes, as well as in amino acid sequence (Gowd et al., 2012). To determine whether Con*Rl*-B interacts with NR2B in a manner similar to Con-R, Con*Rl*-B was assessed for sensitivity towards the group of NR2 chimeras that exhibited the highest sensitivity to Con-R when heterologously expressed in *Xenopus* oocytes,. As shown in Figure 3.5 and summarized in Table 3.2, in a similar manner to Con-R, chimeras with C-terminal NR2B substitutions in both subdomains of the glutamate binding domain (Chimeras 7 and 9, respectively) resulted in receptors with sensitivity

to Con*Rl*-B. However, the simultaneous substitution of the two amino acids in Chimera 15 (D531Y and I534V) that had the greatest effect on sensitivity to Con-R had no effect on sensitivity to Con*Rl*-B (Figure 3.5B and 3.5C). These data suggest the residues important for Con-R inbibition are not identical with those important for Con*Rl*-B. However, the increased sensitivity of Chimeras 7, 9, and 5 also indicate more than one region of the NR2 subunits contribute to Con*Rl*-B sensitivity, suggesting a manner of interaction similar to Con-R.

Ifenprodil, another NR2B selective antagonist, is thought to act noncompetitively with glutamate and glycine at the regulatory domain on the N-terminal extracellular domain of the NR2B subunit (Karakas et al., 2011; Tsai et al., 2005). To determine whether there is any interaction between the residue substitutions important for sensitivity to Con-R (positions 531 and 534) and ifenprodil, NR2D [D531Y I534V] was also tested for sensitivity towards 10 μM ifenprodil. As shown in Figure 3.5D, a Chimera 5, a variant containing the NTD of NR2B was blocked by 10 μM ifenprodil to a similar extent as NR2B, suggesting sensitivity to ifenprodil was unchanged. However, in a manner similar to NR2D, Chimera 15 showed little or no sensitivity to 10 μM ifenprodil (Fig. 3.5D), suggesting no interaction between ifenprodil and the S1 residues identified as important for inhibition by Con-R.

Discussion

Analysis of NR2 subunit chimeras. In this work we generated a series of NR2B and NR2D subunit chimeras to localize the regions important for sensitivity to Con-R and Con*Rl*-B. Chimeras were assessed for sensitivity by performing concentration-response assays on conantokins for each functional mutant we designed. We assessed sensitivity across a range of concentrations to provide a more complete depiction of conantokin-receptor interactions.

Chimera studies can potentially be designed so that the functional outcome for a given mutant (or set of mutants) falls into one of two categories: loss-of-function effects or gain-of-

function effects. In theory, loss-of-function mutations can be interpreted as perturbations of interaction sites or subunit structure that negatively affect ligand binding, the gating of the effect of ligand, or both. While these can be accurate interpretations, a potential caveat of perturbation effects is that they are not necessarily specific to the ligand or molecule of interest. Rather, the perturbations could indicate a more general loss of function (such as a null mutant in the most extreme case).

Gain-of-function mutations, on the other hand, are likely to indicate specific favorable interactions between the mutant subunit and the molecule of interest. The loss-of-function mutants (with respect to Con-R sensitivity) we designed in this study did not yield sufficient current for testing. However, we also chose to focus on gain of function mutants to highlight specific favorable interactions between conantokin peptides and the NR2 subunits. While we do not initially draw such a distinction in our data, increases in sensitivity may be attributed to more favorable interactions for binding, conformational changes favoring conantokin inhibition, or both.

We anticipated one of two potential outcomes for the gain-of-function mutant tests designed in this study: either a single localized region would be important for conantokin sensitivity, or determinants of sensitivity would be distributed across multiple regions in S1 and S2. Previous work demonstrated that determinants of Con*G* sensitivity in NR2B were localized to specific residues in the C-terminal region of S2 (Sheng et al., 2009). In our study, mutants with NR2B substitutions in both S1 and S2 had gain of function effects when compared to NR2D, indicating a plurality of potential regions of interaction for Con-R and Con*Rl*-B.

A number of larger substitutions had increases in sensitivity that could be combined to comprise the whole, additionally indicating that multiple regions are necessary for complete sensitivity. For instance, the NR2B-to-NR2D IC_{50} ratios of Chimeras 2, and 4 could be multiplied to comprise the sensitivity of Chimera 5. Furthermore, additivity was suggested by

comparison of Chimera 5 (containing all the substitutions of Chimeras 2-4) and native NR2B, which were similar in Con-R IC_{50} value.

Notably, some smaller substitutions did not retain the additive properties of the whole-domain NR2B substitutions. The sensitivity ratios of Chimeras 6 and 7 combine to a total that is greater than that of Chimera 4, for instance. While it is possible that this effect may be simply due to random perturbations in protein structure associated with the mutations, the data are suggestive of another interpretation: redundant sets of interactions may occur between conantokins and the NR2 subunits. To illustrate, if a particular set of interactions is removed by a mutation, another set may be strengthened or replaced upon removal of the prior set. In support of this interpretation, it is notable that, in addition to Chimeras 6 and 7, the Con-R sensitivity ratios Chimeras 8 and 9 can be multiplied to yield greater sensitivity ratios that those of the parent construct, Chimera 3. Thus, the redundancy effect is observed for multiple mutants. If this non-additive effect were simply due to changes in conformation as a consequence of random chance, increases in sensitivity (and corresponding super-additive properties) among all four mutants would be extremely unlikely. In contrast, random perturbation effects would predict mutants that were *less* than additive to the whole. In our mutants, nonadditivity was not seen upon substitution of the entire S1 and S2 regions, and was only evident in smaller substitutions, as the contacts for a given lobe are being disrupted. Thus, our data predict redundant interactions on the N- and C-terminal regions of both S1 and S2.

Does Con-R discriminate between subunits via multiple sites? Our data suggest determinants of conantokin sensitivity are distributed across multiple regions of the NR2 subunit. One potential interpretation of these data is that conantokins distinguish between NMDA receptor subtypes via multiple binding sites, suggesting interactions distal from the glutamate-binding site. Studies have confirmed a competitive interaction between conantokins (such as Con*G*) and the glutamate-binding site on the NR2 subunits (Donevan and McCabe 2000), while some work has suggested a possible interaction between conantokins and the polyamine-binding site on the N-

terminal domain (Skolnick et al., 1992). Other studies have shown that Con*G* has biphasic effects on NR2A subunits when coexpressed with certain NR1 splice variants (Ragnarsson et al., 2006), further suggesting the possibility of additional binding sites. Our data confirm the importance of the S1 and S2 glutamate binding subdomains in conantokin inhibition. Interestingly, Chimera 2 showed a 2-fold higher sensitivity to Con-R than Chimera 3, also suggesting a possibility for interactions distal to the glutamate-binding site. The majority of the (30- and 100- fold, respective) differences in sensitivity to Con-R and Con*Rl*-B, however, were attributed to substitutions in the S1 and S2 regions. Thus, our data localize the major determinants for sensitivity to Con-R and Con*Rl*-B as proximal to the glutamate-binding site.

Conantokin interactions at the glutamate-binding site. The work presented in this study identifies novel residues Tyr 507 and Ile 510 on the NR2B subunit (corresponding to NR2D residues Asp 531 and Val 534) as important for Conantokin-R sensitivity. Interestingly, previous work has localized residues in the glutamate binding pocket affecting con*G* sensitivity that are conserved across all four NR2 subunits (Wittekindt et al., 2001), while other work has shown that residues at positions affecting con*G* NR2A and NR2B discrimination are conserved among three (2B, 2C, and 2D) of the four NR2 subunits (Sheng et al., 2009). As all residues at positions previously identified as important for conantokin sensitivity are identical between the NR2B and NR2D subunits (Sheng et al., 2009; Wittekindt et al., 2001), the amino acids important for the differential sensitivity to Con-R were, by exclusion, predicted to be novel.

It is noteworthy that the conantokin-sensitive residues we identified had relatively small effects on response to glutamate upon substitution (~2-fold or less). Previous work has shown some residues important for conantokin sensitivity greatly affected glutamate binding, whereas others had no effect on response to glutamate (Sheng et al., 2009; Wittekindt et al., 2001). In particular, the amino acids conserved across all four NR2 subunits appeared to affect glutamate response (Wittekind et al., 2001), while divergent residues had lesser effects on glutamate sensitivity (Sheng et al., 2009). The effect of nonconserved NR2 residue substitutions on

differential conantokin sensitivity identified in this, and other studies, suggests that residues critical for conantokin activity may be at conserved sites, while the determinants of discrimination among the NR2 subunits may be at positions distinct from those involved in glutamate binding. Indeed, previous data have localized the glutamate-binding residues at sites distinct from NR2B positions 507 and 510 (Laube et al., 1997).

In parallel with studies of NMDA receptor subunits, structure-activity studies of characterized conantokins also indicate that conserved residues at certain positions are critical for activity, whereas other residues are more important for selectivity among the NR2 subunits. For instance, conserved N-terminal residues, including glutamate or aspartate at position 2, appear to be critical for conantokin activity (Blandl et al., 2001), while other amino acid positions, such as Val 5 in Con-R and Lys 8 in Con*Rl*-B, appear to be critical for selecting among the individual NR2 subunits (Twede et al., 2009; Gowd et al., 2012).

When combined, these findings seemingly argue for conserved points of interaction common to both conantokins and NR2 subunits. In particular, they argue for a "core" binding region overlapping the glutamate-binding site, resulting in the observed competitive effect of conantokins. Indeed, docking studies also suggest interactions between the highly conserved residue at position 2 in Con*G*, and conserved residues in the glutamate binding pocket (Wittekindt et al., 2001). However, in addition, the data seem to indicate a nonidentical set of interactions for each conantokin-subunit combination, resulting in differential selectivity profiles among the various conantokins. Interestingly, the double substitution D531Y and I534V in the NR2D subunit had no effect on Con*Rl*-B sensitivity, further suggesting a distinct set of interactions governs the selectivity for each conantokin.

Conservation of NR2 subunits and implications for developing selective conantokins. We generated chimeras for this study using NMDA receptor subunit gene clones from rat; however, a sequence analysis shows NR2B Tyr507 and Val 510 (along with NR2D Asp531 and Ile534) are conserved across the rat, mouse, and human species. Thus, we predict similar Con*R* subtype

selectivity among these species. Analysis of the NMDA receptor subunit sequences in zebrafish, however, shows differences in amino acids at these homologous positions. In mammalian receptors, conantokins generally target the NR2B subunit with the greatest potency. As conantokins presumably evolved to target fish as prey, the effects and targeting specificity of conantokins on fish NMDA receptor subtypes is another question that remains to be addressed. It is interesting to note, however, that the NR2B subunit undergoes significant developmental changes in expression, similar to mammalian species (Cox et al., 2005).

Our findings have implications for the potential development of selective conantokin analogs. These data suggest that conantokins interact with similar regions, but with distinct sets of amino acids for each conantokin. If the core binding site hypothesis is correct, and a distinct set of binding interactions is conserved across conantokins and NMDA receptor NR2 subunits, this necessarily narrows our search for points of interaction that govern selectivity to residues beyond the core binding site. A solved NR2B structure will facilitate endeavors to develop antagonists capable of discriminating among the various NR2 subunits.

Summary. The objective of this study was to elucidate the regions of the NR2B and NR2D subunits important for the high sensitivity of NR2B and low sensitivity of NR2D to Con-R and Con*Rl*-B. To localize these regions, we designed chimeric NR2B and NR2D subunits in order to isolate the sequence components of NR2B that could confer Con-R and Con*Rl*-B sensitivity to the insensitive NR2D subunit when substituted into homologous regions. Our major findings were that the C-terminal regions of both the S1 and S2 domains are important for sensitivity to both Con-R and Con*Rl*-B. We also identified two NR2B residues, Tyr 507 and Val 510, that recapitulate the entire sensitivity of the NR2B S1 region when substituted for the corresponding residues in NR2D (Asp 531 and Ile 534). Our data suggest that, although key residues were identified (i.e., those at positions 531 and 534 in NR2D) multiple residues on the S1 and S2 domains are involved in the discrimination among subunits. The data in this study suggest that, while Con-R and Con*Rl*-B interact with similar regions in the glutamate binding

domains, the two peptides interact with a different set of individual amino acids. Taken together, these data suggest that each conantokin may competitively bind at the glutamate site, while contacting distinct residues outside the binding pocket to govern individual selectivity. Further work defining how conantokins interact with the individual NR2 subunits could lead to the development of highly selective conantokin analogs.

Table 3.1. Glutamate EC_{50} and Con-R IC_{50} values measured for native NMDA receptors and chimeras

NMDAR Composition (NR1b +)	**Amino Acids Changed**[a]	**Glutamate EC_{50} *(μM; 95%CI)***	***Con-R IC_{50} (μM; 95%CI)***	***nH (Con-R)***	***Sensitivity Ratio***[b]
NR2B	--	6.3 (4.8-8.4)	0.14 (0.11-0.18)	-1.51	36.4
NR2D	--	3.7 (2.7-5.0)	5.1 (3.9-6.5)	-0.75	1
Ch2	$1\text{-}567_D \rightarrow 1\text{-}543_B$	13.7 (12-16)	0.81 (.71-.92)	-1.21	6.17
Ch3	$412\text{-}567_D \rightarrow 390\text{-}543_B$	5.3 (3.8-7.4)	1.7 (1.2-2.5)	-0.74	2.9
Ch4	$684\text{-}823_D \rightarrow 660\text{-}799_B$	6.4 (4.4-9.1)	0.88 (.55-1.4)	-0.94	5.7
Ch5	$1\text{-}567_D \rightarrow 1\text{-}543_B$ $684\text{-}823_D \rightarrow 390\text{-}543_B$	6.3 (4.5-8.9)	0.14 (.12-.17)	-1.33	35.7
Ch6	$684\text{-}747_D \rightarrow 660\text{-}723_B$	3.7 (2.9-4.8)	1.2 (1.0-1.5)	-1.11	4.2
Ch7	$748\text{-}823_D \rightarrow 724\text{-}799_B$	3.0 (2.2-4.0)	0.56 (.42-.74)	-1.00	8.9
Ch8	$412\text{-}490_D \rightarrow 390\text{-}467_B$	8.1 (6.9-9.6)	1.3 (.92-1.9)	-0.82	3.8
Ch9	$491\text{-}567_D \rightarrow 467\text{-}543_B$	5.4 (4.5-6.6)	0.15 (.11-.22)	-0.95	33.3
Ch10	$491\text{-}500_D \rightarrow 467\text{-}476_B$	3.4 (2.5-4.5)	5.7 (2.8-12)	-0.70	0.87
Ch11	$501\text{-}540_D \rightarrow 477\text{-}516_B$	2.7 (2.3-3.3)	1.9 (1.4-2.6)	-0.84	2.6
Ch11 S2	$501\text{-}540_D \rightarrow 477\text{-}516_B$ $684\text{-}823_D \rightarrow 660\text{-}799_B$	2.2 (2.7-3.5)	0.18 (.13-.25)	-1.03	27.8
Ch12	$541\text{-}567_D \rightarrow 517\text{-}543_B$	5.8 (5.3-6.4)	9.5 (6.1-15)	-0.72	0.52
Ch13	$D515_D \rightarrow N$ $V517_D \rightarrow T$	4.9 (3.9-6.1)	2.9 (2.3-3.7)	-0.59	1.7
Ch14	$F526_D \rightarrow V$ $Y527_D \rightarrow M$ $Q528_D \rightarrow K$	3.1 (2.7-3.5)	10 (7.5-14)	-1.10	.5
Ch15	$D531_D \rightarrow Y$ $I534_D \rightarrow V$	1.9 (1.5-2.4)	0.99 (.60-1.6)	-0.81	5.1
NR2D [D531Y]	$D531_D \rightarrow Y$	5.9 (4.5-7.7)	2.9 (2.4-3.5)	-0.72	1.7

n>3 oocytes tested for each EC_{50} and IC_{50} value

[a] Corresponding NR2B and NR2D residues shown; NR2B substitutions were made into NR2D background.

[b]Ratio of sensitivity difference from NR2D (NR2D IC_{50}/IC_{50} value for each subunit combination)

Table 3.2. Con*Rl*-B IC_{50} values measured for native NMDA receptors and chimeras

NMDAR Composition (NR1b +)	**ConRl-B IC_{50} (μM; 95%CI)**	**nH**	**10μM / NMDAR IC_{50}**
NR2B	0.1 (0.08-0.12)	-1.49	100
NR2D	>10	--	~1
Ch 5	0.04 (0.03-0.05)	-1.17	250
Ch 7	0.66 (0.39-1.1)	-0.77	15.2
Ch 9	0.36 (0.29-0.45)	-1.38	27.8
Ch 15	>10	--	~1

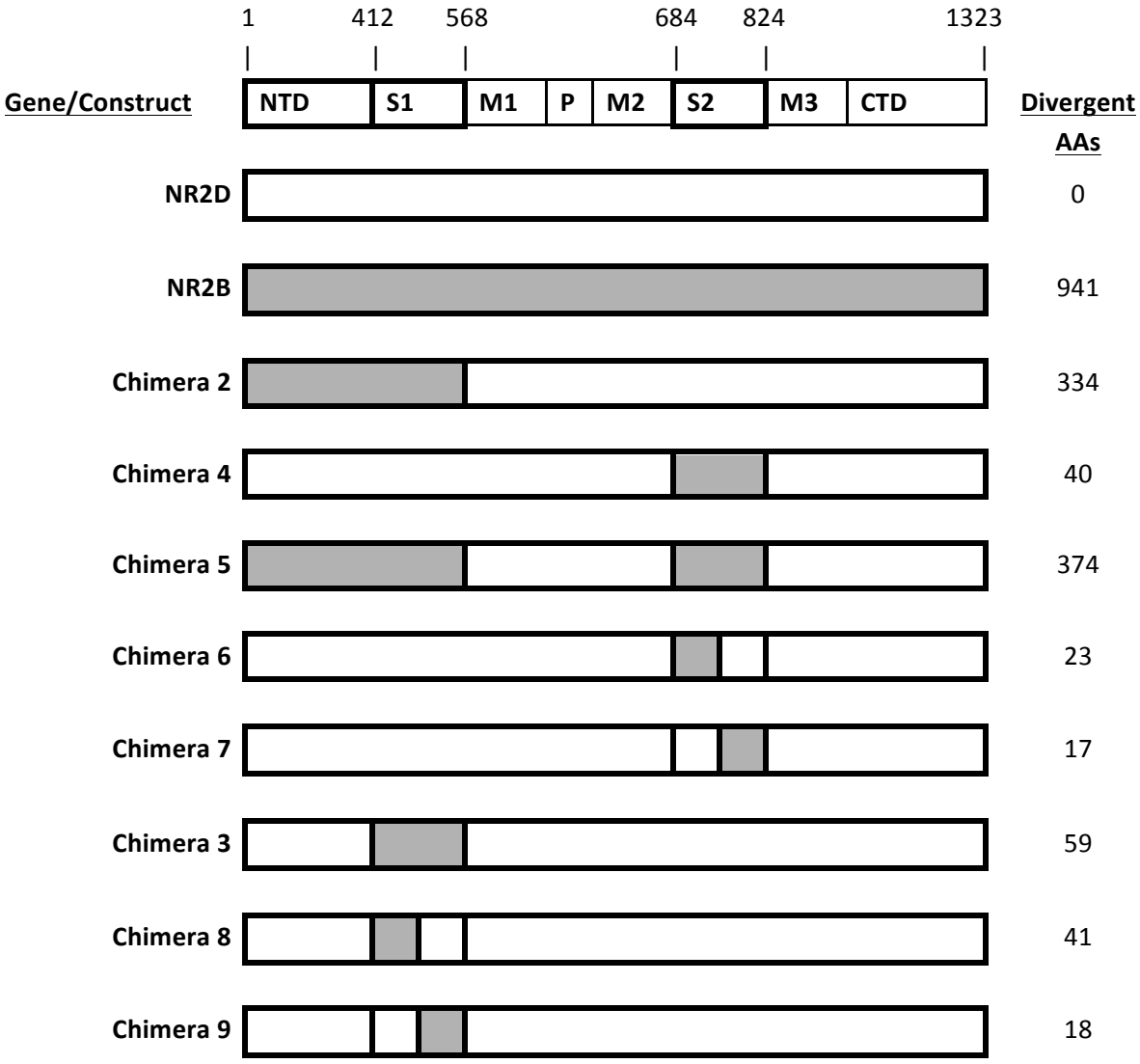

Figure 3.1. Domain topologies of NR2B and NR2D constructs. NR2B regions are shaded in gray and NR2D regions are in white. NTD, N-terminal domain ; S1, Extracellular glutamate binding domain1; M1, transmembrane domain 1; P, pore-lining domain; M2, transmembrane domain 2; S2, Extracellular glutamate binding domain 2; M3, transmembrane domain 3; CTD, C-terminal domain. Regions substituted in this study are highlighted in bold. Numbers of residues that diverge from NR2D for each variant are shown in the column to the right. Numbering scheme at the top indicate amino acid positions of defined regions in the NR2D subunit.

Figure 3.2. Both S1 and S2 are important for sensitivity to Con-R. Concentration response curves shown for Con-R on NR1-b coexpressed with native NR2 subunits (A), extracellular domain chimeras (B), and S1/S2 subregion chimeras (C) in *Xenopus* oocytes (*n*=3-7 oocytes for each concentration and subtype; error bars represent SEM).

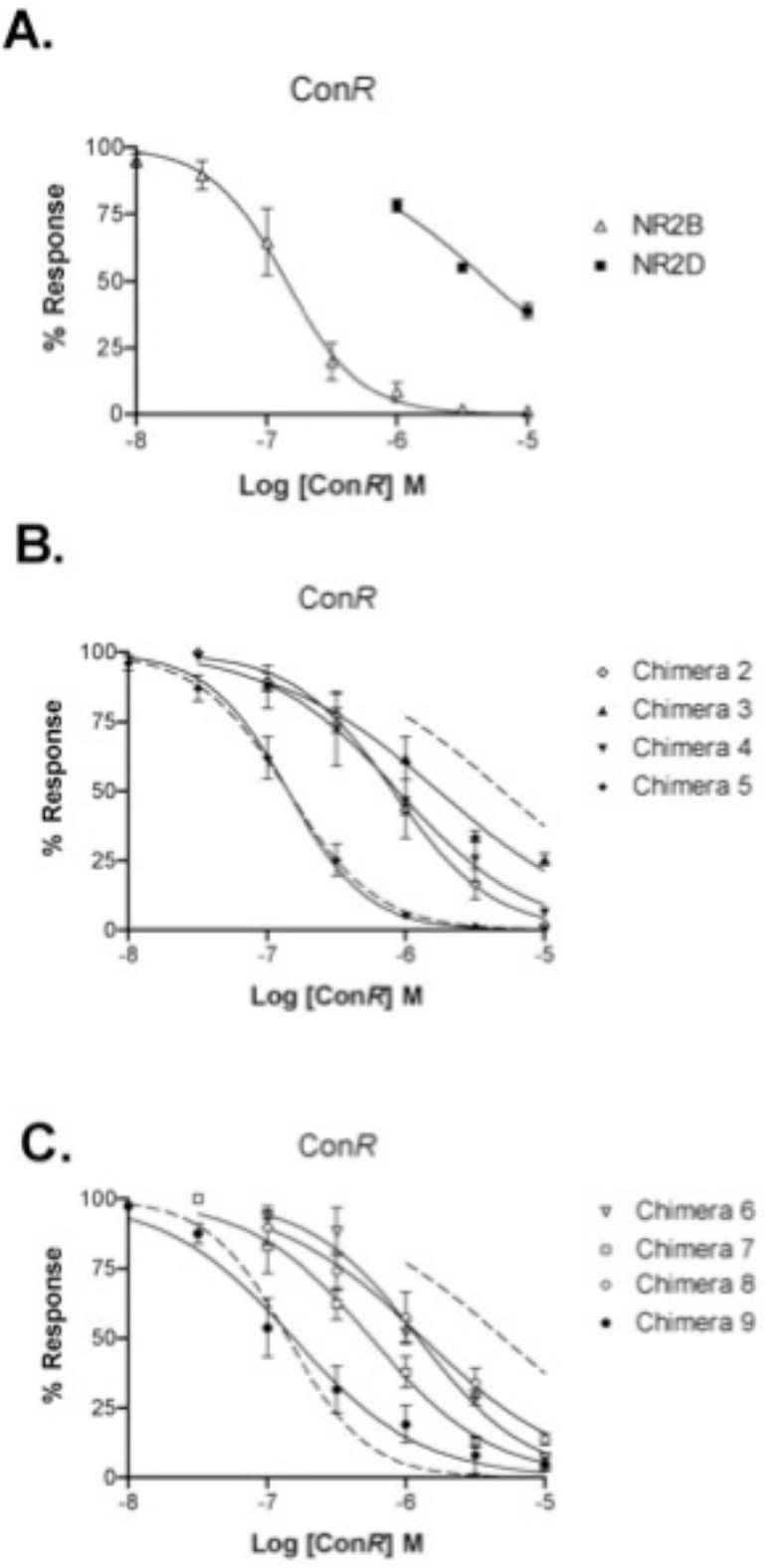
A.
ConR
100
75
50
25
0
% Response
-8
-7
-6
-5
Log [ConR] M
NR2B
NR2D
B.
ConR
100
75
50
25
0
% Response
-8
-7
-6
-5
Log [ConR] M
Chimera 2
Chimera 3
Chimera 4
Chimera 5
C.
ConR
100
75
50
25
0
% Response
-8
-7
-6
-5
Log [ConR] M
Chimera 6
Chimera 7
Chimera 8
Chimera 9

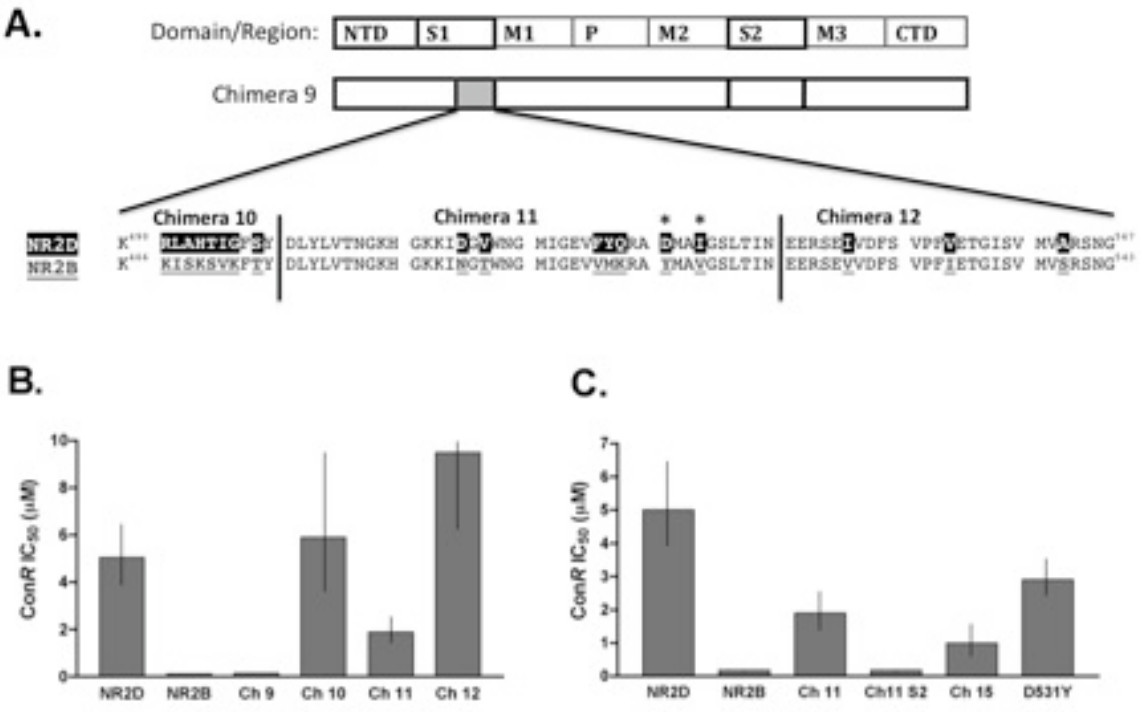

Figure 3.3. Residues in the C-terminal half of S1 contribute to Con-R sensitivity. (A) Alignment of amino acid residues in the C-terminal half of S1. Divergent residues are highlighted (NR2D) or underlined (NR2B). Black bars indicate regions of subdivision for Chimera 10, Chimera 11, and Chimera 12. In all three regions, divergent NR2B residues were substituted into homologous regions of NR2D. Stars indicate the residues that contributed the greatest to sensitivity upon substitution. (B) Comparison of IC_{50} values for chimera 9, 10, 11, and 12. (C) Comparison of Chimera 11 and variants that significantly contributed to sensitivity. Error bars represent 95% confidence intervals for IC_{50} values (n=3-8 oocytes for each concentration response assay).

Figure 3.4. Effect of NR2B substitutions on glutamate sensitivity. Glutamate concentration-response curves for NR1-b coexpressed with native NR2 subunits (A) and selected NR2 mutants (B) in *Xenopus* oocytes (*n*=3-6 oocytes for each concentration and subtype; error bars represent SEM). Dotted line indicates glutamate concentration used in antagonist sensitivity assays.

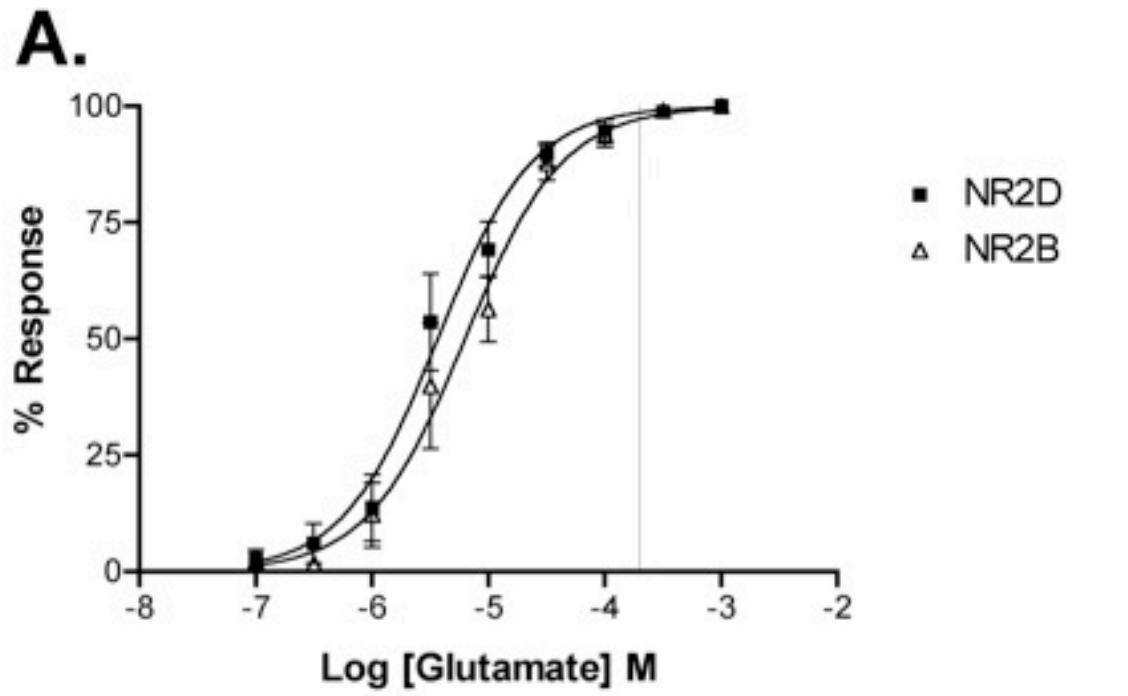
A.
100
75
50
25
0
% Response
-8
-7
-6
-5
-4
-3
-2
Log [Glutamate] M
NR2D
NR2B

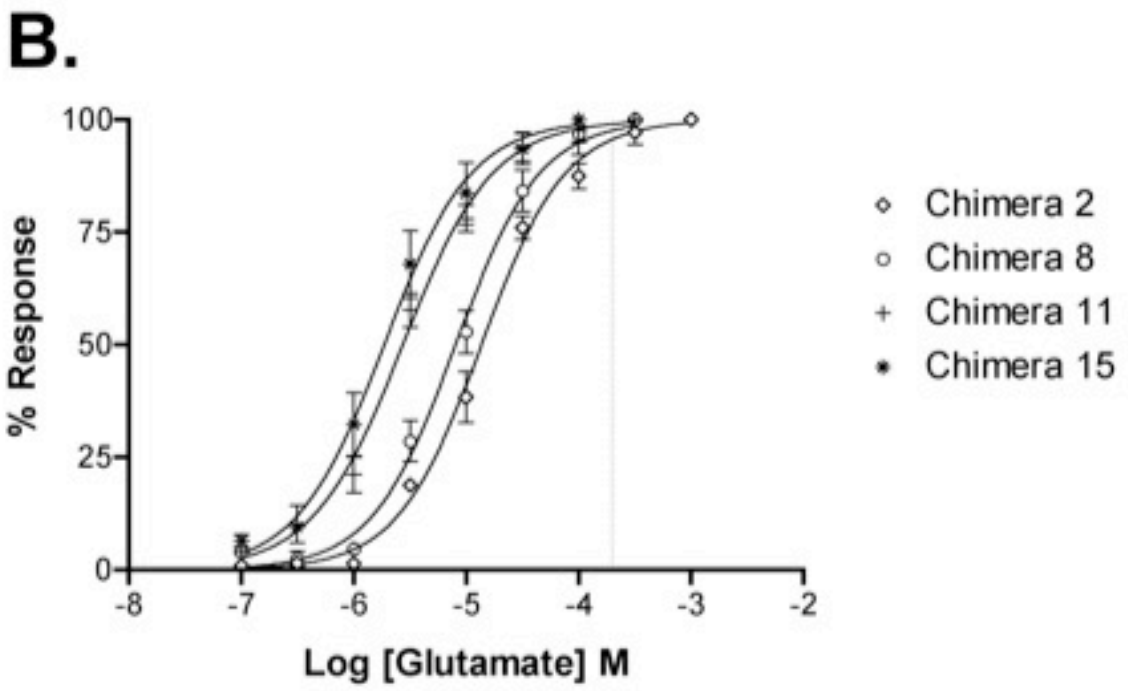
B.
100
75
50
25
0
% Response
-8
-7
-6
-5
-4
-3
-2
Log [Glutamate] M
Chimera 2
Chimera 8
Chimera 11
Chimera 15

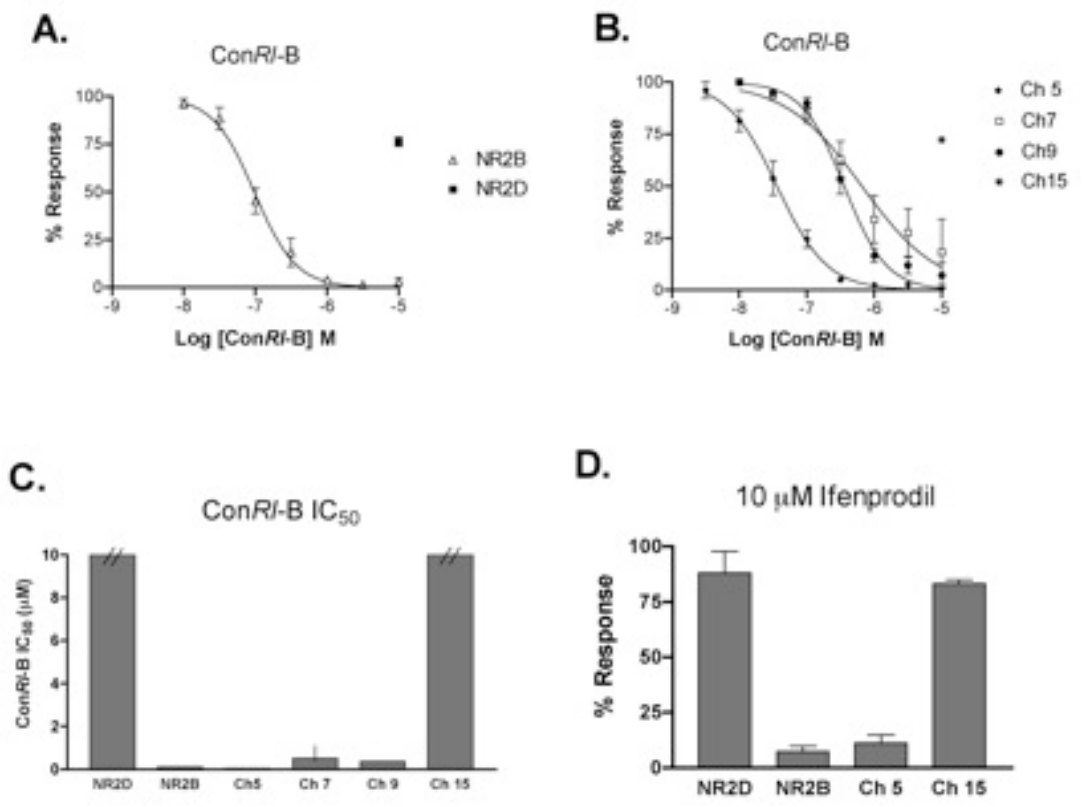

Figure 3.5. NR2B regions important for sensitivity to Con*Rl*-B. Concentration response curves shown for Con*Rl*-B on NR1-b coexpressed with native NR2 subunits (A), or chimeras (B). n=3-oocytes per concentration and subtype; error bars represent SEM. (C) Comparison of approximate Con*Rl*-B IC_{50} values for native receptors and chimeras. IC_{50} values for NR2D and Chimera 15 are estimated at 10 μM. Error bars represent 95% CI. (D) Sensitivity of native receptors and chimeras to 10 μM ifenprodil. Error bars represent SEM. n=3 oocytes per subtype.

References

Anson L.C., Chen P.E., Wyllie D.J., Colquhoun D., Schoepfer R., 1998. Identification of amino acid residues of the NR2A subunit that control glutamate potency in recombinant NR1/NR2A NMDA receptors. J. Neurosci. 18, 581-9.

Cavara, N.A., Hollmann, M., 2008. Shuffling the deck anew: how NR3 tweaks NMDA receptor function. Mol. Neurobiol. 38, 16–26.

Chandler P., Pennington M., Maccecchini M.L., Nashed N.T., Skolnick P., 1993. Polyamine-like actions of peptides derived from conantokin-G, an N-methyl-D aspartate (NMDA) antagonist. J Biol. Chem. 268, 17173-8.

Chen P.E., Johnston A.R., Mok M.H., Schoepfer R., Wyllie D.J., 2004. Influence of a threonine residue in the S2 ligand binding domain in determining agonist potency and deactivation rate of recombinant NR1a/NR2D NMDA receptors. J. Physiol. 558, 45-58.

Chenard B.L. Menniti F.S., 1999. Antagonists selective for NMDA receptors containing the NR2B subunit. Curr. Pharm. Des. 5, 381-404.

Childers W.E., Baudy R.B., 2007. N-methyl-D-aspartate antagonists and neuropathic pain: the search for relief. J. Med. Chem. 50, 2557–2562.

Costa B.M., Feng B., Tsintsadze T.S., Morley R.M., Irvine M.W., Tsintsadze V., Lozovaya N.A., Jane, D.E., Monaghan D.T., 2009. N-Methyl-D-aspartate (NMDA) receptor NR2 subunit selectivity of a series of novel piperazine-2,3-dicarboxylate derivatives: preferential blockade of extrasynaptic NMDA receptors in the rat hippocampal CA3-CA1 synapse. J. Pharmacol. Exp. Ther. 331, 618− 626.

Cox J.A., Kucenas S., Voigt M.M., 2005. Molecular characterization and embryonic expression of the family of N-methyl-D-aspartate receptor subunit genes in the zebrafish. Dev. Dyn. 234, 756-66.

Cull-Candy S., Brickley S., Farrant M., 2001. NMDA receptor subunits: diversity, development and disease. Curr. Opin. Neurobiol. 11, 327–335.

Donevan S.D., McCabe R.T., 2000. Conantokin G is an NR2B-selective competitive antagonist of N-methyl-D-aspartate receptors. Mol. Pharmacol. 58, 614−623.

Erreger K., Geballe M.T., Kristensen A., Chen P.E., Hansen K.B., Lee C.J., Yuan H., Le P., Lyuboslavsky P.N., Micale N., Jørgensen L., Clausen R.P., Wyllie D.J., Snyder J.P., Traynelis S.F., 2007. Subunit-specific agonist activity at NR2A-, NR2B-, NR2C-, and NR2D-containing N-methyl-D-aspartate glutamate receptors. Mol. Pharmacol. 72, 907-20.

Feng B., Tse H.W., Skifter D.A., Morley R., Jane D.E., Monaghan D.T., 2004. Structure-activity analysis of a novel NR2C/ NR2D-preferring NMDA receptor antagonist: 1-(Phenanthrene-2-carbonyl) piperazine-2,3-dicarboxylic acid. Br. J. Pharmacol. 141, 508−516.

Fischer G., Mutel V., Trube G., Malherbe P., Kew J.N., Mohacsi E., Heitz, M.P., Kemp, J.A., 1997. Ro 25-6981, a highly potent and selective blocker of N-methyl-D-aspartate receptors containing the NR2B subunit. Characterization in vitro. J. Pharmacol. Exp. Ther. 283, 1285−1292.

Gonda X., 2012. Basic pharmacology of NMDA receptors. Curr. Pharm. Des. 18, 1558-67. Review.

Gowd K.H., Han T.S., Twede V., Gajewiak J., Smith M.D., Watkins M., Platt R.J., Toledo G., White H.S., Olivera B.M., Bulaj G., 2012. Conantokins derived from the Asprella clade impart conRl-B, an N-methyl d-aspartate receptor antagonist with a unique selectivity profile for NR2B subunits. Biochemistry. 51, 4685-92.

Hammerland L.G., Olivera B.M., Yoshikami D., 1992. Conantokin-G selectively inhibits N-methyl-D-aspartate-induced currents in Xenopus oocytes injected with mouse brain mRNA. Eur. J. Pharmacol. 226, 239-44.

Hollmann M., Heinemann S., 1994. Cloned glutamate receptors. Annu. Rev. Neurosci. 17, 31–108.

Karakas E., Simorowski N., Furukawa H., 2011. Subunit arrangement and phenylethanolamine binding in GluN1/GluN2B NMDA receptors. Nature. 475, 249-53.

Kinarsky L., Feng B., Skifter D.A., Morley R.M., Sherman S., Jane D.E., Monaghan D.T., 2005. Identification of subunit- and antagonist-specific amino acid residues in the N-Methyl-D-aspartate receptor glutamate-binding pocket. J. Pharmacol. Exp. Ther. 313, 1066-74.

Laube B., Hirai H., Sturgess M., Betz H., Kuhse J., 1997. Molecular determinants of agonist discrimination by NMDA receptor subunits: analysis of the glutamate binding site on the NR2B subunit. Neuron. 18, 493-503.

Maier W., Schemm R., Grewer C., Laube B., 2007. Disruption of interdomain interactions in the glutamate binding pocket affects differentially agonist affinity and efficacy of N-methyl-D-aspartate receptor activation. J. Biol. Chem. 282, 1863-72.

Matsuda K., Kamiya Y., Matsuda S., Yuzaki M., 2002. Cloning and characterization of a novel NMDA receptor subunit NR3B: a dominant subunit that reduces calcium permeability. Brain Res. Mol. Brain Res. 100, 43-52.

Meldrum B.S., 1994. The role of glutamate in epilepsy and other CNS disorders. Neurology. 44,

S14–23.

Morris R.G., 2013. NMDA receptors and memory encoding. Neuropharmacology. Apr 26. doi:pii: S0028-3908(13)00151-2. 10.1016/j.neuropharm.2013.04.014. [Epub ahead of print]

Mosley C.A., Acker T.M., Hansen K.B., Mullasseril P., Andersen K.T., Le P., Vellano K.M., Brauner-Osborne H., Liotta D.C., Traynelis S.F., 2010. Quinazolin-4-one derivatives: A novel class of noncompetitive NR2C/D subunit-selective N-methyl-D-aspartate receptor antagonists. J. Med. Chem. 53, 5476−5490.

Mosley C.A., Myers S.J., Murray E.E., Santangelo R., Tahirovic Y.A., Kurtkaya N., Mullasseril P., Yuan H., Lyuboslavsky P., Le P., Wilson L.J., Yepes M., Dingledine R., Traynelis S.F., Liotta D.C., 2009. Synthesis, structural activity-relationships, and biological evaluation of novel amide-based allosteric binding site antagonists in NR1A/NR2B N-methyl-D-aspartate receptors. Bioorg. Med. Chem. 17, 6463−6480.

Perin-Dureau F., Rachline J., Neyton J., Paoletti P., 2002. Mapping the binding site of the neuroprotectant ifenprodil on NMDA receptors. J. Neurosci. 22, 5955–5965.

Ragnarsson L., Yasuda T., Lewis R.J., Dodd P.R., Adams D.J., 2006. NMDA receptor subunit-dependent modulation by conantokin-G and Ala7-conantokin-G. J. Neurochem. 96, 283-91.

Schuler T., Mesic I., Madry C., Bartholomaus I., Laube B., 2008. Formation of NR1/NR2 and NR1/NR3 heterodimers constitutes the initial step in N-methyl-D-aspartate receptor assembly. J. Biol. Chem. 283, 37–46.

Sheng Z., Dai Q., Prorok M., Castellino F.J., 2007. Subtype-selective antagonism of N-methyl-D-aspartate receptor ion channels by synthetic conantokin peptides. Neuropharmacology. 53, 145−156.

Sheng Z., Liang Z., Geiger J.H., Prorok M., Castellino, F.J., 2009. The selectivity of conantokin-G for ion channel inhibition of NR2B subunit-containing NMDA receptors is regulated by amino acid residues in the S2 region of NR2B. Neuropharmacology. 57, 127−136.

Sheng Z., Prorok M., Castellino F.J., 2010. Specific determinants of conantokins that dictate their selectivity for the NR2B subunit of N-methyl-D-aspartate receptors. Neuroscience. 170, 703−710.

Simeone T.A., Sanchez R.M., Rho J.M., 2004. Molecular biology and ontogeny of glutamate receptors in the mammalian central nervous system. J. Child Neurol. 19, 343-360; discussion 361.

Skolnick P., Boje K., Miller R., Pennington M., Maccecchini M.L., 1992. Noncompetitive

inhibition of N-methyl-D-aspartate by conantokin-G: evidence for an allosteric interaction at polyamine sites. J. Neurochem. 59, 1516-21.

Tsai V.W., Dodd P.R., Lewis R.J. 2005. The effects of alanine-substituted conantokin-G and ifenprodil on the human spermine-activated N-methyl-D-aspartate receptor. Neuroscience. 130, 457-64.

Twede V.D., Miljanich G., Olivera B.M., Bulaj G., 2009. Neuroprotective and cardioprotective conopeptides: an emerging class of drug leads. Curr. Opin. Drug Discovery Dev. 12, 231−239.

Twede V.D., Teichert R.W., Walker C.S., Gruszczynski P., Kazmierkiewicz R., Bulaj G., Olivera B.M., 2009. Conantokin- Br from Conus brettinghami and selectivity determinants for the NR2D subunit of the NMDA receptor. Biochemistry. 48, 4063−4073.

White H.S., McCabe R.T., Armstrong H., Donevan S.D., Cruz L.J., Abogadie F.C., Torres J., Rivier J.E., Paarmann I., Hollmann M., Olivera B.M., 2000. In vitro and in vivo characterization of conantokin-R, a selective NMDA receptor antagonist isolated from the venom of the fish-hunting snail Conus radiatus. J. Pharmacol. Exp. Ther. 292, 425-32.

Wittekindt B., Malany S., Schemm R., Otvos L., Maccecchini M.L., Laube B., Betz H., 2001. Point mutations identify the glutamate binding pocket of the N-methyl-D-aspartate receptor as major site of conantokin-G inhibition. Neuropharmacology. 41, 753-61.

Zhou L.M., Szendrei G.I., Fossom L.H., Maccecchini M.L., Skolnick P., Otvos L. Jr., 1996. Synthetic analogues of conantokin-G: NMDA antagonists acting through a novel polyamine-coupled site. J. Neurochem. 66, 620-8.

CHAPTER 4

IDENTIFICATION OF MEMBERS OF THE GLUTAMATE RECEPTOR FAMILIES, INCLUDING NMDA RECEPTOR SUBTYPES AMONG CELL CLASSES IN THE MOUSE VENTRAL RESPIRATORY COLUMN

This chapter appears in part in the following manuscript: Raghraman S,. Garcia A.J., Anderson T., Twede V., Ramirez J.M., Olivera B.M., Teichert R.W., (submitted) Using Constellation Pharmacology to Define CNS Neuronal Subclasses.

Abstract

Previously, we functionally fingerprinted peripheral nervous-system neurons through pharmacologically intensive calcium-imaging experiments that we call "Constellation Pharmacology." Here, we extend Constellation Pharmacology to the central nervous system, demonstrating broad applicability to all nervous system loci. We functionally fingerprinted dissociated cells from the ventral respiratory column (VRC) of mouse brainstem, revealing three major cell classes, each comprising minor subclasses. One minor neuronal subclass of Class B cells responded to substance P, putatively corresponding to inspiratory neurons of the pre-Bötzinger complex (preBötC) that control breathing patterns. Among the three classes, differences were further identified in expression of Glutamate receptors, including a distinction between NR2B subunit-containing NMDA receptor subtypes in Class A cells, and non-NR2B-containing NMDA receptor subtypes in Class B cells. Future studies can determine whether distinct NMDA receptor subtypes functionally mediate fundamental neuronal processes important for the control of respiration in the VRC.

Introduction

Progress in understanding the mammalian brain has been impeded by the extraordinary complexity of cell types that comprise the circuitry and the difficulty in bridging different levels of integration (Bernard et al., 2009; Franco and Muller, 2013; Nelson et al., 2006; Sugino et al., 2006). Systems neuroscientists study the circuitry and high-level functions of the brain, while molecular neuroscientists study the molecular components. The large divide between these two approaches may be bridged by identifying key characteristics that differentiate neuronal and glial cell types in a circuit. Neuronal and glial cell types exhibit functional variation conferred by the differential expression of genes encoding critical signaling proteins, such as neurotransmitter receptors, transporters, ion channels, etc. Cell-specific combinations of receptor- and ion-channel subtypes are functionally coupled to fine tune each neuronal subtype for specific physiological

functions. We refer to a cell-specific combination of signaling proteins as a cell-specific "constellation" (Teichert et al., 2012).

Recently we have demonstrated an experimental strategy that we call Constellation Pharmacology to identify neuronal cell types by their by cell-specific constellations of receptors and ion channels (Teichert et al., 2012a; Teichert et al, 2012b). As proof-of-principle, we initially demonstrated this experimental strategy with cells of the peripheral nervous system (PNS): specifically, dissociated mouse dorsal-root ganglion neurons. In the present study, we demonstrate that Constellation Pharmacology can be extended to the central nervous system (CNS) to identify and characterize different neuronal and glial cell types. This report firmly establishes the broad applicability of Constellation Pharmacology for profiling cell types within the CNS.

In this report, we have investigated cells from the ventral-respiratory column (VRC) of the mouse brainstem. The VRC contains a variety of neurons that are active during either inspiratory or expiratory phases of breathing. One key network within the VRC is the pre-Bötzinger complex (preBötC), which contains the circuitry responsible for generating respiratory rhythms (Gray et al., 2010; Ramirez et al., 1998; Smith et al., 1991; Tan et al., 2008). This network of inspiratory neurons is heterogeneous, encompassing neurons with unique pharmacological profiles (Gray et al., 1996; Lieske et al., 2000; Pena et al., 2004; Pena and Ramirez, 2004; Ramirez et al., 2012). Moreover, the tissue immediately surrounding the preBötC also contains neuronal networks important to cardiovascular control, such as cardiac parasympathetic vagal neurons of the nucleus ambiguus and noradrenergic neurons of the A2/C2 region (Dergacheva et al., 2010; Zanella et al., 2006). By investigating the cell-specific constellations within different cell types in the VRC, we may ultimately integrate molecular and systems level data that allow us to differentiate neurons involved in autonomic control, including those that play a role in controlling breathing.

Using the Constellation-Pharmacology strategy, we have identified three major classes of VRC cells, which can be subdivided further into additional cellular subclasses. Through Constellation Pharmacology, we probe a heterogeneous culture of dissociated cells with a panel of selective pharmacological agents, among other physicochemical perturbations, while we simultaneously monitor the individual responses of more than 100 cells by calcium imaging. By monitoring the different response phenotypes, we can parse cell populations into major cell classes and minor subclasses. Among other functional markers, we characterize the expression of glutamate receptors within the identified cell classes. In addition, we use the subtype-selective NMDA receptor antagonist conantokin*Rl*-B (Con*Rl*-B) to begin to dissect particular NMDA receptor subtypes present within the cellular classes of the VRC. The identification of cellular subclasses constitutes an essential first step towards unraveling the physiological roles of these cells in future studies.

Materials and methods

Preparation of solutions. The medium for culturing VRC neurons, minimal essential media (MEM) + supplements, was MEM (Invitrogen) supplemented with 10% (vol/vol) FBS (HyClone), penicillin (100 U/mL), streptomycin (100 µg/mL), 1X Glutamax (Invitrogen), 10 mM Hepes, and 0.4% (wt/vol) glucose. The medium was adjusted to pH 7.4 with NaOH and then filtered through a 0.22-µm filter under sterile conditions. Before use, the medium was stored at 4 °C. It was allowed to warm to 37 °C in a tissue culture incubator with 5% CO2 atmosphere just before use.

We used artificial cerebrospinal fluid (aCSF) for tissue preparations (brain slices and microdissection) and calcium-imaging experiments. It consisted of the following (in mM): 118 NaCl, 3 KCl, 1.5 $CaCl_2$, 1 $MgCl_2$, 25 sodium bicarbonate, 1 sodium phosphate monobasic, and 30 glucose. For use in tissue preparations, we bubbled carbogen (95% Oxygen/5% CO_2) through the aCSF to oxygenate the solution and to adjust its pH to 7.4. For use in calcium-imaging

experiments, aCSF was adjusted to pH 7.4 with HCl, and then stored at 4 °C until used in calcium-imaging experiments at room temperature.

All stock solutions of pharmacological agents were stored at −20 °C in small-volume aliquots to avoid repetitive freezing and thawing. All working concentrations were obtained by diluting stock solutions into aCSF. The following stocks were kept in aqueous solutions, typically either physiological saline or water: 2 mM histamine dihydrochloride (Acros Organics), 1 mM ATP disodium salt trihydrate (Sigma-Aldrich), 1 M acetylcholine chloride (Sigma-Aldrich), 200 μM Substance-P (Peptides International), 1 mM Bradykinin, 20 mM Norepinephrine, 3M Glutamate (Sigma-Aldrich). Fura-2-acetoxymethyl ester (Fura-2-AM; Invitrogen) stocks were 1 mM in DMSO, distributed into single-use aliquots and stored at −20 °C.

Mouse cell preparations and culture. The following methods apply to preparation and culture of mouse VRC cells. All procedures in this study comply with the rules and regulations in the National Institutes of Health Guide for the Care and Use of Laboratory Animals and were approved by the Institutional Animal Care and Use Committee (IACUC) of the University of Utah Health Sciences Center. WT C57BL/6 mice between the ages of 7 and 8 days postnatal were anesthetized by rapid hypothermia on ice prior to rapid decapitation.

The head was pinned to the sylgard plate and the skin and the connective tissues were removed. Using fine scissors, the skull was cut along the sutures to separate the interparietal region of the skull. This resulted in the exposure of superior colliculus, inferior colliculus and cerebellum. Ice-cold aCSF was applied to keep the tissue moist and cold. A one-sided razor blade was used to make a deep cut along the interface between the inferior colliculus and cerebellum, followed by removal of the cerebellum to isolate the brainstem. The brainstem and upper cervical spinal cord were isolated in ice-cold aCSF, bubbled with Carbogen. The brainstem was glued to a slant agar block using cyano acrylate with its rostral end up and its dorsal side attached to an agar block which was mounted and secured on a specimen tray. The agar block was cut at a slant forming a 110 degree angle between the agar block surface and the horizontal specimen tray (20

degree angle from vertical). The vibratome blade was set to a 20 degree angle below horizontal, which consequently sliced at a right angle to the surface of the agar block. Slicing at this angle enabled us to observe the projections from preBötC to the XII nucleus and from the XII nucleus to the rootlets.

We sectioned the brainstem serially from a rostral to caudal direction. The first slice was cut at a thickness of 200 μm from the top (rostral end). From this point onwards, slices were made to observe facial nerves (first landmark). It varied with preparations, but usually a slice of 400-500 μm from the top had to be removed to observe facial nerves. These facial nerves were observed over a thickness of 250-300 μm. Thus, a slice of 300 μm was made from the point of observing facial nerve. The next landmark was to observe the opening of ventricle at the brainstem-agar block interface. A slice of ~300-400 μm was cut to reveal the opening of the ventricle. From this point, slices of 200 μm were cut until the ventricle closed. The last three slices before the complete ventricle closure were taken and were called rostral, medial and caudal, respectively. To ensure that we were cutting at the level of the preBötC, we calculated the percentage of substance P (a marker for preBötC) responsive Class B cells within dissociated cell cultures obtained from each slice: as expected, the 200-μm-thick medial slice, on average, had the highest percentage of Substance P responsive cells (8.6%) compared to the rostral (7.3%) and caudal (4.1%) slices (n = 7 preparations). This suggested that the medial slice, on average, was near the center of the preBötC. In these slices, a faint hypoglossal nerve was observed and the nucleus ambiguus was sometimes observed in the rostral slice.

The medial slice was placed in ice-cold HBSS, where the segments that contained the VRC and preBötC were microdissected and then transferred with a large-diameter fire-polished Pasteur pipette to a 15-mL conical tube. The total volume was adjusted to 900 μL with HBSS. Then 100 μL 2.5% (wt/vol) trypsin was added (for a working concentration of 0.25% (wt/vol) trypsin), and the tube was incubated at 37 °C in a water bath for 3-4 minutes. After incubation,

the intact tissue segments were washed three times with 4 mL MEM + supplements. Each wash was performed by adding 4 mL MEM + supplements, allowing microdissected segments to settle to the bottom of the tube, and removing as much medium as possible with a fire-polished Pasteur pipette while avoiding the accidental removal of any tissue. After the final wash, the tissue segments were resuspended in 1.5 mL MEM + supplements. The VRC suspension was triturated 5–10 times (or until there was no resistance) through a series of fire-polished pipettes, where each successive pipette had a smaller tip diameter. The solution became cloudy as individual cells dissociated from the slice.

The cell suspension was centrifuged at 50 × g for 10 minutes. After centrifugation of the cell suspension, the supernatant was removed by aspiration, leaving behind the volume of medium required to plate dissociated VRC neurons, typically into six wells (130 μL total). Neurons were resuspended in the remaining medium by gentle trituration with a 100 μL disposable plastic pipette tip. In several of the inner wells of a 24-well plate, 20 μL of the cell suspension was placed in the center of a 3 mm inner-diameter silicone ring, attached to the floor of each well, as described previously (Teichert et al., 2012b). The wells at the edge of the plate were half-filled with sterile water to humidify the culture. Each plate was then placed in the 37 °C incubator for 45–60 minutes to allow cells to settle and adhere. One mL MEM + supplements solution was added very gently at the edge of each well to avoid dislocating any loosely adherent cells within the silicone ring. The plates were placed in a 37 °C, 5% CO2 tissue culture incubator, and the cultures were used for imaging after 18–36 hours.

Calcium imaging. We have previously described the calcium-imaging methods in detail (Teichert et al., 2012a; Teichert et al., 2012b). Briefly, the cells were loaded with Fura-2-AM in their growth medium for 1 hour at 37 degrees C, followed by 30 minutes at room temperature, after which the medium containing Fura-2-AM was replaced with aCSF at room temperature for calcium imaging. Changes in cytoplasmic calcium concentration, $[Ca^{2+}]_c$, were monitored over

time by standard ratiometric calcium imaging methods, i.e. the ratio of fluorescence intensities at 510 nm obtained from intermittent (typically once per two seconds) excitation by 340 nm and 380 nm light (labeled as "340/380 nm" in Y-axis of calcium-imaging figures and described as "340/380 nm ratio" in the text). Upward or downward deflection of a calcium-imaging trace represents an increase or decrease in $[Ca^{2+}]_c$, respectively. In all figures, arrows indicate a 15-second application of the specified compound or other perturbation. Horizontal bars indicate when other compounds were present in the bath solution.

Statistical analysis. The values shown under "Average response to 100 mM $[K^+]_e$ ± S.D." in Table 4.1 were calculated using all of the individual responses of Class A, B and C cells from 5 independent experimental trials, where "S.D." is the standard deviation calculated from all of the individual responses. The quantification of the response shown in Table 4.1 is the magnitude change in the 340/380 nm ratio elicited by 100 mM $[K^+]_e$, as described above, and as depicted in the Y-axis of traces from Figure 4.1. Larger numbers indicate a greater response or greater relative change in $[Ca^{2+}]_c$ elicited by 100 mM $[K^+]_e$. In the Results section, the p-value reported for the difference between Class A and B cells in the average response to 100 mM $[K^+]_e$ was derived as follows: for each independent experimental trial (each trial included more than 100 cells), a sample mean was calculated separately for Class A and B cells for the response to 100 mM $[K^+]_e$. Then the sample means for Class A and B cells were compared from five independent experimental trials using Student's t-test (two-tailed, paired samples).

Results

Calcium imaging of dissociated VRC cell cultures. We prepared cultures of dissociated VRC cells as described in Materials and Methods. Briefly, for each culture, we prepared a brainstem slice of ~200 microns thick, at the level of the preBötC, from a postnatal day 7-8 (P7-8) mouse. We followed the same experimental approach and same protocols that we developed for producing rhythmically active slice preparations (Lieske et al., 2000; Pena et al., 2004;

Ramirez et al., 1996). The region containing the preBötC and surrounding VRC was micro-dissected from the slice, after which the cells were dissociated by enzymatic (trypsin) and mechanical methods. Cells were cultured overnight, prior to performing calcium-imaging experiments.

In Figure 4.2, we show images of dissociated VRC cell cultures of inadequate, optimal and excessive density. In our hands, the optimal plating density was ~800 cells/mm^2 (not all cells survive). This plating density allowed us to perform calcium-imaging experiments in which we could simultaneously monitor the individual responses of more than 100 cells, while avoiding an excessive number of cells that overlapped or made contact with neighboring cells. This enabled us to confidently report the intrinsic responses of individual cells in this study.

Figure 4.2 also shows an example of a VRC cell culture that was used for a calcium-imaging experiment. Panels D-G in Figure 4.2 are images of the same field of view. Panel D is bright field image. Panel E is a fluorescence image of the same cells loaded with Fura-2-AM dye (380 nm excitation and 510 nm emission). Panel F is a pseudo-colored ratiometric image of cells loaded with Fura-2-AM dye at rest. The ratio of fluorescence intensities at 510 nm emission, when excited alternately with 340 nm and 380 nm light, provides a relative measure of cytoplasmic calcium concentration, $[Ca^{2+}]_c$. Panel G is a ratiometric image, immediately after a stimulus to which a subset of the cells in the culture responded with an increase in $[Ca^{2+}]_c$.

Pharmacological profiling of VRC cells. Figure 4.1 exemplifies calcium-imaging traces from selected VRC cells in response to a set of receptor agonists and to depolarization by a high concentration (e.g., 100 mM) of extracellular potassium (high $[K^+]_e$). Abbreviations and concentrations are summarized in Table 4.2 for each of the pharmacological agents and other cellular perturbations used in this study. Three major classes of cells within these cultures could be differentiated by their distinct response properties.

The first major cell class, "Class A," was defined by responsiveness to high $[K^+]_e$ and by the lack of responses to a panel of receptor agonists (Fig. 4.1A and Table 4.1). The second major

cell class, "Class B," was defined by responsiveness to high $[K^+]_e$ and one or more receptor agonists tested (Fig. 4.1B and Table 4.1). Notably, responsiveness to glutamate was excluded as a criterion for classifying cells, because approximately 80% of both Class A and B cells responded to glutamate (a receptor agonist for both metabotropic and ionotropic receptors). However, only Class B cells responded to the other receptor agonists (Table 4.1). In fact, the majority of Class B cells responded to each of the receptor agonists, with the exceptions of the neuropeptides, substance P and bradykinin, to which a minority of the Class B cells responded (Table 4.1).

On average, Class A cells responded to depolarization by high $[K^+]_e$ with large transient increases in $[Ca^{2+}]_c$ (Fig. 4.1A and Table 4.1), indicating that they express high levels of voltage-gated calcium channels, characteristic of neurons. On average, Class B cells responded less strongly to depolarization by high $[K^+]_e$ than Class A cells (Fig. 4.1B and Table 4.1). This difference was statistically significant (p-value = 0.001, Student's t-test). It is presently unclear whether Class B cells are neurons, glia or a mixed population of neurons and glia.

Class B cells were subdivided into subclasses, based on the response profiles of individual cells, as shown in Table 4.3. The subclasses depicted in Table 4.3 represent 82% of the Class B cells. Other Class B subclasses each represented less than 1% of the Class B cells, and were not included in Table 4.3. Table 4.3 demonstrates that there are many variant forms of Class B cells, which presumably play different functional roles within this medullary region.

The third major cell class, "Class C," is comprised of putative nonneuronal cells (glial cells and potentially other nonneuronal cells) that did not respond to depolarization by high $[K^+]_e$ (or responded very weakly, i.e., change in 340/380 nm ratio < 0.1) (Fig. 4.1C and Table 4.1), suggesting that they do not express voltage-gated calcium channels, or only express very low levels, unlike neurons. A small minority of Class C cells responded to each of the receptor agonists tested (Table 4.1). However, when we reduced the resting $[K^+]_e$ from 3 mM to 0.2 mM, 30% of the Class C cells responded with an increase in $[Ca^{2+}]_c$ (Fig. 4.3). Such responses (putatively mediated by $K_{ir}4.1$) have been shown to be specific to astrocytes in the VRC (Hartel

et al., 2007; Hartel et al., 2009). This evidence supports the hypothesis that many Class C cells are glial (astrocytes and other glial cells). Furthermore, none of the Class A cells responded to 0.2 mM $[K^+]_e$, which also supports the hypothesis that Class A cells are all neurons. Six percent of the Class B cells responded to 0.2 mM $[K^+]_e$, which suggests that some of the Class B cells are astrocytes.

Glutamate-receptor expression in VRC cell classes. Cells were parsed into Classes A, B and C by the following criteria: cells were considered Class A if they only responded to high $[K^+]_e$ and Class B if they responded to high $[K^+]_e$ and either ACh (in the absence of PNU) or ATP (Fig. 4.4). Class C cells were determined by the same criterion as in Table 4.1 (change in 340/380nm ratio < 0.1 in response to high $[K^+]_e$). On average, the Class A cells exhibited greater responses to high $[K^+]_e$ than Class B cells, as expected, and as demonstrated in Figure 4.4C. Notably, the majority of Class A cells functionally express NMDA receptors and metabotropic glutamate receptors, with or without detectable expression of non-NMDA (AMPA or kainate) receptors (Fig. 4.44A & C). In contrast to Class A cells, the majority of Class B cells functionally express AMPA and/or kainite receptors, but not NMDA receptors (Fig. 4.4B & C). Class C cells also did not express NMDA receptors (Fig. 4.4C).

NMDA-receptor subtype expression in VRC cell classes. Cells were divided into Classes A, B and C in a similar manner to the criteria used to define cell types for glutamate-receptor expression, with the exception of the use of the marker Substance P and the absence of the marker ATP. Cells were considered Class A if they responded only to high $[K^+]_e$ and Class B if they responded simultaneously to high $[K^+]_e$ and either ACh or SP. Cells were considered to be Class C by the same criterion as in Table 4.1 (change in 340/380nm ratio < 0.1 in response to high $[K^+]_e$). Following a protocol to identify cell classes, Mg^{2+} was removed from the bath solution, and cells were assayed for NMDA receptor expression. Similar to experiments assessing glutamate-receptor expression, the majority of Class A cells express NMDA receptors, whereas the majority of Class B and Class C cells do not (Fig. 4.5A and 4.5B; Table 4.4.). Con*Rl*-B, a

conopeptide that selectively blocks NMDA receptor subtypes containing the NR2B subunit, was administered following the first application of NMDA and D-serine, and block was measured during co-application with the second pulse of NMDA and D-serine (Fig. 4.5A and 4.5B). Notably, the majority (96%) of Class A cells were blocked by con*Rl*-B, with an average block of 68% (Figure 4.5A; Table 4.4). In contrast, none of the Class B cells were blocked by con*Rl*-B, indicating a relative lack of abundance of NR2B-containing NMDA receptor subtypes in this class (Fig. 4.5B; Table 4.4). Among cells in Class C, 50% were blocked by con*Rl*-B, suggesting a mixture NMDA receptor subtypes are expressed in a small population (3%) of non-neuronal cells (Table 4.4). NMDA-receptor mediated calcium signal in all cells that were either not blocked or partially blocked by con*Rl*-B showed a complete inhibition by AP5, indicating the presence of non-NR2B NMDA receptor subtypes mediating calcium signal unblocked by con*Rl*-B (Fig. 4.5A and 4.5B; Table 4.4).

Discussion

Here, we show the characterization of VRC cell classes within the mouse brainstem at the level of the preBötC. Three major cell classes, designated Class A, Class B, and Class C were identified. It is notable that functional divergence within each cell class suggests that each of these major classes may be further subdivided into minor subclasses based on their responsiveness to the set of pharmacological tools used in this study. With additional pharmacological markers, each subclass may ultimately be divided into specific cellular subtypes with distinct pharmacological roles. A long-term goal of this work is to identify all of the cellular subtypes present in these cultures, to the point to where a physiological role for each cellular subtype may be inferred.

On average, the Class A cells in this study responded strongly to a depolarizing stimulus. In addition, most Class A cells also responded to glutamate, but failed to respond to the other agonists tested (see Table 4.1). Class B cells, in contrast, responded relatively weakly on average

to a depolarizing stimulus, with the majority of cells responding to an array of receptor agonists (Fig. 4.1 and Table 4.1). Class C cells responded either very weakly or not at all to a depolarizing stimulus, suggesting that they potentially include glial cells or other nonneuronal cells (Fig 4.1 and Table 4.1). Approximately 30% of Class C cells responded to 0.2 mM $[K^+]_e$, a response suggesting that a proportion of Class C cells are astrocytes.

Glutamate receptors were present in the majority of both Class A and Class B cells (Fig 4.4). Pharmacological dissection revealed that NMDA receptors are predominant in Class A cells, with concurrent expression of AMPA/Kainate receptors. Among Class B cells, glutamate receptors largely belong to the AMPA/Kainate classes, with relatively little expression of NMDA receptors. These data suggest a potential functional role for NMDA receptors among Class A cells. It is notable that a large proportion (>50%) of Class A cells also tentatively express metabotropic glutamate receptors, as assessed by a glutamate-mediated calcium signal unaffected by CNQX (Figure 4.4). Interestingly, both metabotropic glutamate receptors and NMDA receptors have been shown to contribute to inspiratory drive potentials in preBötC neurons, potentially through a common calcium-activated target (Pace et al., 2007). Metabotropic glutamate receptors also have a modulatory role on NMDA receptor function in certain cell types (Conn and Pin, 1997). Additional experiments using dissociated VRC cells can be used to reveal whether the functional relationships elucidated among NMDA receptors and metabotropic glutamate receptors correspond to particular cell types identified in this work.

A distinction between NMDA receptor subtypes was also observed among the VRC cell classes. Among Class A cells, NR2B subunit-containing NMDA receptors are the predominant subtype expressed (Table 4.4). In contrast, among Class B cells, no NR2B subunit-containing NMDA receptor subtypes were detected (Fig. 4.5; Table 4.4). Class B cells that respond to NMDA represent a relatively small proportion of the total population (approximately 2-5% in Class B; Fig. 4.4 and Table 4.4). Nevertheless, this relatively small population of cells expressing non-NR2B-containing NMDA receptor subtypes may be functionally significant: VRC cells

responding to Substance P are hypothesized to be important for the generation of rhythmic breathing patterns (Palgiardini et al., 2005), and have been shown to co-express NMDA receptor protein in rats (Liu et al., 2001). Thus, a distinct subtype of NMDA receptor may be present in cells that mediate vital respiratory function. Through the use of additional subtype-selective NMDA receptor antagonists, future studies can begin to identify further NMDA receptor subtypes within these cell populations.

Table 4.1. Summary of responses from the profiling experiments depicted in Figure 4.1.

	Criteria for Classification			% of Responsive Cells in Each Cell Class							
Cell Class	**Average Response to 100 mM $[K^+]_e$ ± S.D.**	**Responsiveness to Pharmacological Compounds**	**Total Cells**	**% of Total Cells**	**SP**	**ACh**	**ATP**	**NE**	**H**	**B**	**G**
Ventral Respiratory Column (P7-8 Mouse)											
Class A	0.8 ± 0.4	Responsive to glutamate only & response to 100 mM $[K^+]_e \geq 0.1$	220	13%	0%	0%	0%	0%	0%	0%	78%
Class B	0.3 ± 0.2	Responsive to other receptor agonists & response to 100 mM $[K^+]_e \geq 0.1$	574	33%	8%	91%	68%	65%	74%	35%	76%
Class C	0.0 ± 0.0	Response to 100 mM $[K^+]_e < 0.1$	965	55%	1%	6%	8%	4%	5%	6%	6%

The "Average response to 100 mM $[K^+]_e$ ± S.D." is a relative measure of the change in $[Ca^{2+}]_c$ elicited by 100 mM $[K^+]_e$ (i.e., change in 340/380 nm ratio shown in figures and described in Materials and methods). Larger numbers indicate a greater response or greater relative change in $[Ca^{2+}]_c$ elicited by high $[K^+]_e$. The VRC data set was compiled from five independent experimental trials, using cells prepared separately from four different mice.

Table 4.2. Abbreviations of compounds cited in figures and tables.

Abbreviation	Compound	Working Concentration
ACh	Acetylcholine	1 mM
AP5	2-amino-5-phosphopentanoic acid	100 μM
ATP	Adenosine 5' triphosphate	20 μM
B	Bradykinin	10 μM
C	Control	NA
CNQX	6-cyano-7-nitroquinoxaline-2,3-dione	10 μM
Con*Rl*-B	Conantokin*Rl*-B	3.3 μM
G	Glutamate	300 μM
H	Histamine	50 μM
K	$[K^+]_e$	100 mM
NE	Norepinephrine	20 μM
NMDA D-Ser	N-methyl-D-aspartate and D-Serine	100 μM 10 μM
SP	Substance-P	1 μM

Table 4.3. Subclasses of VRC Class B cells.

SP	ACh	ATP	NE	Histamine	Brady	Glutamate	No. of Cells	% of Class B
-	+	+	+	+	-	+	128	22%
-	+	+	+	+	+	+	84	15%
-	+	-	+	+	+	+	33	6%
-	+	-	+	+	-	+	30	5%
-	+	+	-	+	-	+	30	5%
-	+	+	-	-	-	+	22	4%
-	+	-	-	-	-	+	21	4%
+	+	+	+	+	-	+	15	3%
+	+	+	+	+	+	+	13	2%
-	+	-	-	+	-	+	12	2%
-	+	+	-	-	-	-	12	2%
-	+	-	-	+	+	+	10	2%
-	+	+	+	+	-	-	10	2%
-	+	+	+	-	-	+	10	2%
-	+	+	-	+	+	+	9	2%
-	+	+	+	+	+	-	8	1%
-	+	-	+	+	+	-	8	1%
-	+	+	-	+	-	-	7	1%

Subclasses were sorted in order of observed frequency within Class B cells. These subclasses represent 82% of the Class B cells. Shading and "+" indicates responsiveness and "-" indicates lack of responsiveness to the respective compounds. This data set was compiled from five independent experimental trials, using cells prepared separately from four different mice.

Table 4.4. NR2B subunit-containing NMDA receptor expression among VRC cell classes

Cell Class	**% Responsive to NMDA**	**% NMDA-responsive cells blocked by con*Rl*-B**	**Average calcium signal block by con*Rl*-B (SD)**
Class A	79%	96%	68% (25%)
Class B	5%	0%	0% (0%)
Class C	3%	50%	33% (38%)

Average block represents the percent inhibition of calcium signal amplitude. Data set was compiled from five independent experimental trials, using cells prepared separately from five different mice.

Figure 4.1. Example calcium-imaging traces from dissociated VRC cells in culture. Each trace is the response of a single cell to the experimental protocol depicted at the bottom of the figure. In each experimental trial, the individual responses of >100 cells were monitored simultaneously. The X-axis and experimental protocol at the bottom of the figure apply to all traces in the figure. The units of the X-axis are time in minutes. The arrows identify time points when various types of stimuli were applied to the cells for 15 seconds. The abbreviations for these stimuli are defined in Table 4.2. "C" represents a control that is the replacement of bath solution (aCSF) with identical bath solution, which allowed us to exclude cells from further analysis that responded to the mere exchange of bath solution. The Y-axis for each trace is the ratio of fluorescence intensities obtained at 510 nm emission from the alternating excitation by 340 nm or 380 nm light. It is a measure of relative changes in $[Ca^{2+}]_c$. The aforementioned facts also apply to Figures 4.3 – 4.5. These traces were obtained from an experimental protocol employing a set of receptor agonists and high $[K^+]_e$. (A) Example traces from Class A cells. Both cells responded strongly to depolarization by high $[K^+]_e$, but only one responded to glutamate with an increase in $[Ca^{2+}]_c$. (B) Example traces from Class B cells. Notably, these cells responded less strongly to high $[K^+]_e$, than Class A cells. They typically responded to several receptor agonists, as shown. (C) Example traces from Class C cells. These either did not respond to depolarization by high $[K^+]_e$ or only responded very weakly.

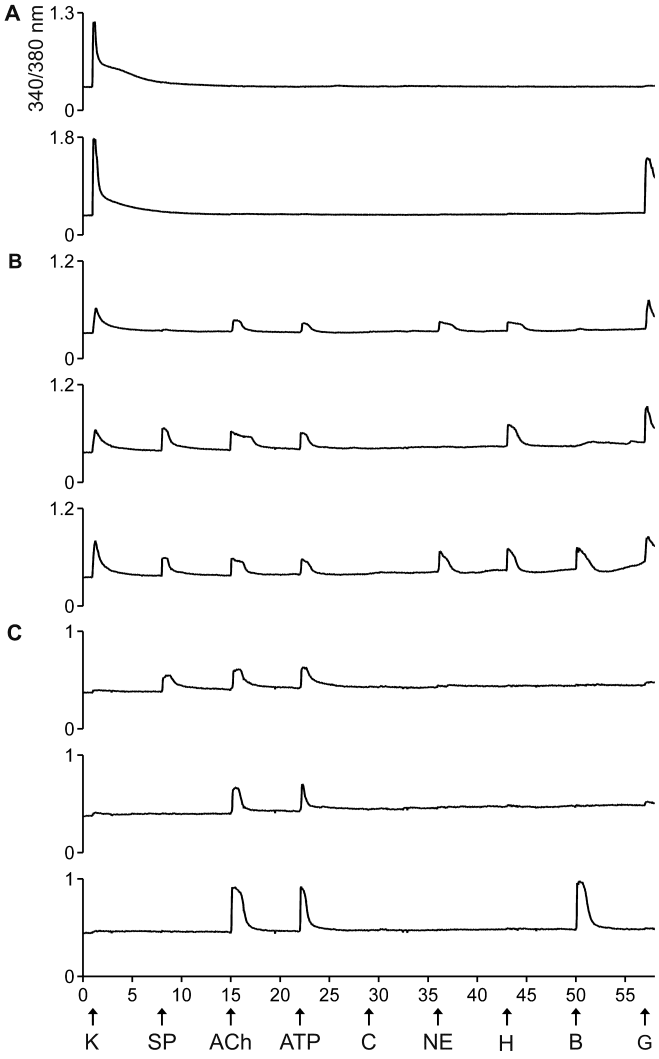
A
340/380 nm
1.3
0
1.8
0
B
1.2
0
1.2
0
1.2
0
C
1
0
1
0
1
0
0 5 10 15 20 25 30 35 40 45 50 55
K SP ACh ATP C NE H B G

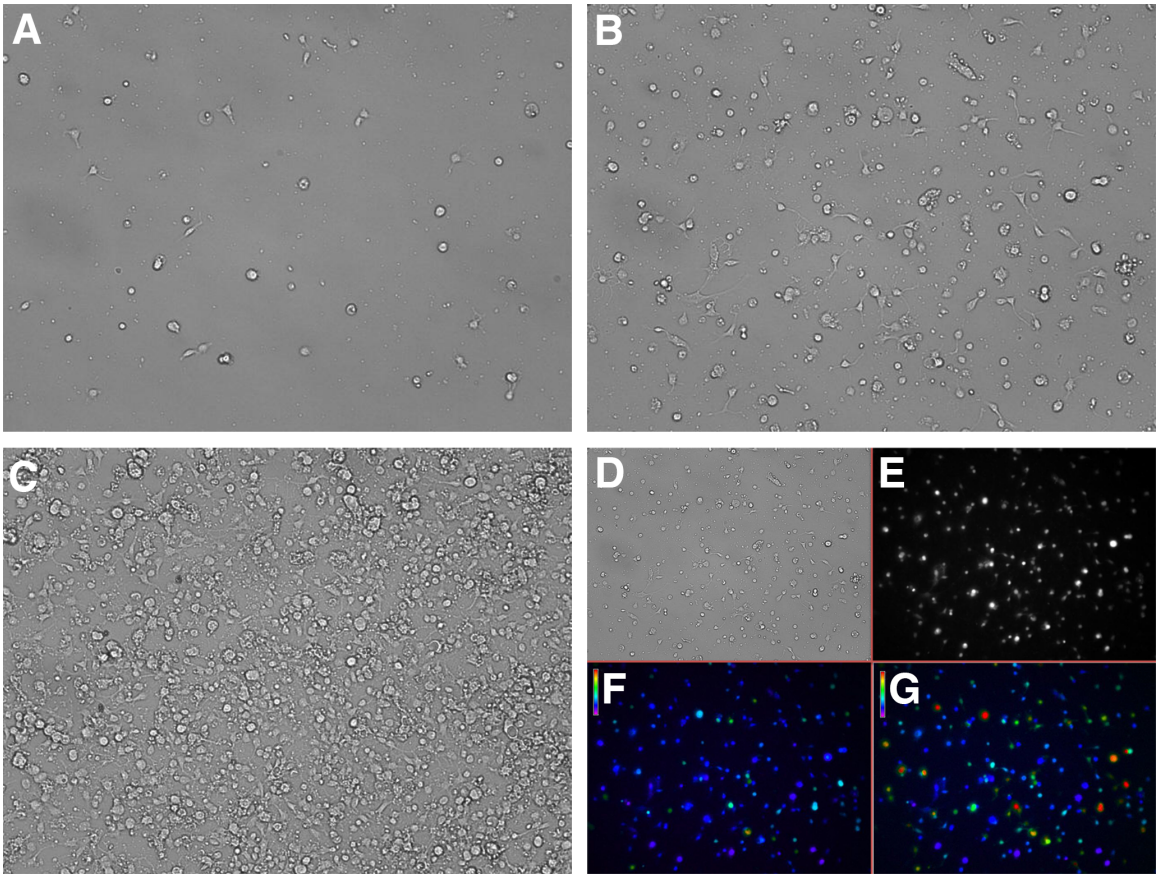

Figure 4.2. Bright field images of dissociated VRC cells in culture. This shows cells of inadequate density (A), optimal density (B) and excessive density (C) for calcium-imaging experiments. Cells were plated at the following densities for these images: (A) 400 cells/mm^2, (B) 800 cells/mm^2 and (C) 2000 cells/mm^2. (D-G) Same field of view. (D) Bright field image of dissociated VRC cells. (E) Fluorescence image of the cells loaded with Fura-2-AM dye (380 nm excitation and 510 nm emission). (F) Pseudo-colored ratiometric image of cells at rest. The ratiometric image is a relative measure of $[Ca^{2+}]_c$, which is obtained from the ratio of fluorescence intensities obtained at 510 nm emission by alternately exciting by 340 nm and 380 nm light. (G) Pseudo-colored ratiometric image of cells immediately following a stimulus, demonstrating that only a subset of the cells responded to the stimulus with an increase in $[Ca^{2+}]_c$ (color scale in F and G indicates relative $[Ca^{2+}]_c$).

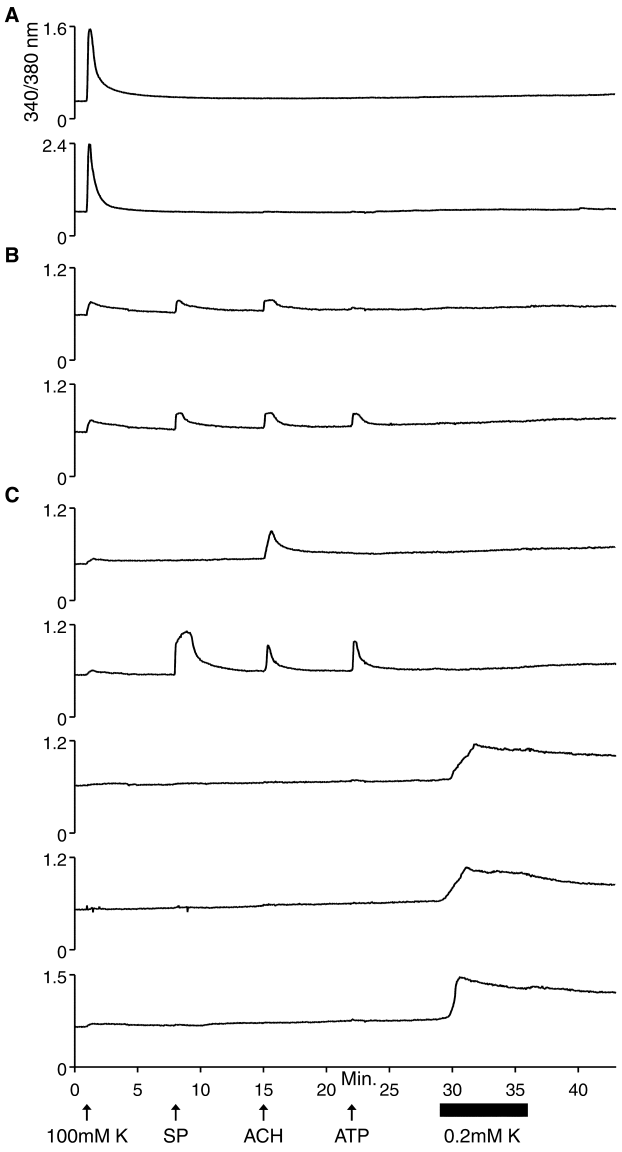

Figure 4.3. Example calcium-imaging traces demonstrating responses to 0.2 mM $[K^+]_e$ in VRC Class C cells, and the lack of responses to 0.2 mM $[K^+]_e$ in Class A and B cells. (A) Two examples are shown of Class A cells that did not respond to 0.2 mM $[K^+]_e$ with an increase in $[Ca^{2+}]_c$. (B) Two examples are shown of Class B cells that did not respond to 0.2 mM $[K^+]_e$. (C) Two examples (top two traces) are shown of Class C cells that did not respond to 0.2 mM $[K^+]_e$ with an increase in $[Ca^{2+}]_c$ and three examples (bottom three traces) are shown of Class C cells that did respond to 0.2 mM $[K^+]_e$ with an increase in $[Ca^{2+}]_c$.

Figure 4.4. Example calcium-imaging traces from experiments investigating glutamate receptors in VRC cells. The black horizontal bar indicates when 100 μM AP5 (NMDA receptor inhibitor) was present in the bath, which did not block the response to the second application of 300 μM glutamate. The open horizontal bar indicates when 10 μM CNQX (AMPA/kainite receptor inhibitor) was present in the bath. CNQX had differential effects on Class A and B cells. The grey horizontal bar (last bar to the right) indicates when the bath solution (aCSF) was changed to Mg^{2+}-free aCSF, because Mg^{2+} blocks NMDA receptors (without a depolarizing stimulus; compare with NMDA/D-Ser application at minute 22). This demonstrated that Class A cells expressed NMDA receptors but Class B cells generally did not. (A) Example traces from Class A cells. (B) Example traces from Class B cells. (C) Compilation of data for Class A and B cells. This data set was compiled for 435 cells from 6 independent experimental trials, using cells prepared separately from 3 different mice.

A

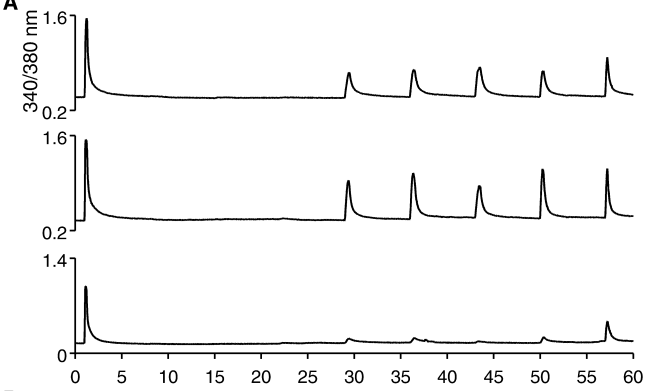

B

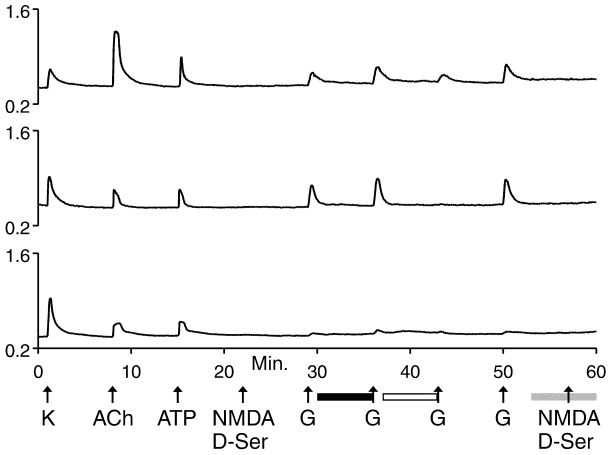

C

			% of responsive cells in each cell class			
Cell Class	**Avg Resp. to 100 mM $[K^+]_e$**	**% of Total Cells**	**NMDA-R**	**Non-NMDA-R**	**Glu Resp. Blocked by CNQX (>5% block)**	**Avg %block by CNQX(S.D.)**
A	0.9	15%	85%	64%	50%	36% (35%)
B	0.3	31%	2%	81%	99%	69% (22%)
C	0.0	54%	0%	3%	86%	64% (27%)

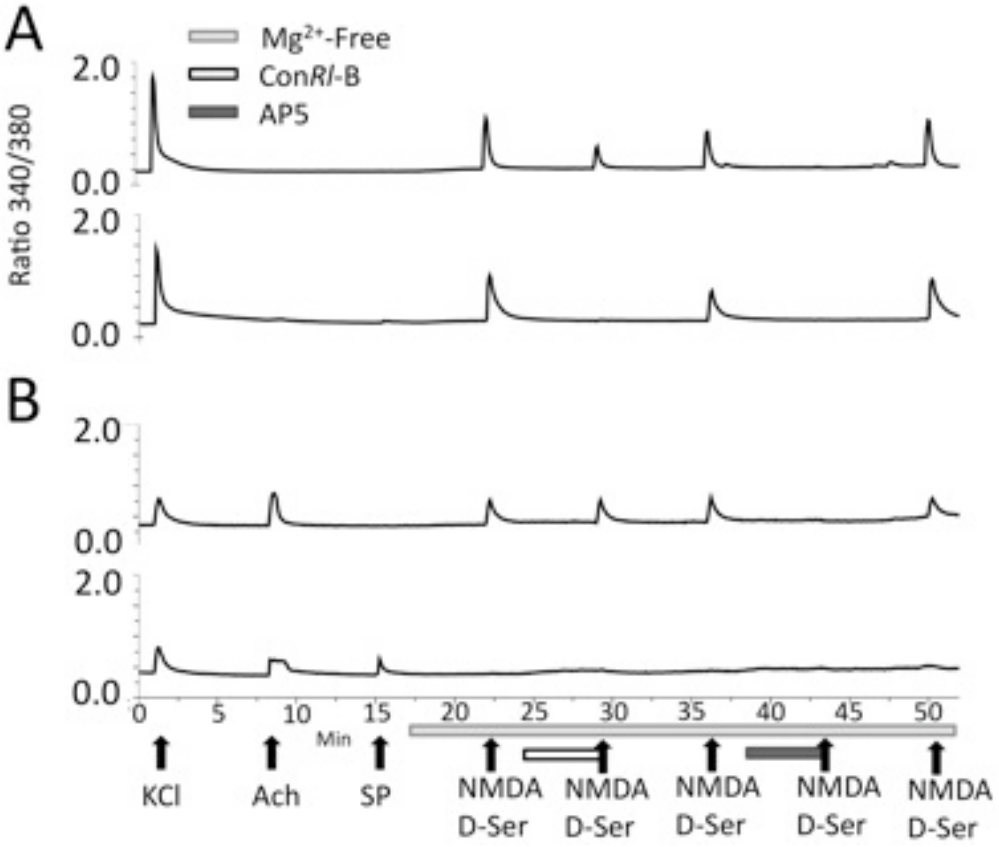

Figure 4.5. Example traces from calcium-imaging protocol investigating NMDA receptor subtype expression in VRC cells. The light-grey horizontal bar indicates replacement of aCSF with Mg^{2+}-free aCSF solution in the bath. The open horizontal bar indicates when 3.3 μM con*RI*-B (a NR2B-selective NMDA receptor inhibitor) was present in the bath. The dark-grey horizontal bar indicates when 100 μM AP5 was present in the bath. (A) Example traces from Class A cells. The majority of Class A cells were either partially blocked (top) or completely blocked (bottom) by con*RI*-B. (B) Example traces from Class B cells. The majority of Class B cells did not respond to NMDA (bottom). Among Class B cells that responded to NMDA, none were blocked by con*RI*-B (top). This data set was compiled for 575 cells from 5 independent trials, using cells prepared separately from 5 difference mice.

References

Bernard A., Sorensen S.A., Lein E.S., 2009. Shifting the paradigm: new approaches for characterizing and classifying neurons. Curr. Opin. Neurobiol. 19, 530-536.

Conn P.J., Pin J.P., 1997. Pharmacology and functions of metabotropic glutamate receptors. Annu. Rev. Pharmcacol. Toxicol. 37, 205-37. Review.

Dergacheva O., Griffifoen K.J., Neff R.A., Mendelowitz D., 2012. Respiratory modulation of premotor cardiac vagal neurons in the brainstem. Respiratory Physiology & Neurobiology. 174, 102-110.

Franco S.J., Muller U., 2013. Shaping our minds: stem and progenitor cell diversity in the Mammalian neocortex. Neuron. 77, 19-34.

Gray P.A., Hayes J.A., Ling G.Y., Llona I., Tupal S., Picardo M.C., Ross S.E., Irata T., Corbin J.G., Eugenin J., Del Negro C.A., 2010. Developmental origin of preBotzinger complex respiratory neurons. J Neurosci. 30, 14883-14895.

Gray R., Rajan A.S., Radcliffe K.A., Yakehiro M., Dani J.A., 1996. Hippocampal synaptic transmission enhanced by low concentrations of nicotine. Nature. 383, 713-716.

Hartel K., Schnell C., Hulsmann S., 2009. Astrocytic calcium signals induced by neuromodulators via functional metabotropic receptors in the ventral respiratory group of neonatal mice. Glia. 57, 815-827.

Hartel K., Singaravelu K., Kaiser M., Neusch C., Hulsmann S., Deitmer J.W., 2007. Calcium influx mediated by the inwardly rectifying K+ channel Kir4.1 (KCNJ10) at low external K+ concentration. Cell Calcium. 42, 271-280.

Lieske S.P., Thoby-Brisson M., Telgkamp P., Ramirez J.M., 2000. Reconfiguration of the neural network controlling multiple breathing patterns: eupnea, sighs and gasps. Nat. Neurosci. 3, 600-607.

Liu Y.Y., Ju G., Wong-Riley M.T., 2001. Distribution and colocalization of neurotransmitters and receptors in the pre-Botzinger complex of rats. J. Appl. Physiol. 91, 1387-95.

Nelson S.B., Sugino K., Hempel C.M., 2006. The problem of neuronal cell types: a physiological genomics approach. Trends Neurosci. 29, 339-345.

Pace R.W., Mackay D.D., Feldman J.L., Del Negro C.A., 2007. Inspiratory bursts in the preBotzinger complex depend on a calcium-activated non-specific cation current linked to glutamate receptors in neonatal mice. J. Physiol. 582, 113-25.

Palgiardini S., Adachi T., Ren J., Funk G.D., Greer J.J., 2005. Fluorescent tagging of rhythmically active respiratory neurons within the pre-Botzinger complex of the rat medullary slice preparations. J. Neurosci. 25, 2591-6.

Pena F., Parkis M.A., Tryba A.K., Ramirez J.M., 2004. Differential contribution of pacemaker properties to the generation of respiratory rhythms during normoxia and hypoxia. Neuron. 43, 105-117.

Pena F., Ramirez J.M., 2004. Substance P-mediated modulation of pacemaker properties in the mammalian respiratory network. J. Neurosci. 24, 7549-7556.

Ramizez J.M., Doi A., Garcia A.J., 3rd, Elsen F.P., Koch H., Wei A.D., 2012. The cellular bulding blocks of breathing. Comprehensive Physiology. 2, 2683-2731.

Ramirez J.M., Quellmalz U.J., Richter D.W., 1996., Postnatal changes in the mammalian respiratory network as revealed by the transverse brainstem slice of mice. J. Physiol. 491 (Pt 3), 799-812.

Ramirez J.M., Schwarzacher S.W., Pierrefiche O., Olivera B.M., Richter D.W., 1998. Selective lesioning of the cat pre-Botzinger complex in vivo eliminates breathing but not gasping. J. Physiol. 507 (Pt 3), 895-907.

Smith J.C., Ellenberger H.H., Ballanyi K., Richter D.W., Feldman J.L., 1991. Pre-Botzinger complex: a brainstem region that may generate respiratory rhythm in mammals. Science. 254, 726-729.

Sugino K., Hempel C.M., Miller M.N., Hattox A.M., Shapiro P., Wu C., Huang Z.J., Nelson S.B., 2006. Molecular taxonomy of major neuronal classes in the adult mouse forebrain. Nat. Neurosci. 9, 99-107.

Tan W., Jancezewski W.A., Yang P., Shao X.M., Callaway E.M., Feldman J.L., 2008. Silencing preBotzinger complex somatostatin-expressing neurons induces persistent apnea in awake rat. Nat. Neurosci. 11, 538-540.

Teichert R.W., Raghuraman S., Memon T., Cox J.L., Foulkes T., Rivier J.E., Olivera B.M., 2012a. Characterization of two neuronal subclasses through constellation pharmacology. Proc. Natl. Acad. Sci. USA. 109, 12758-12763.

Teichert R.W., Smith N.J., Raghuraman S., Yoshikami D., Light A.R., Olivera B.M., 2012b. Functional profiling of neurons through cellular neuropharmacology. Proc. Natl. Acad. Sci. USA. 109, 1388-1395.

Zanella S., Roux J.C., Viemari J.C., Hilaire G., 2006. Possible modulation of the mouse respiratory rhythm generator by A1/C1 ceuronses. Resporatory Physiology & Neurobiology. 153, 126-138.

CHAPTER 5

DISCUSSION

Summary

In Chapters 2, 3, and 4, three different approaches were taken to further the development and applicability of utilizing conantokin peptides for the development of selective NMDA receptor antagonists. In Chapter 2, a structure-activity relationship approach was used to identify sequence determinants of conantokin peptides that govern selectivity towards NR2D subunit-containing NMDA receptor subtypes. The work in Chapter 3 addresses a similar question by localizing regions on the NR2 subunits important for Conantokin-R and Conantokin*Rl*-B discrimination between NR2D- and NR2B-containing NMDA receptor subtypes. Lastly, the experiments in Chapter 4 address the applicability of utilizing highly selective conantokins to identify particular NR2 subunits expressed in particular cell types in a localized brain region.

Significance of findings and perspectives for future research: Chapter 2

Two key findings are reported in Chapter 2: the discovery and functional characterization of a conantokin that has a high potency on NR2D-containing NMDA receptor subtypes, and the identification of amino acid position 5 as a determinant for NR2D potency in the conantokins Con-R and Con-Br. The combination of these two findings has had a significant impact on subsequent research. *Conus brettinghami*, the species from which Con-Br was isolated, belongs to the Asprella clade of cone snails. Molecular phylogeny, a research approach by which discovery of novel peptides (with desirable pharmacological properties) is guided by utilizing the phylogenetic relationship between species to search for homologous peptides in closely related species, has been successfully used to discover and characterize alpha-conotoxins of desired target specificity (Olivera, 2006). Using this strategy, combined with sequence predictions guided our structure-activity relationship data, we identified, synthesized, and functionally characterized three conantokins from another species in the Asprella clade, *Conus bocki,* with novel pharmacologies: each of these three peptides had an unprecedented inhibitory preference (among conantokin peptides) for NR2D-containing NMDA receptor subtypes over those

containing other NR2 subunits (Platt et al., submitted). These subsequent findings demonstrate the power of combining sequence prediction data with guided phylogenetic searches to identify novel pharmacological tools.

The finding that the amino acid at position 5 in Con-R and Con-Br is important for inhibition of NR2D subunit-containing NMDA receptor subtypes, is in addition, of significance in determining the basis for NR2 subunit selectivity in conantokin peptides. In particular, the conclusions that can be drawn from this study are that sequence determinants can be used to predict selectivity towards the NR2D subunit. Interestingly, prior studies have indicated that the amino acids at Positions 5 and 8 (and others) also govern selectivity among the NR2A and NR2B subunits in other conantokins (Klein et al., 2001; Sheng et al., 2007; Sheng et al., 2010). Thus, certain common amino acid positions are potentially important for distinguishing among all of the NR2 subunits. It is notable that not all conantokins appear to selectively inhibit NMDA receptor subtypes by a common set of sequence determinants. For instance, structure activity studies of Con*Rl*-B show no effect the substitution of the amino acid ad position 5 on subunit selectivity, and rather, amino acids at positions 8-10 including a lysine at position 8, appear to be important determinants (Gowd et al., 2012). It is therefore possible that structural differences may contribute to conantokin selectivity in addition to sequence determinants. A corollary of this hypothesis is that different sets of interactions at distinct amino acid positions could occur between different conantokins and the same NR2 subunit to govern selective inhibition. A particular peptide "scaffold," or milieu of amino acid sequences, may therefore be important for exhibiting selective preference over particular NR2 subunits. Future studies to reveal the crystal structures of novel conantokin peptides, in their free form, as well as bound to NMDA receptors, are warranted to provide further insight into how conantokins discriminate among the various NR2 subunits.

Significance of findings and perspectives for future research: Chapter 3

The results of key significance in Chapter 3, are that Con-R and Con*Rl*-B interact with both subdomains of the glutamate binding pocket (S1 and S2) to determine selectivity between the NR2B and NR2D subunits. Moreover, specific NR2 subunit mutants were used to determine that Con-R and Con*Rl*-B likely interact with similar regions of the subunits, but through a distinct set of amino acid residues. These results can be interpreted in the context of the findings from Chapter 2 to provide insight into how conantokins and NR2 subunits are likely to interact to distinguish among the various NMDA receptor subtypes. The conclusions in Chapter 2 and Gowd et al. (2012) suggest that, because the peptide determinants of selectivity on Con-R and Con*Rl*-B occur at different positions, interactions governing selectivity on the NR2 subunits are predicted to occur through distinct sets of amino acids. Consistent with this prediction, the double point mutant NR2D [D531Y; I534V] had an increase in effects on sensitivity to Con-R, but not Con*Rl*-B (Chapter 3, Figs. 3.3 & 3.5). It is also notable that these two peptides interacted similarly with NR2 subunit mutants that had larger regions of substitution than a few amino acids. These results indicate that the positioning for these two peptides within the glutamate-binding pocket (and likely other conantokins) are largely similar. Future studies utilizing mutant cycle analysis can reveal precise points of interaction between Con-R, Con*Rl*-B and the NR2B and NR2D subunits. Such studies could examine, for instance, whether coupling occurs between the valine to tyrosine substitution at position 5 in Con-R and either of the amino substitutions D531Y or I34V in the NR2D subunit.

Other studies have indicated that another conantokin, Con*G*, discriminates between the NR2A subunit and NR2B subunit through two amino acids in the S2 subdomain of the glutamate binding pocket (Sheng et al., 2009). While this is not inconsistent with the findings reported in this dissertation, it is interesting to note that a single locus of interaction was identified for ConG on the NR2A and NR2B subunits, while multiple loci of interaction are suggested by results assessing the effects of Con-R and Con*Rl*-B on NR2B and NR2D mutants. One explanation of

this is that the differences in the number of discriminatory sites may vary among conantokins for each NR2 subunit. Thus, the NR2B and NR2D subunits may simply have more sites for conantokin discrimination than the NR2A and NR2B subunits. One could easily test this hypothesis through the use of Con*Rl*-B (which also discriminates between the NR2A and NR2B subunits) using a similar set of mutants, to determine whether the loci of discrimination overlap with Con*G*. Additional work investigating the points of interaction for each conantokin-subunit combination could lead to predictions that could be utilized as rationale for the discovery and design of novel and highly selective conantokin peptides.

Significance of findings and perspectives for future research: Chapter 4

Three principal findings are described in Chapter 4: first, it was demonstrated that through Constellation Pharmacology, cells in the ventral respiratory column can be divided into three broad cell classes; second, it was demonstrated that differences in glutamate receptor types occur among the cell classes; and third, we show that selective conantokins can be used to identify differences in NMDA receptors subtypes among different cell types. These are among the first experiments to identify NMDA receptor subtypes in particular cell types using conantokins. The results show that Class A cells are largely NR2B-predominant, whereas Class B cells have a notable absence of NR2B-containing NMDA receptor subtypes. Presumably, Class A cells and Class B cells have unique functional roles within the functional network of the preBötC. Indeed, cells responding to Substance P (presumably a subpopulation of Class B cells identified in our assay), have been linked to critical functioning in the ventral respiratory column (Palgiardini et al., 2005). Further experiments using conantokins with more broad pharmacologies such as Con-R (which targets both NR2A- and NR2B-subunit-containing NMDA receptor subtypes; see Chapter 2) can be used to dissect the NMDA receptor subtypes present in the Class B cell population.

These results are of further significance because application of NMDA receptor antagonists have been associated with certain types of network activity in the preBötC, such as enhancing fictive sighs and inhibiting normal breathing patterns, that are distinct from other glutamate receptors (Lieske and Ramirez, 2005). A greater understanding of how NMDA receptors function in different cell types could lead to insight into how these particular cells behave in functioning networks. Through Constellation Pharmacology, we can begin to make predictions regarding which cell types may correspond to functioning cells within an intact brain region, and test these predictions through electrophysiological recordings. Such an approach has been used to predict VRC cell types responding to Substance P that function in whole brain slices (Raghuraman et al., in preparation). In future studies, the development and use of selective conantokins in dissociated cell calcium-imaging assays, brain slice preparations, and whole animals, will hopefully reveal the functional roles of these NMDA receptor subtypes in the VRC and other brain regions.

Therapeutic applications of subtype selective conantokins

The conantokins discovered and characterized thus far have shown effectiveness in both clinical and preclinical trials for the treatment of various nervous system diseases. Con*G* has reached phase I clinical trials for the treatment of epilepsy in humans (Bialer et al., 2002). In addition, five conantokins have shown preclinical efficacy in animal models of pain, epilepsy, or neuroprotection following ischemia (Gowd et al., 2012; Jiminez et al., 2002; Malmberg et al., 2003; Twede et al., 2009; White et al., 2000;; Williams et al., 2000). Some small molecule compounds have been developed that preferentially target some NMDA receptor subtypes (such as NR2B) with a high degree of selectivity (Fischer et al., 1997); however, conantokins have the added advantage of lacking off-target activity on non-NMDA receptor targets (Gowd et al., 2012). Thus, conantokin peptides may prove highly useful in targeting NMDA receptor subtypes in whole animal systems with a great deal of specificity.

Notably, not all conantokins are equivalent in their efficacy or toxicity in preclinical models of disease (Twede et al., 2009). For instance, Con*G* appears to exhibit less behavioral toxicity than Con*T* in models of pain, and certain Con*G* analogs appear to be more effective at inhibiting pain than their native peptide counterparts (Malmberg et al., 2003; Xiao et al., 2008). Interestingly, the conantokins that are most effective or exhibit the fewest side effects, are generally more selective for NR2B-containing NMDA receptor subtypes than their counterparts. Thus, high selectivity of conantokin peptides may correlate with improved efficacy and reduced toxicity in preclinical models of disease. Conantokin*Rl*-B shows an approximate 100-fold selectivity for NR2B-containing NMDA receptor subtypes over any other NMDA receptor subtype, and has demonstrated anticonvulsant activity in mice (Gowd et al., 2012), and is the most NR2B-selective conantokin identified to date. One hypothesis that merits further testing is that Con*Rl*-B will exhibit greater efficacy and less toxicity than other conantokins when compared in other animal models of nervous system dysfunction.

The testing of highly selective conantokins in additional models of disease is also of potential therapeutic relevance. Recently, inhibition of NR2B and NR2D NMDA receptor subtypes was shown to alleviate A-Beta-induced inhibition of long-term potentiation in a rat model of Alzheimer's disease (Zhang et al., 2013). Selective conantokins that block NR2B- or NR2D- containing NMDA receptor subtypes could therefore be of potential use in treating early symptoms of Alzheimer's disease. NR2B-selective conantokins have further potential use in a number of disorders leading to cell death. Con*G* was found to promote cell survival in hippocampal neurons, whereas a less NR2B- selective conantokin (Con*T*) was found to be less effective (Balsara et al., 2012). This effect has been attributed to the preferential inhibition of cell death extrasynaptic NMDA receptor-mediated pathways associated with NR2B subtypes (Balsara et al., 2012). NR2D-containing NMDA receptors may also be associated with cell death, as proteins that negatively regulate the function of the NR2D subunit are thought to promote cell survival by the inhibition of this NMDA receptor subtype (Bai et al., 2013). NR2D is expressed

at the highest levels in midbrain structures in the central nervous system (Laurie et al., 1997). The development of NR2D-selective conantokins is therefore of potential benefit in devising effective strategies for promoting cell survival in disorders that affect this region of the brain, such as dopaminergic loss in substantia nigra cells in Parkinson's disease.

It should be noted that potential therapeutic applications for selective conantokin peptides need to ideally be considered on a disease-specific basis. One potential caveat of studies of NMDA receptor subunit expression in normal mammalian systems, is that there may not be a complete correspondence with the subtype expression in pathogenic animals. For instance, certain models of epilepsy show a differences in expression of NR2A, but not NR2B subtypes (Gibbs et al., 2011; Zhu et al., 2004). Contrastingly, some models of neuropathic pain show an increase in NR2B expression (Wilson et al., 2005). This underscores the need to develop a toolkit of highly selective conantokins for many NMDA receptor subtypes, which can then be evaluated for further therapeutic merit in the context of specific nervous system pathologies. Thus far, conantokins have been discovered that target NR2B-containing NMDA receptor subtypes while simultaneously targeting various other NR2 subunit combinations. The discovery of NR2D-preferring conantokins, and the findings described in this dissertation point towards the potential for developing highly selective conantokins for each particular NMDA receptor subtype. The continued development of these novel compounds may lead to a pharmacological toolkit that can be used to target an array of nervous system disorders.

Scientific contributions of this work

The experiments in this dissertation essentially tackle two broad questions. First, how do we go about developing highly subtype-selective NMDA receptor antagonists from a particular class of conopeptides? Second, can a highly selective conantokin peptide be used to identify NMDA receptor subtypes in the nervous system? Through structure-function studies and structure-activity relationship studies, this work has provided insights that have already been used

to predict conantokin peptide sequences with novel inhibitory activities. Hopefully, this work will provide additional information that may be used to achieve this objective. By testing selective conantokin peptides in dissociated cell calcium imaging assays, we have begun to identify particular NMDA receptor subtypes in particular brain regions and cell types. It is hoped that the continued development of selective conantokins will reveal further distinctions among NMDA receptor subtypes in brain regions of significant scientific or therapeutic merit.

References

Bai N., Hayashi H., Aida T., Namekata K., Harada T., Mishina M., Tanaka K., 2013. Dock3 interaction with a glutamate-receptor NR2D subunit protects neurons from excitotoxicity. Mol. Brain. 6, 22.

Balsara R., Li N., Weber-Adrian D., Huang L., Castellino F.J., 2012. Opposing action of conantokin-G on synaptically and extrasynaptically-activated NMDA receptors. Neuropharmacology. 62, 2227-38.

Bialer M., Johannessen S.I., Kupferberg H.J., Levy R.H., Loiseau P., Perucca E., 2002. Progress report on new antiepileptic drugs: a summary of the Sixth Eilat Conference (EILAT VI). Epilepsy Res. 51, 31-71.

Fischer G., Mutel V., Trube G., Malherbe P., Kew J.N., Mohacsi E., Heitz M.P., Kemp, J.A., 1997, Ro 25-6981, a highly potent and selective blocker of N-methyl-D-aspartate receptors containing the NR2B subunit. Characterization in vitro. J. Pharmacol. Exp. Ther. 283, 1285−1292.

Gibbs S., Chattopadhyaya B., Desgent S., Awad P.N., Clerk-Lamalice O., Levesque M., Vianna R.M., Rébillard R.M., Delsemme A.A., Hébert D., Tremblay L., Lepage M., Descarries L., Di Cristo G., Carmant L., 2011. Long-term consequences of a prolonged febrile seizure in a dual pathology model. Neurobiol. Dis. 43, 312-21.

Gowd K.H., Han T.S., Twede V., Gajewiak J., Smith M.D., Watkins M., Platt R.J., Toledo G., White H.S., Olivera B.M., Bulaj G., 2012. Conantokins derived from the Asprella clade impart conRl-B, an N-methyl d-aspartate receptor antagonist with a unique selectivity profile for NR2B subunits. Biochemistry. 51, 4685-92.

Jimenez E.C., Donevan S., Walker C., Zhou L.M., Nielsen J., Cruz L.J., Armstrong H., White H.S., Olivera B.M., 2002. Conantokin-L, a new NMDA receptor antagonist: determinants for anticonvulsant potency. Epilepsy Res. 51, 73-80.

Klein R.C., Prorok M., Galdzicki Z., Castellino F.J., 2001. The amino acid residue at sequence position 5 in the conantokin peptides partially governs subunit-selective antagonism of recombinant N-methyl-D-aspartate receptors. J. Biol. Chem. 276, 26860-7.

Laurie D.J., Bartke I., Schoepfer R., Naujoks K., Seeburg P.H., 1997. Regional, developmental and interspecies expression of the four NMDAR2 subunits, examined using monoclonal antibodies. Brain Res. Mol. Brain Res. 51, 23-32.

Lieske S.P., Ramirez J.M., 2006. Pattern-specific synaptic mechanisms in a multifunctional network. I. Effects of alterations in synapse strength. J. Neurophysiol. 95, 1323-33.

Malmberg A.B., Gilbert H., McCabe R.T., Basbaum A.I., 2003. Powerful antinociceptive effects of the cone snail venom-derived subtype-selective NMDA receptor antagonists conantokins G and T. Pain. 101, 109-16.

Olivera B.M., 2006. Conus peptides: biodiversity-based discovery and exogenomics. J. Biol. Chem. 281, 31173-7.

Pagliardini S., Adachi T., Ren J., Funk G.D., Greer J.J., 2005. Fluorescent tagging of rhythmically active respiratory neurons within the pre-Bötzinger complex of rat medullary slice preparations. J. Neurosci. 25, 2591-6.

Platt R.J., Curtice K.J., Twede V.D., Watkins M., Gruszczynski P., Bulaj G., Horvath M.P., Olivera B.M., *submitted*. Conantokins from *Conus bocki*: from molecular phylogeny towards differentiating pharmacology for NMDA receptor subtypes.

Sheng Z., Dai Q., Prorok M., Castellino F.J., 2007. Subtype-selective antagonism of N-methyl-D-aspartate receptor ion channels by synthetic conantokin peptides. Neuropharmacology. 53, 145-56.

Sheng Z., Liang Z., Geiger J.H., Prorok M., Castellino F.J., 2009. The selectivity of conantokin-G for ion channel inhibition of NR2B subunit-containing NMDA receptors is regulated by amino acid residues in the S2 region of NR2B. Neuropharmacology. 57, 127-36.

Sheng Z., Prorok M., Castellino F.J., 2010. Specific determinants of conantokins that dictate their selectivity for the NR2B subunit of N-methyl-D-aspartate receptors. Neuroscience. 170, 703-10.

Twede V.D., Miljanich G., Olivera B.M., Bulaj G., 2009. Neuroprotective and cardioprotective conopeptides: an emerging class of drug leads. Curr. Opin. Drug. Discov. Devel. 12, 231-9. Review.

White H.S., McCabe R.T., Armstrong H., Donevan S.D., Cruz L.J., Abogadie F.C., Torres J., Rivier J.E., Paarmann I., Hollmann M., Olivera B.M., 2000. In vitro and in vivo characterization of conantokin-R, a selective NMDA receptor antagonist isolated from the venom of the fish-hunting snail Conus radiatus. J. Pharmacol. Exp. Ther. 292, 425-32.

Williams A.J., Dave J.R., Phillips J.B., Lin Y., McCabe R.T., Tortella F.C., 2000. Neuroprotective efficacy and therapeutic window of the high-affinity N-methyl-D-aspartate antagonist conantokin-G: in vitro (primary cerebellar neurons) and in vivo (rat model of transient focal brain ischemia) studies. J. Pharmacol. Exp. Ther. 294, 378-86.

Wilson JA, Garry EM, Anderson HA, Rosie R, Colvin LA, Mitchell R, Fleetwood-Walker SM. NMDA receptor antagonist treatment at the time of nerve injury prevents injury-induced changes in spinal NR1 and NR2B subunit expression and increases the sensitivity of

residual pain behaviours to subsequently administered NMDA receptor antagonists. Pain. 2005 Oct;117(3):421-32.

Xiao C., Huang Y., Dong M., Hu J., Hou S., Castellino F.J., Prorok M., Dai Q., 2008. NR2B-selective conantokin peptide inhibitors of the NMDA receptor display enhanced antinociceptive properties compared to non-selective conantokins. Neuropeptides. 42, 601-9.

Zhang J., Wang C., Deng T., Xue Z., Chen X., Chang L., Wang Q., 2013. The preventive effect of NR2B and NR2D-containing NMDAR antagonists on Aβ-induced LTP disruption in the dentate gyrus of rats. Metab. Brain Dis. 28, 697-704.

Zhu L.J., Chen Z., Zhang L.S., Xu S.J., Xu A.J., Luo J.H., 2004. Spatiotemporal changes of the N-methyl-D-aspartate receptor subunit levels in rats with pentylenetetrazole-induced seizures. Neurosci. Lett. 356, 53-6.